NASA Contractor Report 4129
Part II

Acoustically Excited Heated Jets

II—In Search of a Better Understanding

J. Lepicovsky, K. K. Ahuja, W. H. Brown,
M. Salikuddin, and P. J. Morris

CONTRACT NAS3-23708
JUNE 1988

NASA Contractor Report 4129
Part II

Acoustically Excited Heated Jets

II—In Search of a Better Understanding

J. Lepicovsky, K. K. Ahuja,
W. H. Brown, and M. Salikuddin
Lockheed Aeronautical Systems Company–Georgia
Marietta, Georgia

P. J. Morris
Pennsylvania State University
University Park, Pennsylvania

Prepared for
Lewis Research Center
under Contract NAS3-23708

National Aeronautics
and Space Administration

**Scientific and Technical
Information Division**

1988

FOREWORD

This report was prepared by Lockheed Aeronautical Systems Company - Georgia Division, Marietta, Georgia for NASA-Lewis Research Center, Cleveland, Ohio under contract NAS3-23708, entitled "Experimental Investigation of the Effects of Acoustic Excitation on Hot Jet Mixing." The work was performed under a two phase effort.

Mr. James R. Stone was the Project Manager for NASA-Lewis Research Center for the Phase I effort. Lockheed's Program Manager was Dr. H. K. Tanna. Dr. Ed Rice was the Project Manager for NASA-Lewis Research Center for the Phase II effort. Lockheed's Program Manager was Dr. K. K. Ahuja.

The program was conducted over a period of five years. During this period, however, the originally proposed goals for this study were substantially modified by the NASA project manager and emphasis was put on the ivnestigation of excitability of high speed, highly heated jets. Because of this, the final report presents a chronological rather than a thematic development of the subject.

Technical help from Messrs. R. H. Burrin, C. R. Huie, and J. F. Songer is particularly acknowledged.

The authors are particularly grateful to Mr. Uwe von Glahn of NASA-Lewis for his continuous support, various lively discussions and useful suggestions during the course of this work.

This Page Intentionally Left Blank

CONTENTS

SUMMARY

This is Part 2 of a three-part report on the excitability of heated jets under the influence of acoustic excitation. Our efforts to understand the lack of excitability of high speed heated jets by internal excitation are described here. The theoretical predictions discussed in Part 1 are examined in detail to find explanations for the observed discrepancies between the measured and the predicted results. Additional testing was performed by studying the self excitation of the shock containing hot jets and also by exciting the jet by sound radiated through source tubes located externally around the periphery of the jet. The effects of nozzle-exit boundary layer conditions on jet excitability was also investigated. It is concluded that high speed, heated jet mixing rates and consequently also the jet excitability strongly depends on nozzle exit boundary layer conditions. Considerable further work is still needed to understand the excitability of the heated jets before they can be controlled effectively by artificial excitation.

1.0 INTRODUCTION

This report is Part 2 of a three-part report on the excitability of heated jets under the influence of acoustic excitation. The effects of internal excitation on jet mixing were described in detail in Part 1. The excitation sound in this case emitted from eight acoustic drivers located some distance upstream of the nozzle exit. Effects of boundary layer thickness, jet Mach number, excitation level, and excitation frequency were measured for both heated and unheated jets. Detailed flow visualization was also made to substantiate most of the observed effects. The most important conclusion of these results was that we were able to excite unheated jets at all jet Mach numbers examined, but the highly heated jets were found to be excitable only at the low jet Mach numbers. For example, at a jet Mach number (M_j) of 0.3, the heated jet was even more excitable than the unheated jet, but at an M_j = 0.8, the heated jet did not appear to be excitable.

This lack of excitability for the high Mach number jets was not only disappointing, but was contradictory to the theoretical predictions according to which heated jets should in fact be somewhat more excitable at a given jet Mach number and excitation level and excitation Strouhal number.

In this Part 2 of the report are described our efforts to understand the above anomalous behavior of hot jets. After having discovered the above results, we repeated our experiments and indeed the same results were obtained. The first step, therefore, was to reexamine the theoretical predictions and look for some obvious explanation. An assessment of the predictions versus measurements was, therefore, made first and is described in the next section. As a result of this assessment, it was concluded that a new and more powerful acoustic source was required. In addition, a new method of directly measuring the acoustic excitation levels was needed. It was decided that the use of an external excitation source will fulfill these requirements. But before designing and fabricating this source, some unique experiments were performed that indicated what kind of excitation levels will be needed if the experiments with the external source were to be successful. These experiments are described in Section 3.0. The results from these experiments, which incorporated studying the effects of naturally occurring screech in supersonic jets on jet flow behavior, helped us reach some very important conclusions about the excitability of the heated jets. The adopted method of excitation level measurement is also presented in the same section.

The results for the external excitation are presented in Section 4.0. The jet in this case was excited by sound impinging right at the nozzle lip.

The sound was directed at the lip by eight equispaced tubes connected to eight electroacoustic drivers. Since the tube openings were located outside the flow, true levels of excitation were measured just outside the nozzle lip.

Finally, the last section, Section 5.0, describes experiments on the effects of nozzle-exit boundary layer conditions on jet excitability. This task was added to the original program in an effort to understand limited excitability of highly heated jets at certain jet operating conditions. The results, acquired under this task, indicate that nozzle-exit boundary layer conditions play an important role as far as jet excitability is concerned.

However, this conclusion is based on a narrow range of jet operating conditions. Further work is still needed to generalize the derived conclusions for a broader range of jet operating conditions.

2.0 A CLOSER LOOK AT THE DISCREPANCIES BETWEEN MEASUREMENTS AND THEORETICAL PREDICTIONS

2.1 INTRODUCTARY REMARKS

The purpose of this section is to examine the response of a high Mach number heated jet to upstream acoustic excitation. The predictions are based on an analysis which has been reported in References [2.1], [2.2], and [2.3]. The details of the analysis will not be repeated here. However, it is useful to review the elements of the model. For a given excitation level and frequency and given jet operating conditions, the coupling between the acoustic excitation and the jet instability waves is calculated. The degree of coupling is a function of the local width of the jet. Once the instability wave, which has zero amplitude at the jet exit, is excited, its growth is calculated on the basis of inviscid instability theory. The development of the jet flow itself, which may be characterized by a few scaling parameters, such as the jet mixing layer thickness, the jet centerline velocity and the maximum turbulent kinetic energy, is determined from an integral energy analysis. Simple models, based on the eddy viscosity concept, have been used to describe the production of turbulent kinetic energy and the interaction between the excited instability wave and the small-scale turbulence. It should be emphasized that the model is based on a compressible flow analysis. An analytic solution to the thermal energy equation, Crocco's relationship, is used to relate the local static temperature to the local jet velocity.

This section first considers the predicted and measured response of an unheated jet at both low and high Mach numbers. The effects of jet heating are then examined. The influence of the jet exit boundary layer thickness on the jet response is also considered. Finally, a discussion of the discrepancies between prediction and experiment, and suggestions for key experiments to either confirm or invalidate the prediction model for high temperatures, is given.

2.2 CALCULATIONS

2.2.1 The Effect of Jet Exit Mach Number

For unheated jets some comparisons between prediction and experiment were given in References [2.1] and [2.3]. Those experiments were conducted at Mach numbers of 0.58 and 0.78. Further comparisons are made here with the

data given by Chan [2.4] for a Mach number of 0.2 and further data given in Reference [2.1] at a Mach number of 0.78. These comparisons provide further confirmation that the model predicts successfully the properties of cold, excited jets for a wide range of Mach numbers.

A critical test of the prediction scheme is its ability to predict the pressure level of the excited instability wave on the jet centerline. This level provides an indication of the presence of an instability wave which influences the development of the jet. It should be noted that the model predicts the absolute level of the excited instability wave for a given excitation level.

Figure 2.1 shows a comparison between the predicted centerline pressure level and the measurements by Chan [2.4]. Taking the pressure level at the jet exit to be 125 dB, the predicted maximum wave amplitude on the jet centerline is 2.5 dB below the measured value. Taking an excitation level of 130 dB gives only a 1 dB difference. For these levels of excitation, which are well above the 'threshold' level for this jet Mach number, the non-linear response of the jet can be seen. The peak moves closer to the jet exit. This corresponds to an increase in the spreading rate of the jet and decrease in the potential core length. The more rapid drop in the instability wave amplitude with axial distance compared to the measured values is probably due to the influence of small-scale pressure fluctuations towards the end of the potential core.
A similar comparison between prediction and experiment is shown in Figure 2.2. Several excitation levels are considered for this jet exit Mach number, however, this time for high jet exit Mach number of 0.8. The predicted 'threshold' level for this Mach number is much higher, at about Le = 122 dB, so the instability wave response is nearly linear. This can be seen by comparing the relative amplitude between the instability wave peak and the excitation level. In all cases, this ratio is approximately 21 dB. This is confirmed by the measurements and the agreement, bearing in mind the absolute nature of the predictions, is excellent.

Figure 2.3 shows the effect of excitation level on the relative Mach number on the jet centerline at X/D = 9. This ratio was used extensively in Reference [2.2] and is the ratio of the centerline Mach number for the excited case to its value in the unexcited case. The predictions indicate that there is no change for excitation levels less than 120 dB. This is confirmed by the measurements. This excitation level corresponds to the 'threshold' level reported by Moore [2.5] of 0.08 percent of the jet exit dynamic head. The measurements indicate that at the highest excitation levels, the relative Mach number is as low as 0.83. This value is not predicted by the present model. This is probably related to the simplicity of the turbulence models for production and dissipation. For the sake of simplicity, it has been assumed that these models have the same empirical coefficients in all regions of the jet. This assumption could be relaxed

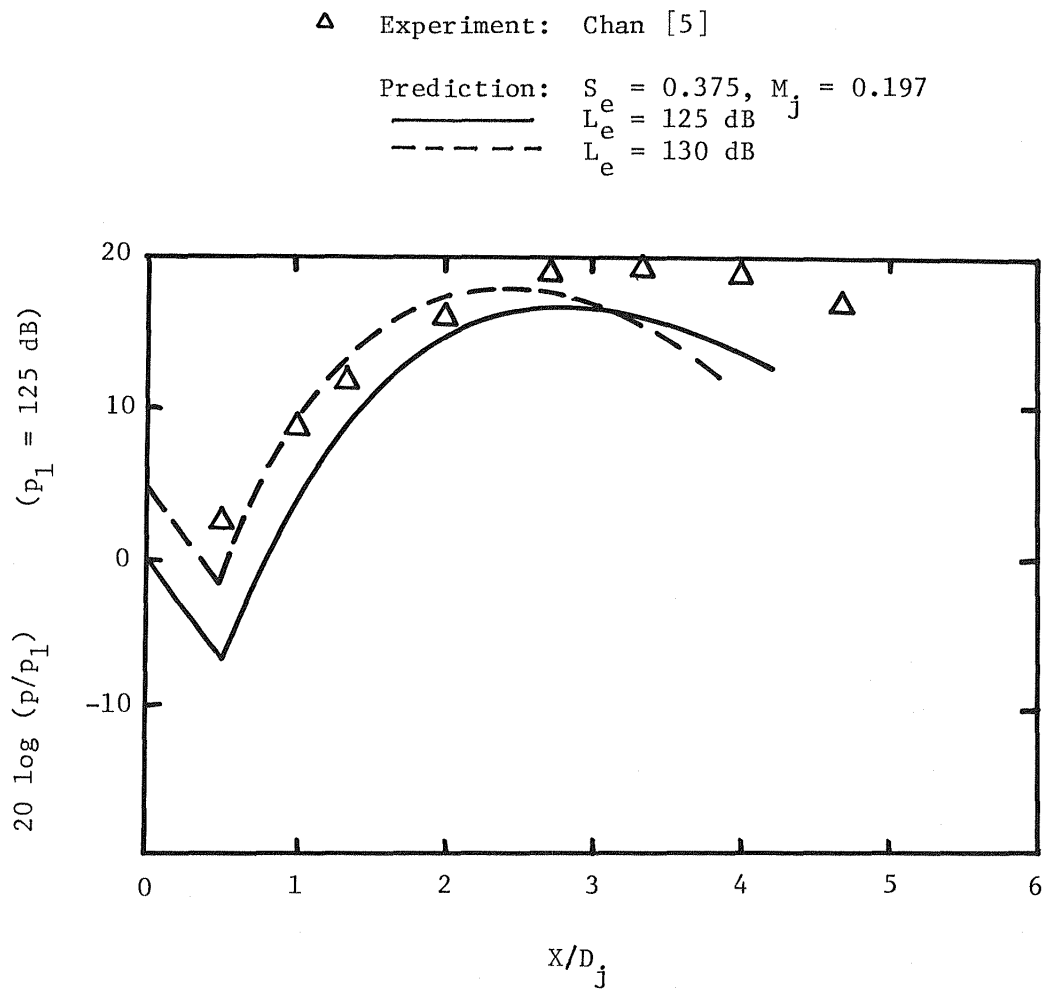

Figure 2.1 Centerline pressure level in a low Mach number, unheated jet

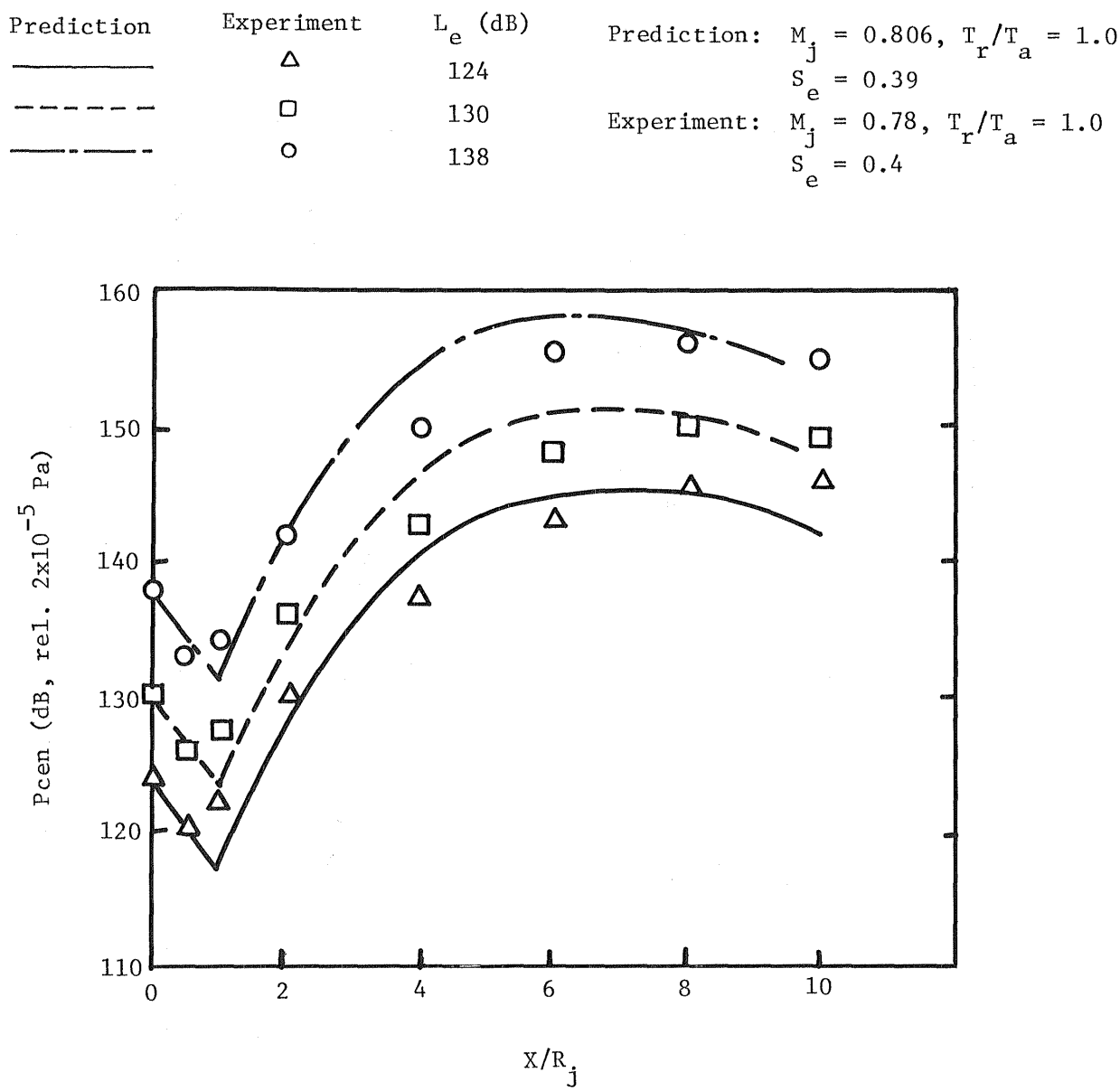

Figure 2.2 Centerline pressure level in a high Mach number, unheated jet

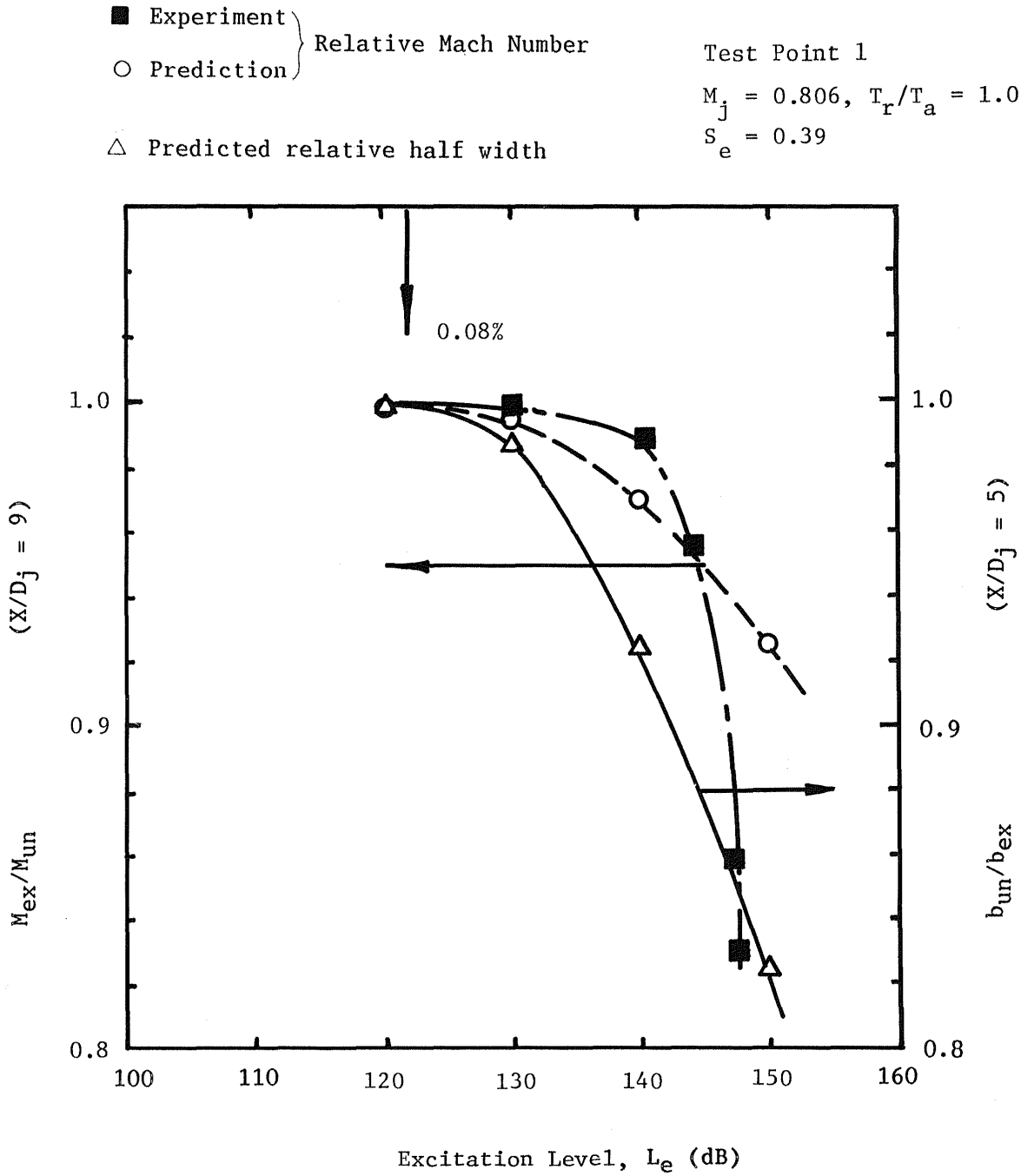

Figure 2.3 Effect of excitation level on centerline Mach number and jet width

and somewhat better agreement obtained, but this would violate the basic intent of the model, which attempts to model the basic physical processes with the minimum of empiricism. The overall good agreement between the predictions and experiments provides justification for this approach.

Also shown in Figure 2.3 is the predicted relative half-width of the jet at X/D = 5. These predictions indicate that there is a larger relative change in this parameter with excitation than in the centerline Mach number further downstream. Thus this ratio would be used as a measure of the response of the jet.

These calculations, and those previously reported, indicate that the prediction model is based on the correct physical processes. In the next subsection, the effects of jet temperature on the response of the jet to excitation is examined.

2.2.2 The Effect of Jet Temperature

Figure 2.4 shows the predicted response of a jet to excitation for the same Mach number as in Figure 2.3. However, the jet is heated in this case to a stagnation temperature ratio of 2.29. The threshold level is seen to have been reduced slightly by the increase in the jet temperature. The relative changes in the centerline Mach number and the jet thickness are somewhat lower than the predicted changes for the unheated case as can be seen by comparison with Figure 2.3. However, the measured values indicate that there is no change in the jet centerline Mach number for the range of excitation levels considered and the excitation Strouhal number of 0.39.

From the viewpoint of the predictions, the decrease in the jet's response with higher temperature is readily understood. The details of the prediction model and definition of the coupling coefficients used in this model are given in Reference 2.3. Here, Figure 2.5 shows a comparison of the calculated coupling coefficients for the heated and unheated cases. The real and imaginary parts are shown since the relative phase of the acoustic excitation wave and the excited instability wave is important. However, the magnitude of the coupling coefficient gives a gross indication of the receptivity of the jet. Since the magnitude is relatively independent of the jet temperature, it can be inferred that the initial growth in amplitude of the instability wave or the receptivity of the jet will be similar in both cases. Figure 2.6 shows the calculated growth rate of the instability wave as a function of the local jet width for the two cases. Though the maximum growth rate for the heated case is higher, the unheated case shows growth for a wider range of jet thicknesses. This results in the centerline pressure levels shown in Figure 2.7. The excited instability wave grows to a high amplitude close to the jet exit and then decays rapidly. The instability wave in the unheated case has a large

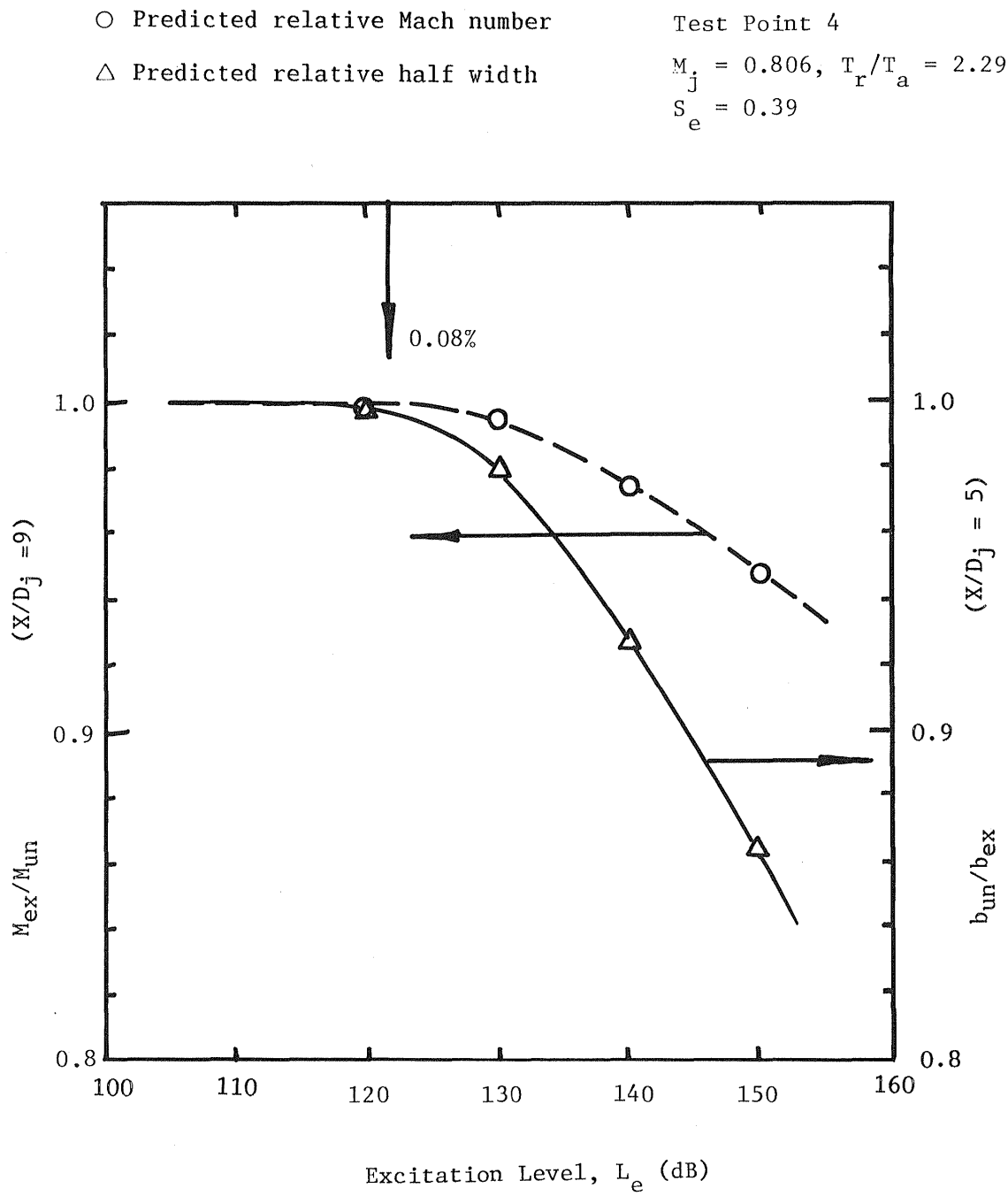

Figure 2.4 Effect of excitation level on centerline Mach number and jet width

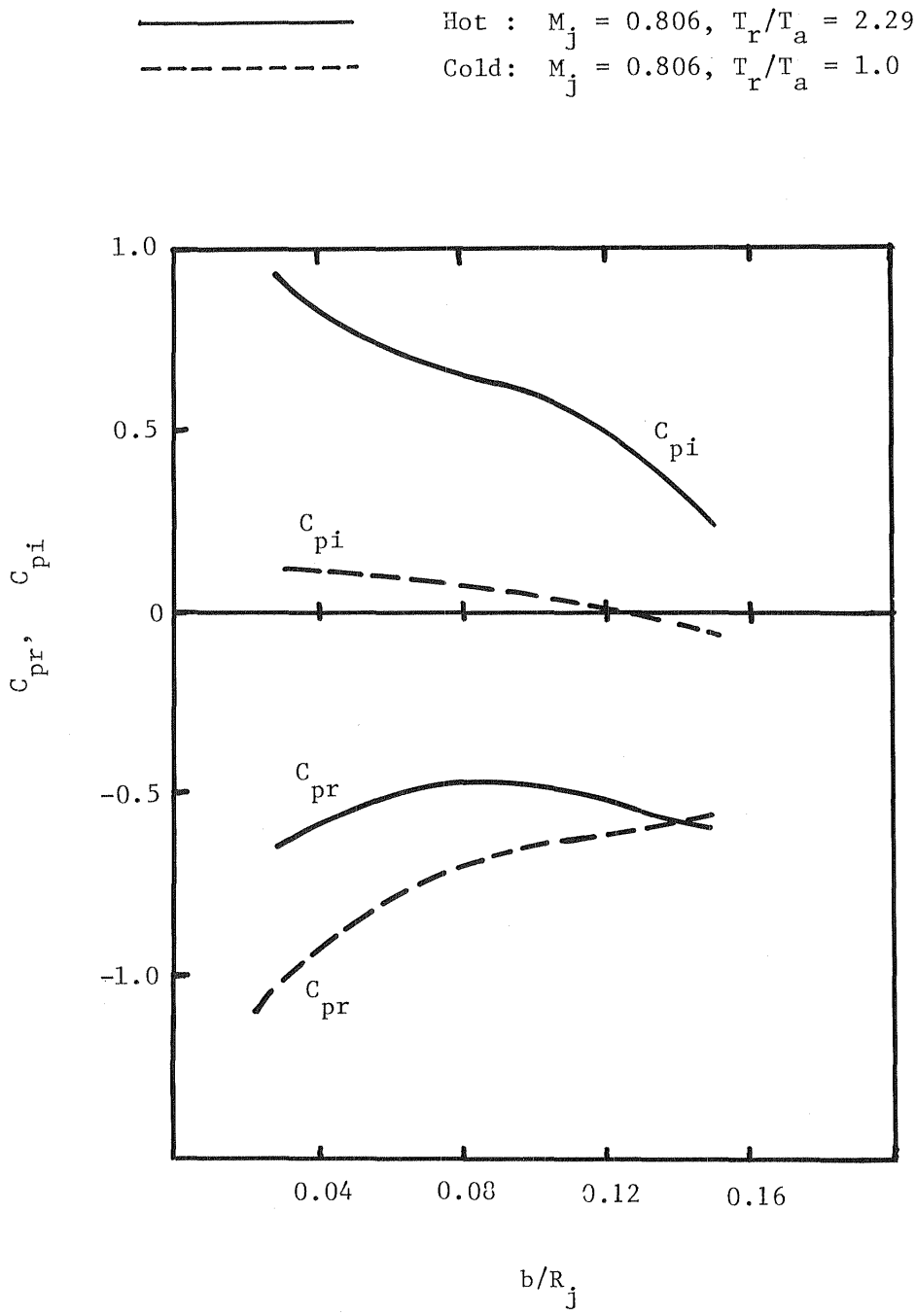

Figure 2.5 Variation of coupling coefficients with jet width for heated and unheated jets

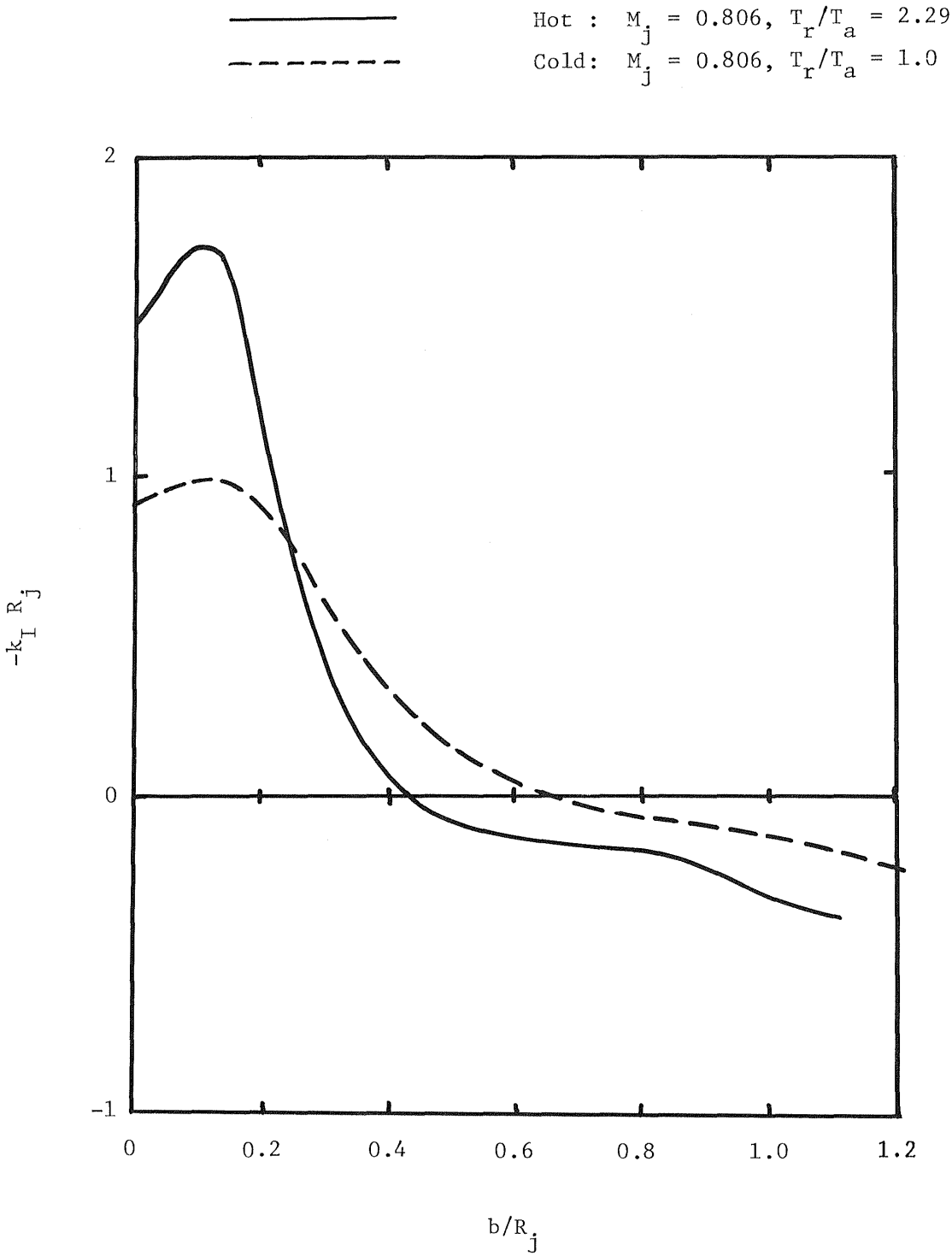

Figure 2.6 Variation of axial growth rate with jet width for heated and unheated jets

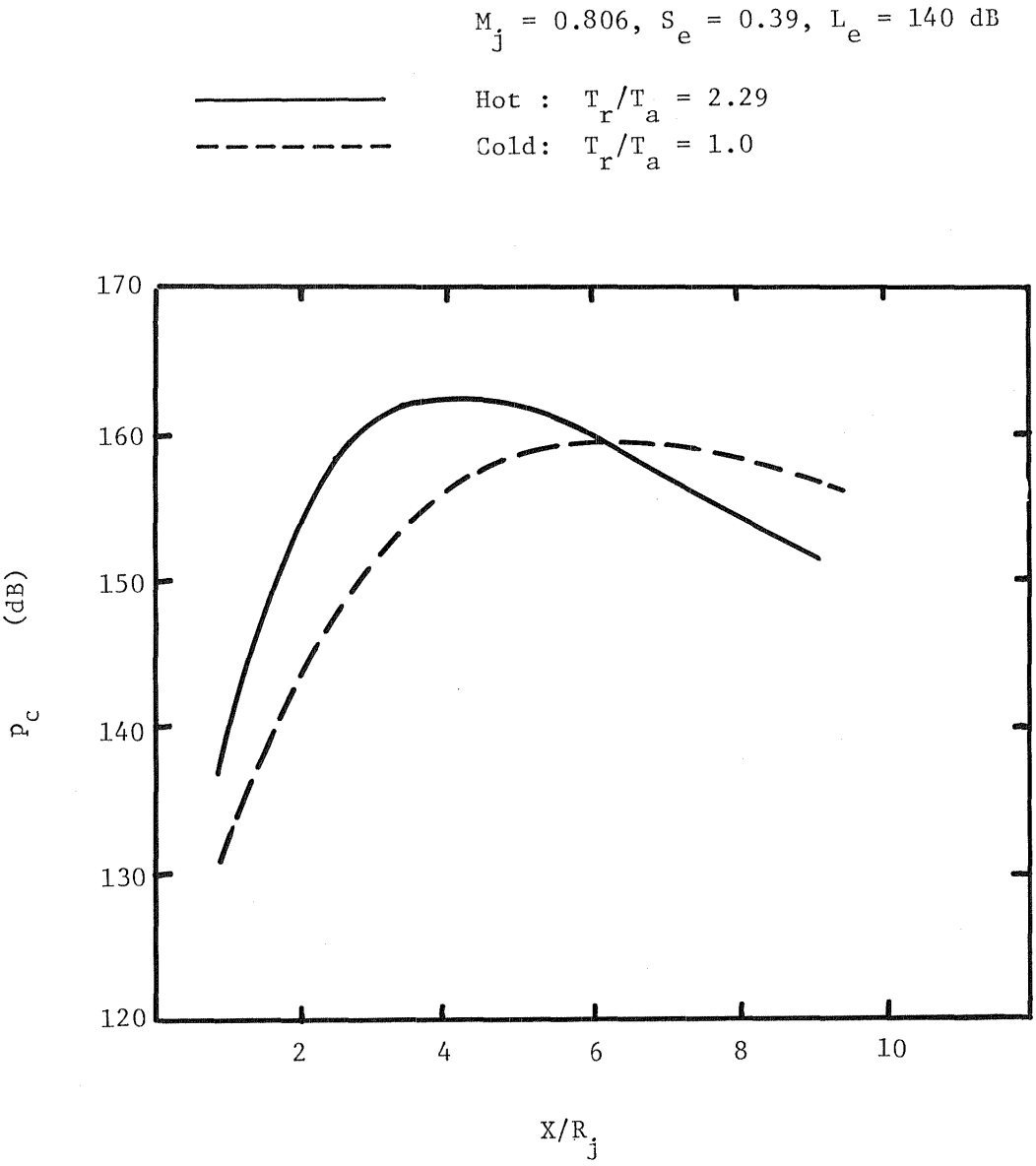

Figure 2.7 Comparison of the predicted centerline pressure levels for heated and unheated jets

amplitude over a larger axial extent. Since the finite amplitude wave only influences the jet development when it is above a particular high level, approximately a local value of 150 dB in this case*, the instability wave for the unheated jet interacts significantly over a wider range. This results in a greater change in the jet properties in the unheated case.

Figures 2.8 and 2.9 show the predicted effect of excitation level on the relative Mach number and the jet thickness for a Mach number of 0.305 with no heating and a stagnation temperature ratio of 2.74 respectively. It can be seen that the 'threshold' level is reasonably predicted. As in the high Mach number case, the relative changes are greater in the unheated case for values of excitation well above the 'threshold' level. However in this case, though measurements of the effect of excitation level were not made, the measurements reported in Reference [2.2] and in Part I show that the heated jet is more responsive to excitation than the unheated jet.

Thus it is clear that the prediction scheme is unable to match the measured data for the case of heated jets. In order to find the reason for this discrepancy, the influence of the initial boundary layer thickness and the effects of jet heating on the development of the unexcited jet have been examined.

2.2.3 The Effect of Initial Boundary Layer Thickness

Careful measurements of the initial boundary layer thickness as a function of jet temperature have been made [2.2]. These indicate that at a fixed exit Mach number, the boundary layer thickness decreases as the stagnation temperature increases.

In the prediction model the mean velocity is assumed to have a Gaussian shape at all points downstream of the jet exit. In fact, there is a transition from a boundary layer profile to this Gaussian form. Thus the choice of an initial thickness of $b/R_J = 0.02$ was based on matching the momentum thicknesses of the boundary layer and by a comparison between the predicted jet development and measurements in the unexcited case [2.1]. Figure 2.10 shows the effect of the initial jet thickness on the peak level of the instability wave on the jet centerline. The location of this peak may vary along the jet centerline. For a range of initial thicknesses up to twice the value used in the present calculations, there is little change in the peak value. There is also very little change in all the other predicted properties of the developing jet. It is only for very thick initial boundary layers that the jet's response to acoustic excitation is reduced.

---

*This level is an estimate based on calculations for a wide range of jet conditions [2.1].

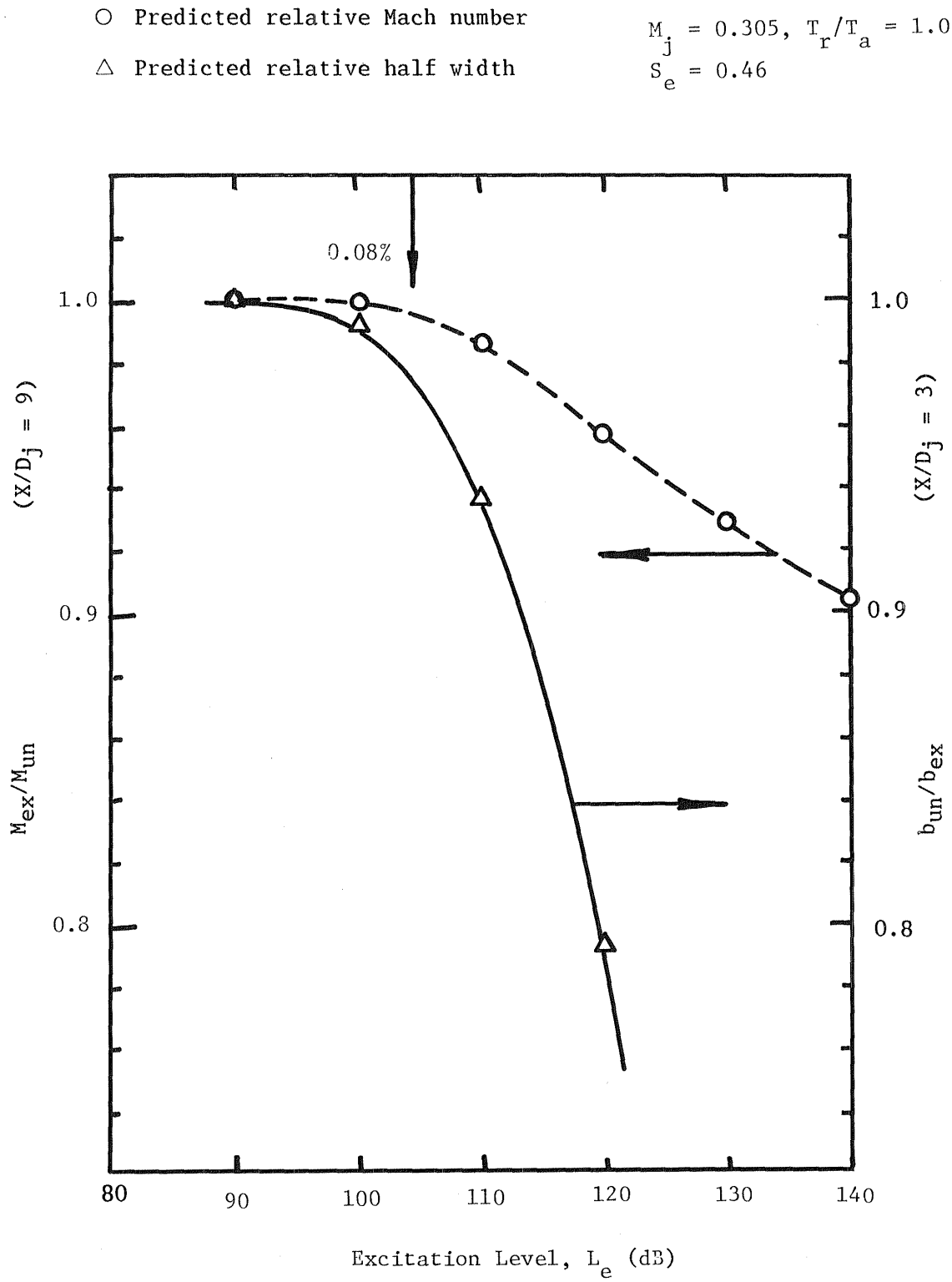

Figure 2.8 Effect of excitation level on the jet centerline Mach number and jet width

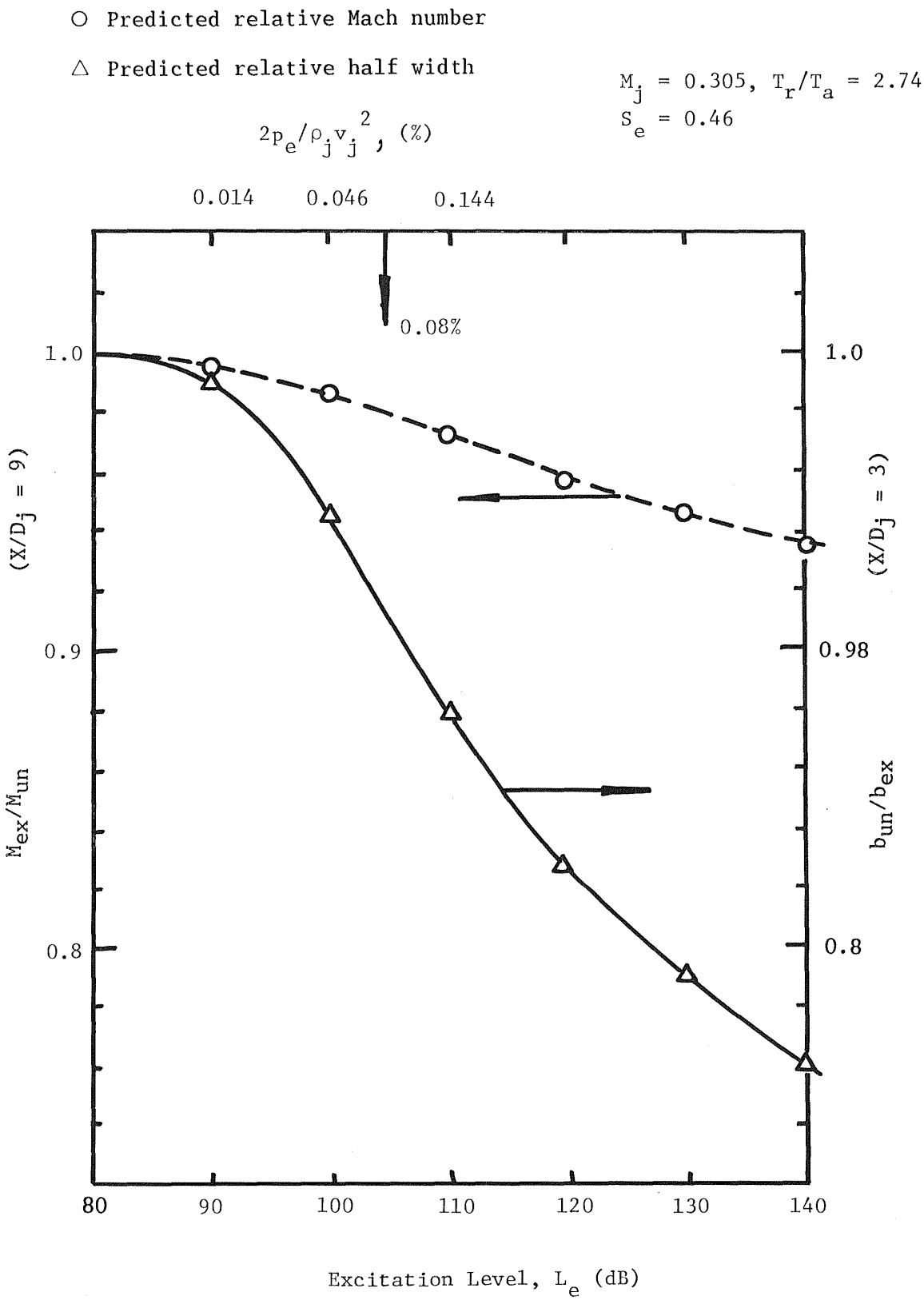

Figure 2.9 Effect of excitation level on the jet centerline Mach number and jet width

$M_j = 0.806$, $T_r/T_a = 2.29$
$S_e = 0.39$, $L_e = 140$ dB

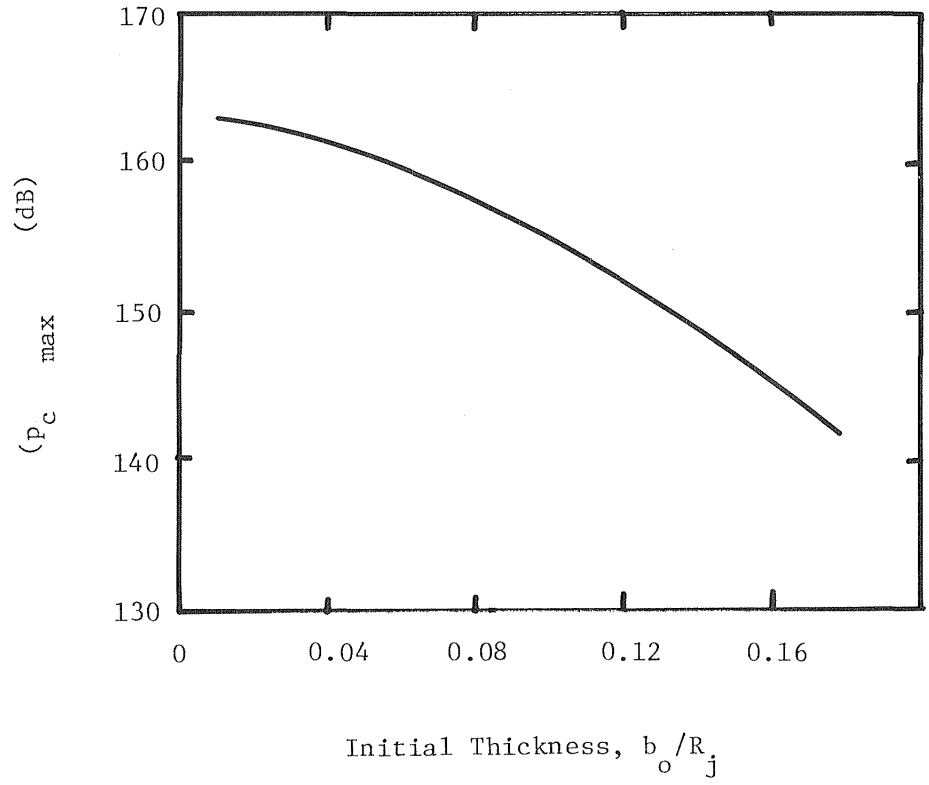

Figure 2.10 Predicted effect of initial thickness of jet mixing layer on peak centerline pressure level

2.2.4 The Development of the Unexcited Jet

It is important to assure that the unexcited jet development is being well predicted, since the spreading rate of the jet, for example, has a significant effect on the development of the instability wave. It is known that both the jet Mach number and the jet temperature alter the rate at which a jet develops. Figures 2.11 and 2.12 show a comparison between the measured and predicted centerline Mach numbers for the unheated and heated jets respectively. The simple nature of the integral scheme is the cause of the discontinuity in the derivative of the centerline Mach number at the end of the potential core. Though the agreement is not perfect, it is clear that the model is able to predict the different rates of development of both heated and unheated jets.

2.3 DISCUSSION OF THE THEORETICAL PREDICTIONS

The reason for the discrepancies between the predicted response of the heated jet and its measured response remains unclear. In view of the success of the model for the unheated case it would seem that the essential physical processes have been correctly modeled. In order to either confirm or invalidate the theory further measurements are required. These are discussed below.

It is essential that the excitation level at the jet exit be known. This is particularly important at the high Mach number condition since the 'threshold' level is so high. The measurement of the excitation level should be as direct as possible. It should be noted that the best agreement between prediction and experiment occurs when the pressure level at the jet exit, and along the jet centerline, has been measured directly. It is probable that the transmission coefficient of the nozzle is influenced by the flow velocity and temperature. This influence should be determined. Without a confident measurement of the excitation level the experimental data may be misleading.

The prediction scheme is based on velocity as a dependent variable and the Mach numbers have been computed using Crocco's relationship. In case this relationship does not hold, particularly in the developed jet and for high temperatures, the experimental data should be converted to velocity data using the corrected total temperature measurements.

The single point measurement of the relative Mach number on the jet centerline at 9 diameters provides a useful means for measuring the

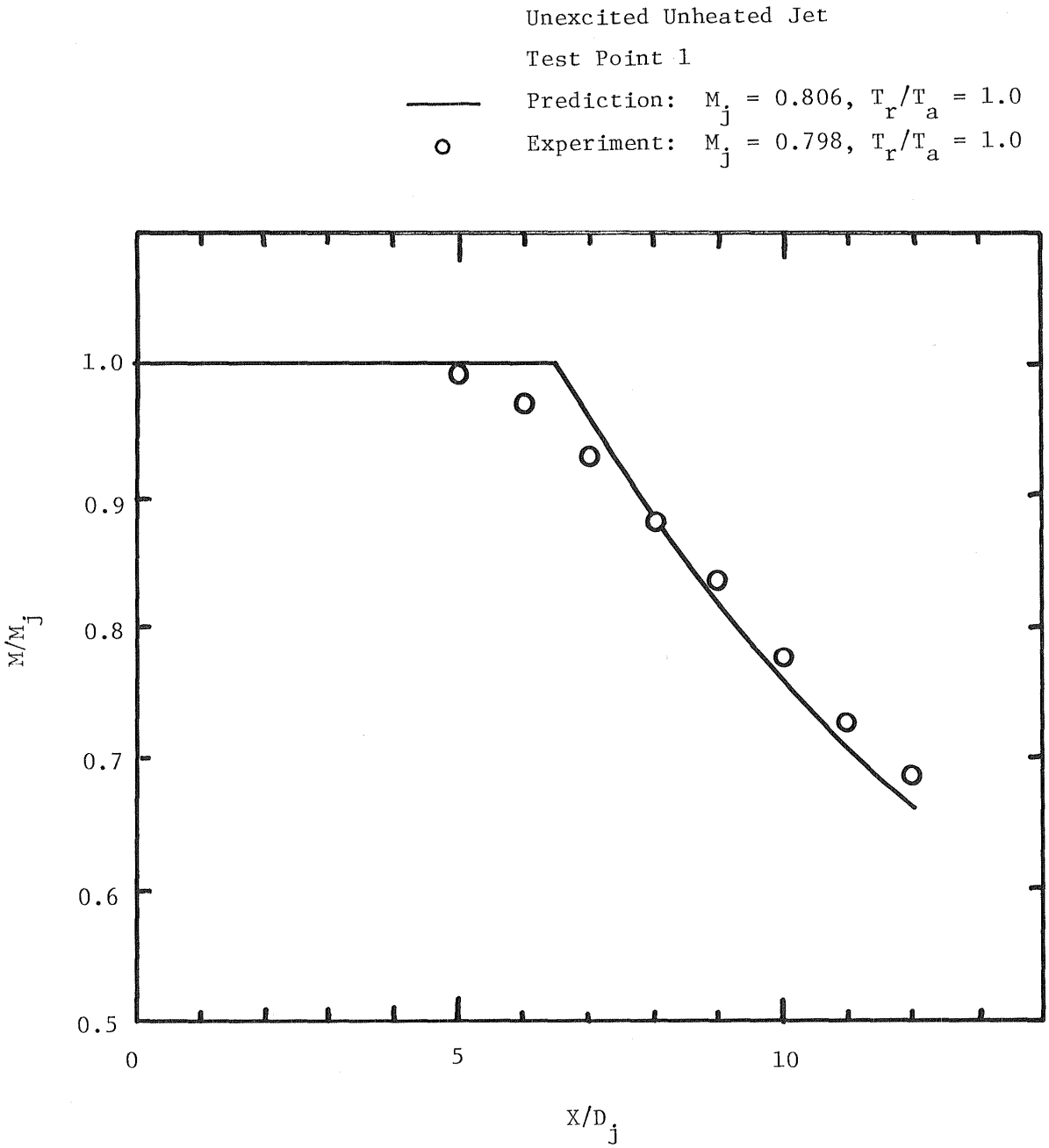

Figure 2.11 Variation of the centerline Mach number with axial distance

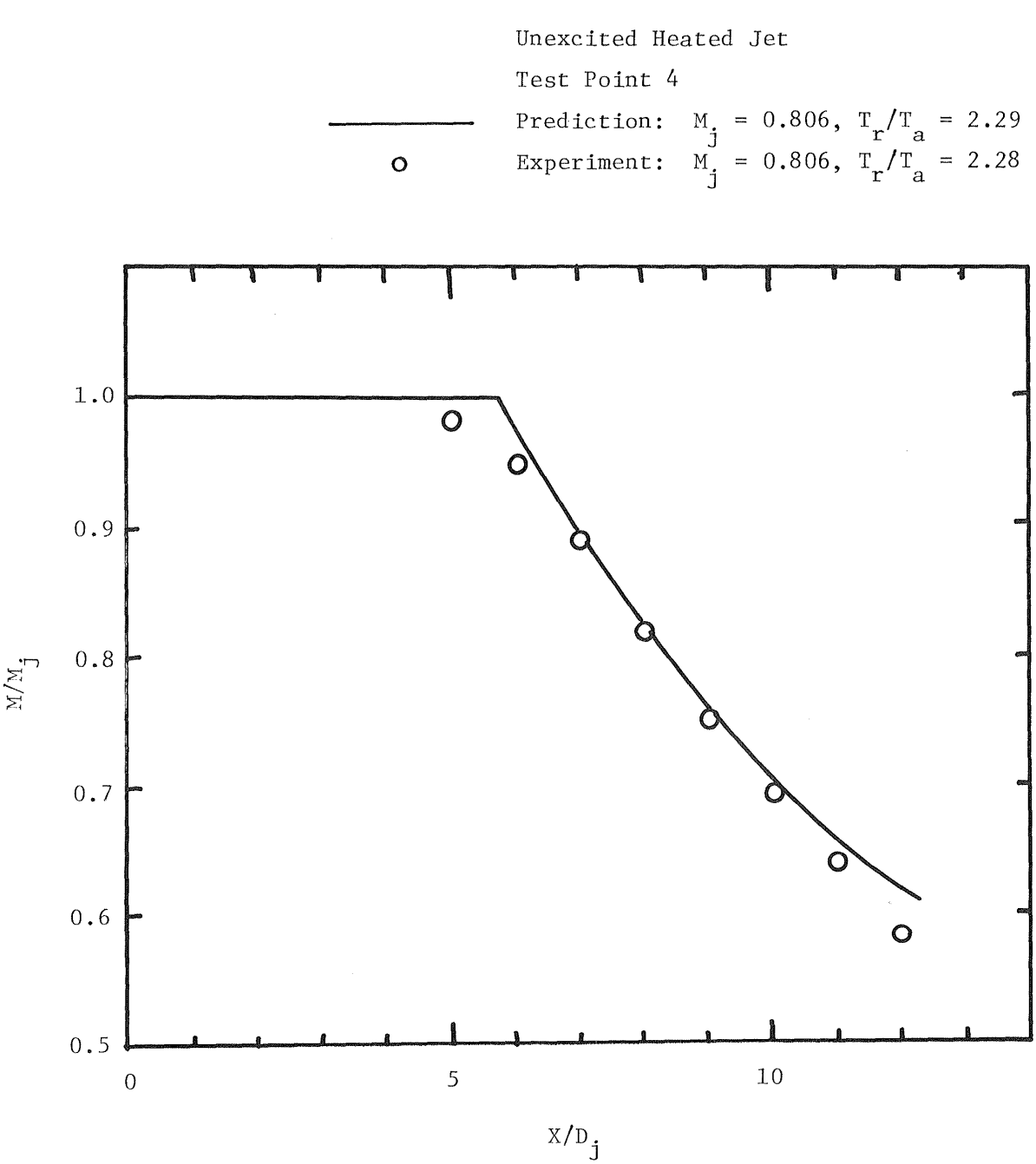

Figure 2.12 Variation of the centerline Mach number with axial distance

response of the jet to excitation. However, it is to be expected that the greatest influence of the jet excitation will be observed closer to the jet exit. Thus it is proposed that radial traverses in the annular mixing region of the jet be performed. These can be used to calculate the relative jet half-width as predicted in subsection 2.2. It is expected that these relative changes will be greater than those for the Mach number further downstream and will provide a more sensitive measure of the jet's receptivity.

Once the excitation level has been accurately determined, the laser velocimeter can be used, in the heated jet, to detect the presence and properties of the excited instability wave. This is most easily accomplished using the phase averaging technique along the jet centerline.

A detailed survey of the mean velocity and turbulence levels will provide data to further confirm that the properties of the unexcited jet are being correctly modeled. They will also enable the predicted changes in the turbulent kinetic energy to be verified. The use of the laser velocimeter will enable a direct measurement to be made of velocity and will verify the previous measurements based on total pressure and temperature probes.

The availability of this data, particularly the careful verification of the actual excitation level, will provide essential data to either confirm or suggest improvements in the present prediction procedure.

It should be noted that at the time these recommendations were made, it was expressed by the NASA technical monitor that it was important to demonstrate that high Mach number heated jets can be controlled by excitation. As discussed in Section 1.0 and in the subsequent section, not all the recommendations given above could be followed through. Instead, attempts were made to increase the excitation levels at the exit by installing an external excitation source, the levels of which could be measured directly around the jet periphery.

3.0 SELF-EXCITATION TESTS

As explained in the previous section, it was conceivable that for the test conditions at which little change was observed in the jet structure as a result of acoustic excitation, the true excitation levels were not high enough. It was, therefore, decided to install a new source of sound so that the opening of the source tubes were located just outside the heated jet. It was expected that by so doing, the effects of flow on sound propagation to the nozzle lip will be minimized, and also it will be possible to measure the true levels of excitation sound by placing a microphone right at or near the jet lip outside the jet flow.

Before embarking upon a detailed design of an external sound source, however, it was important to have some guidelines as to the possible magnitude of excitation that might be adequate.

In this section some unique tests are described that enabled us to design the external excitation source and which also let us derive some categorical conclusions about the excitability of supersonic hot jets.

3.1 MEASUREMENT PHILOSOPHY

It is a well known fact that screech from supersonic shock-containing jets is, in essence, a result of some form of self excitation of the jet by the sound emitted from some distance downstream of the jet [Ref. 3.1 - 3.3]. In fact, if the jet cannot be excited, the screech will not be present. It was decided, therefore, to first determine if the heated jet used in our study showed the evidence of the presence of screech. If present, a measurement of its amplitude near the nozzle lip will indicate an order of magnitude that is needed to excite the hot, high speed jet used here.

While we were acquiring these data, it was thought that some extremely useful results would be obtained if we could come up with a method to modify the level of screech at the nozzle lip with simultaneous measurement of the flow behavior. Based upon some earlier experience at Lockheed [3.4], it was decided to mount a large baffle just upstream of the nozzle lip as shown in Figure 3.1. In a similar study by Ahuja [3.4, 3.5], it was found that by moving the baffle axially, the screech could be modified, and in some cases suppressed completely. It was confirmed by Ahuja that the presence of screech excited a well defined large-scale structure or instability wave in the jet, which completely disappeared on suppressing the screech. A typical result from this study is shown in Figure 3.2 for an unheated jet.

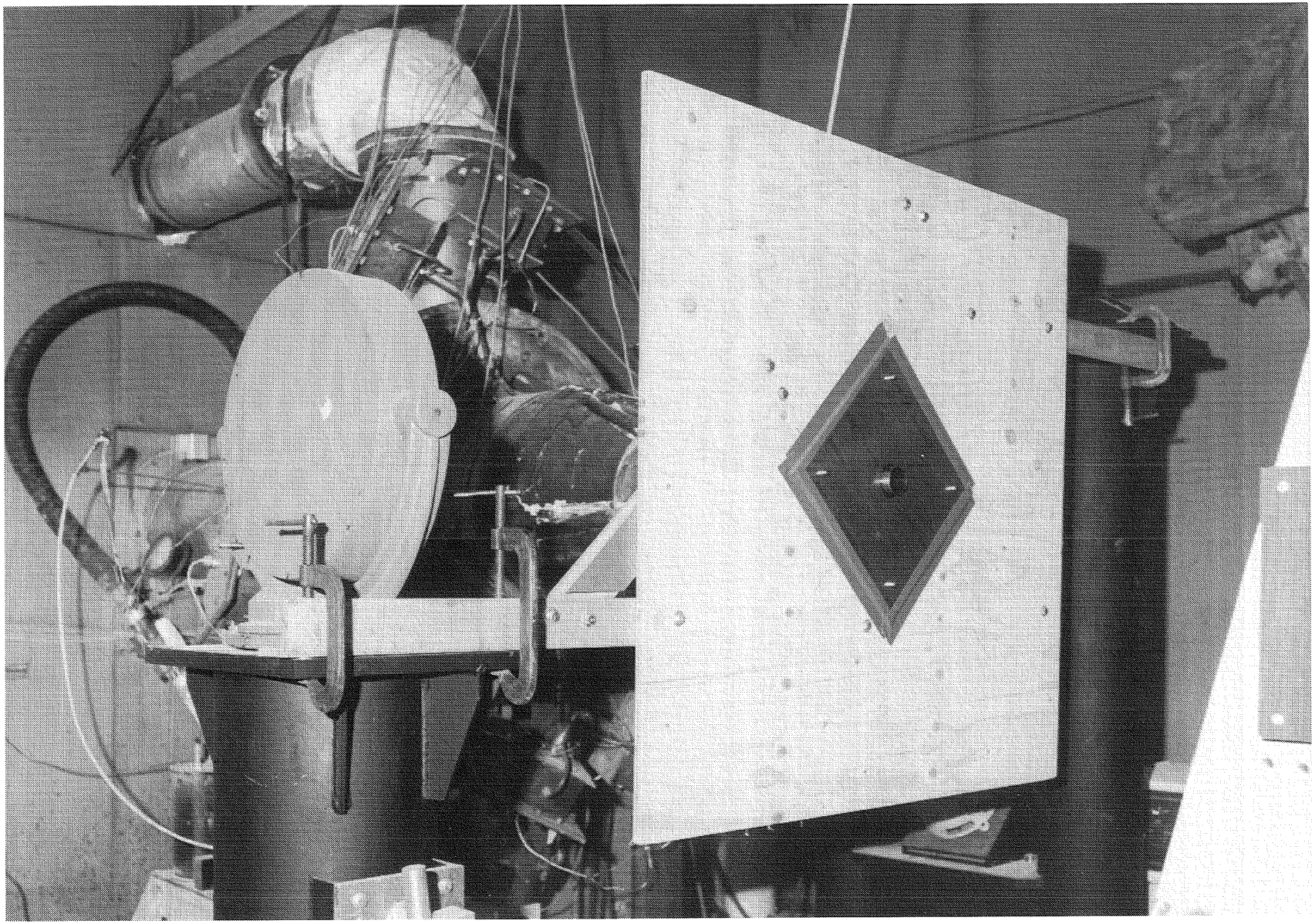

Figure 3.1 Baffle arrangement for the "Self Excitation" tests

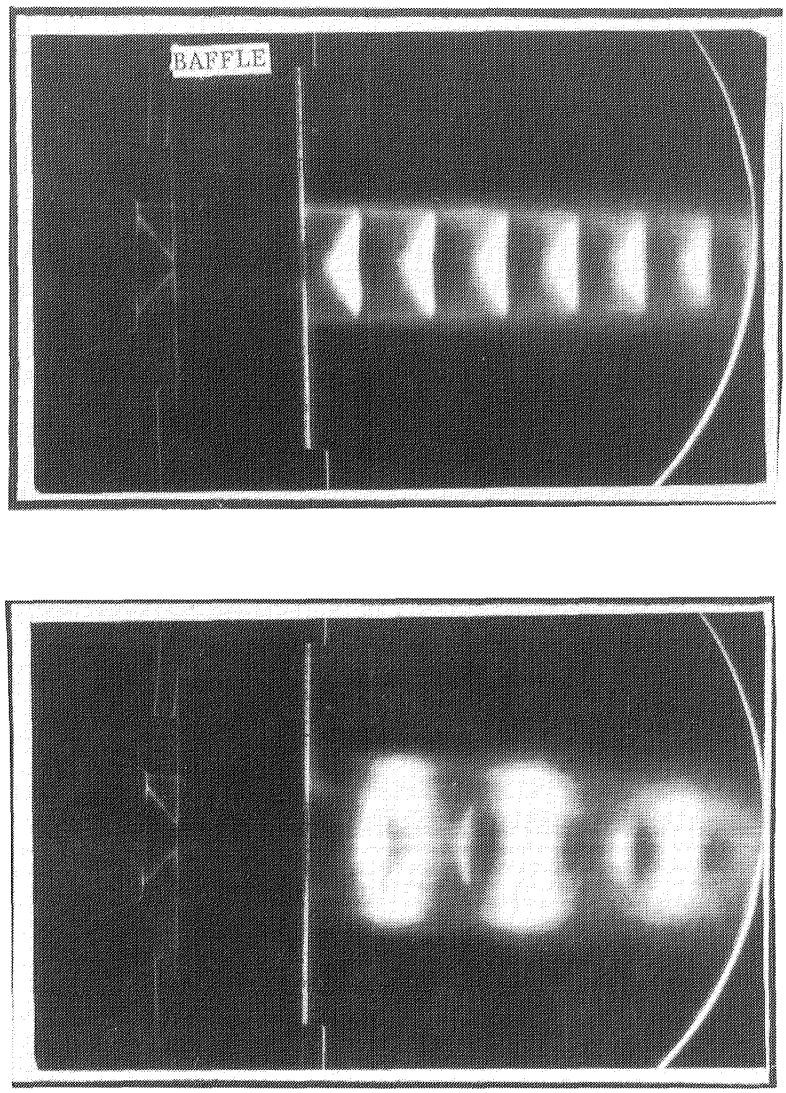

Figure 3.2 Changes produced in the jet flow structure by traversing the baffle by less than 0.16 cm (1/16 in). (PR = 2.197)

In the present tests, the jet was heated to reservoir temperature of 670 K and it was exhausted at a Mach number of 1.12. These are the same conditions at which internal excitation was found to have little effect on the jet flow structure.

3.2 TEST RESULTS

3.2.1. Unbaffled Jet Data

The noise spectra from the heated supersonic jet were monitored at 2.54 cm (1 inch) from the nozzle lip in the plane of the jet exit. As shown in Figure 3.3, a well defined tone was observed, which became noticeable only when the jet became supersonic. This is the tone associated with the screech. The level associated with this screech tone was found to be 137 dB. In our internal excitation studies, this high level could not be achieved at this jet operating condition and could be part of the explanation as to why we were unable to excite the heated supersonic jet.

The mere presence of a screech in the heated jet indicated that the heated jet is excitable and negated the earlier tendencies of concluding, based upon the results obtained from internal excitation, that heated jets may not be excitable.

3.2.2 Baffled Jet Data

Having established the evidence of the presence of screech and its magnitude near the lip, the baffle shown in Figure 3.1 was mounted, and the corresponding noise spectra measured by the microphone mounted near the nozzle lip. This time, the baffle was also traversed by small distances upstream of the nozzle lip. The corresponding spectra are shown in Figure 3.4. Clearly the screech magnitudes changed drastically, as a function of the baffle location. (This is because of the change in the feedback path length [see Reference 3.4]).

For those baffle locations for which the screech noise levels were different, the jet total pressure distribution along the centerline was measured with a pitot probe. It was indeed found, that the higher the screech level, the larger was the jet Mach-number decay rate. Typical results are shown in Figure 3.5. Although no measurements were made to establish the effects of the presence of the baffle on entrainment, it is expected, based upon available evidence [3.6], that the baffle will have little effect on the velocity profiles.

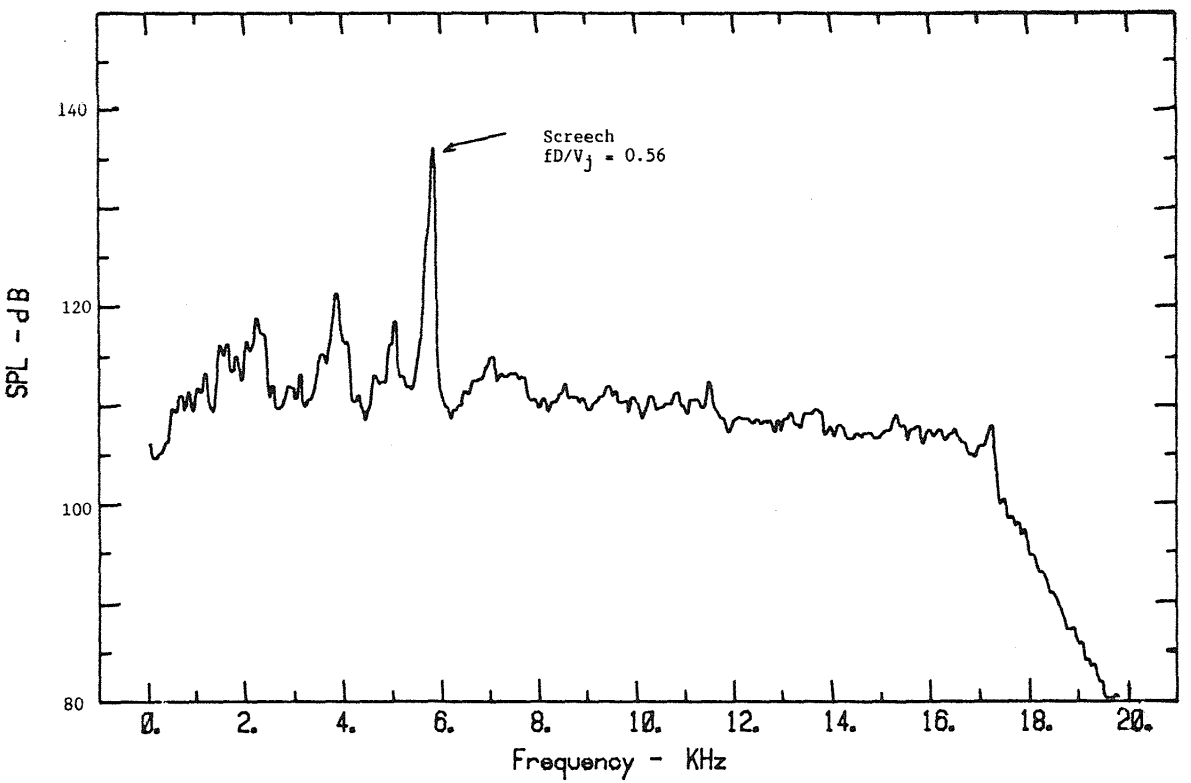

Figure 3.3 Near field jet noise sepectrum of the bare jet (M_j = 1.12, T_t = 670 K, R = 2.54cm, θ^* = 90°)

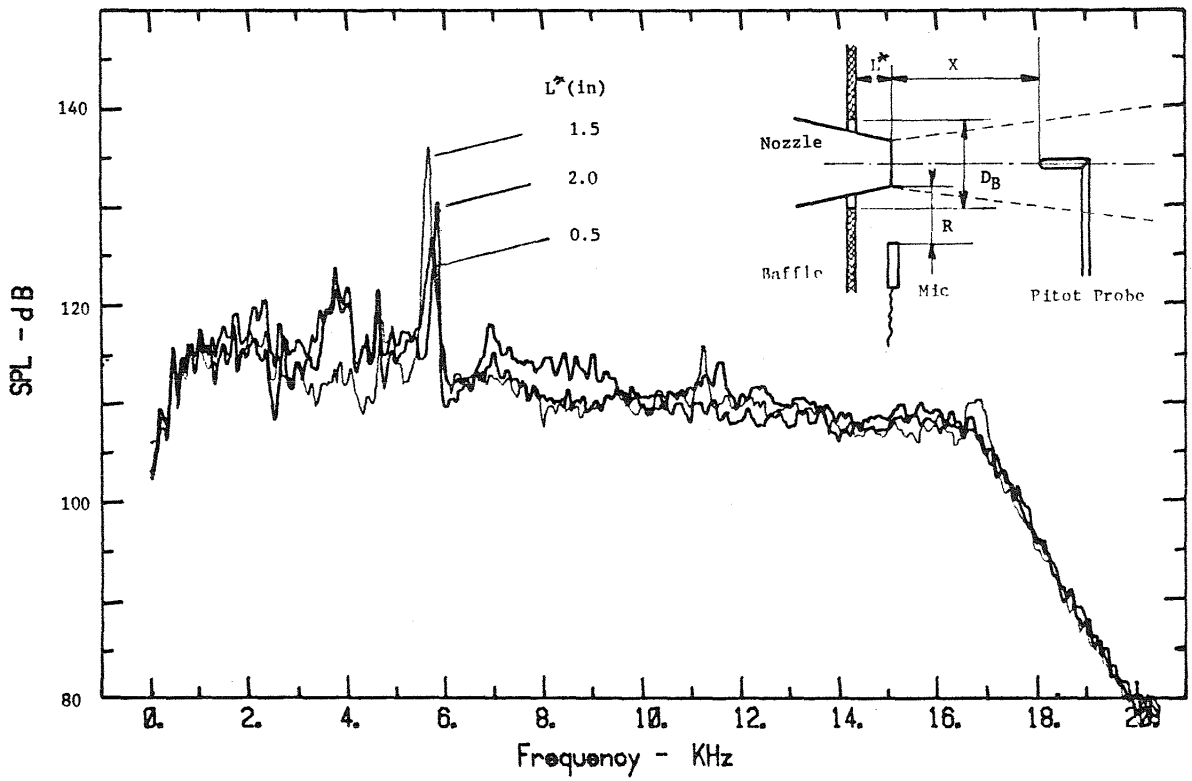

Figure 3.4 Near field jet noise spectra with the baffle located at different position.
(M_j = 1.12, T_t = 670K, R = 2.54cm, θ^* = 90°)

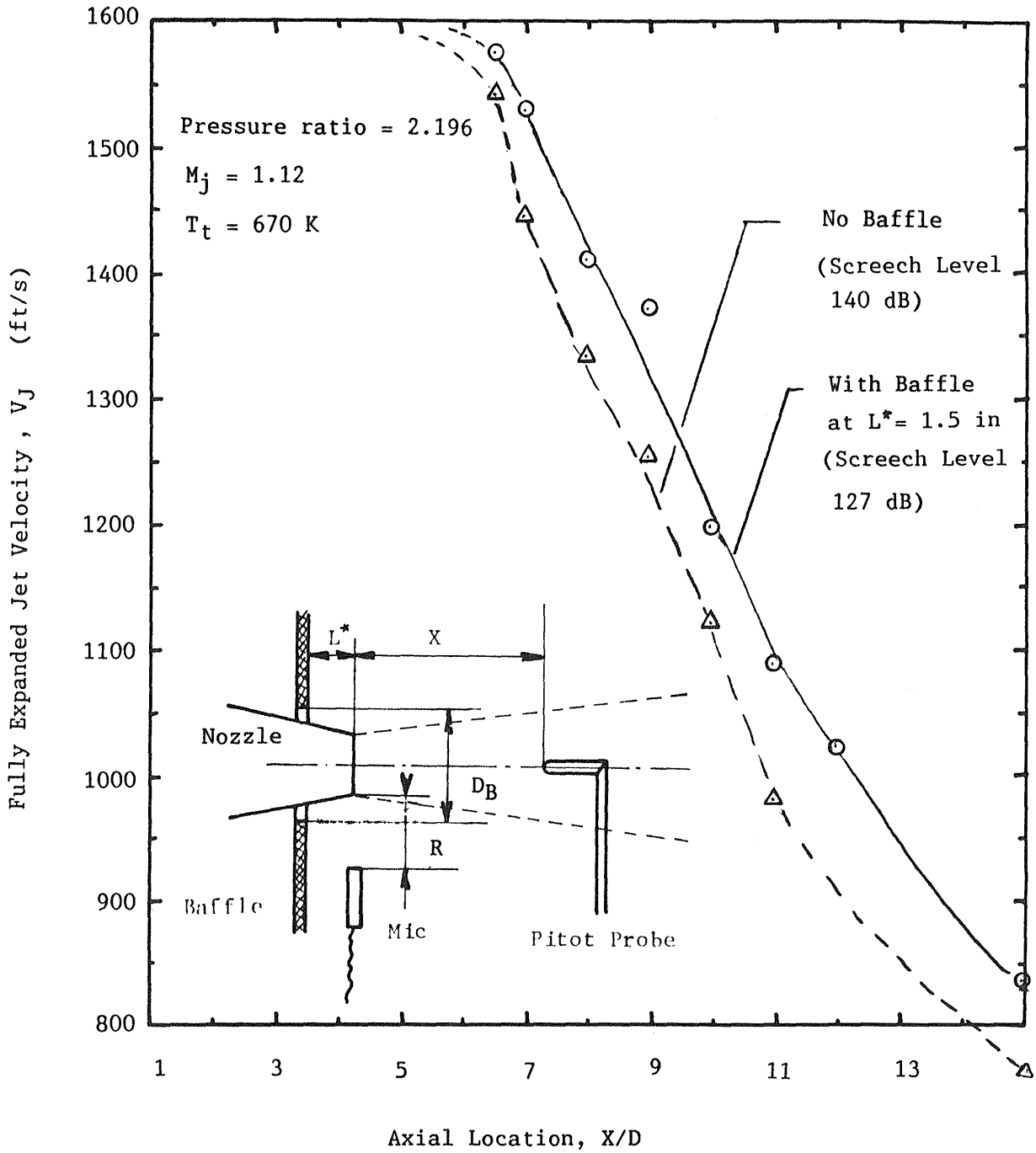

Figure 3.5 Effect of suppressing screech noise on centerline mean velocity decay
(D = 5.08 cm, D_{BAFF} = 8.7 cm)

3.2.3 Conclusions for the Self-Excitation Tests

The results presented here are rather important in that they point out that a heated supersonic jet is excitable so long as the excitation levels are high enough. They also provided us an impetus to go ahead and design and fabricate the external excitation source.

4.0 EXTERNAL EXCITATION OF HEATED JETS

4.1 GENERAL REMARKS

It was shown in Part 1 of this report that high-speed, highly heated jets do not appear to respond to internal upstream acoustic excitation as strongly as the low speed heated and unheated jets. One of the possible reasons for this behavior was attributed to the fact that the actual excitation levels at the nozzle exit plane might not have been sufficiently high to produce the desired response in the high-speed, high temperature jets. In addition, the excitation levels at the nozzle exit plane were not measured directly for the heated jets, but were deduced from the cold jet measurements assuming no effect of the flow temperature on the efficiency of the acoustic excitation source section and the supply duct.

To improve the efficiency of the excitation source and overcome the above mentioned uncertainty, it was decided to design and fabricate a new source section which would excite the flow externally. The new external excitation source is described in the next subsection. The adopted method of excitation level measurement is presented in Subsection 4.3.

4.2 TEST FACILITY AND THE EXTERNAL EXCITATION SOURCE

A detailed description of the Lockheed's jet flow facility and associated instrumentation is given in Part 1 of this report. Here, a description of the external excitation source only is presented.

Before the new external excitation source section was designed, three separate source configurations, shown in Figure 4.1, were checked out for their acoustic performance. Configuration #1 consisted of a 3.5 cm diameter tube connected directly to the 3.5 cm opening of an Altec driver body, whereas in configuration #2 a converging duct with an inlet of 10 cm diameter and a source opening of 3.15 cm diameter was used. Thus in configuration #2, the sound from the Altec driver opening (dia = 3.5 cm) escaped into a larger space before converging back into a smaller opening. As shown below, this arrangement radiated up to 20 dB less noise through the final source opening.

To determine if noise amplitude could be increased considerably by decreasing the size of the source opening, configuration #3 was tested. In this configuration, an inverse conical horn was used such that the duct

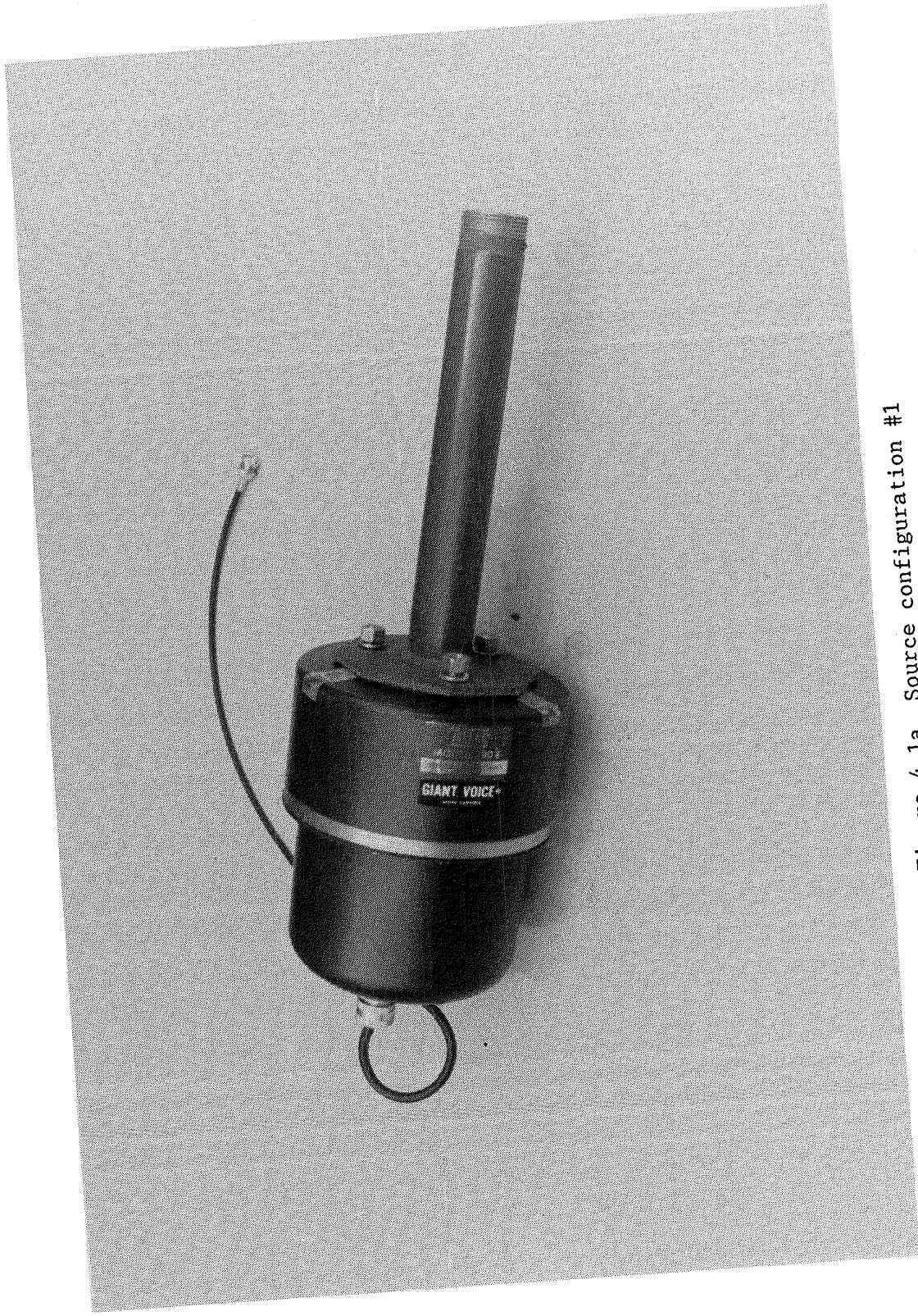

Figure 4.1a Source configuration #1

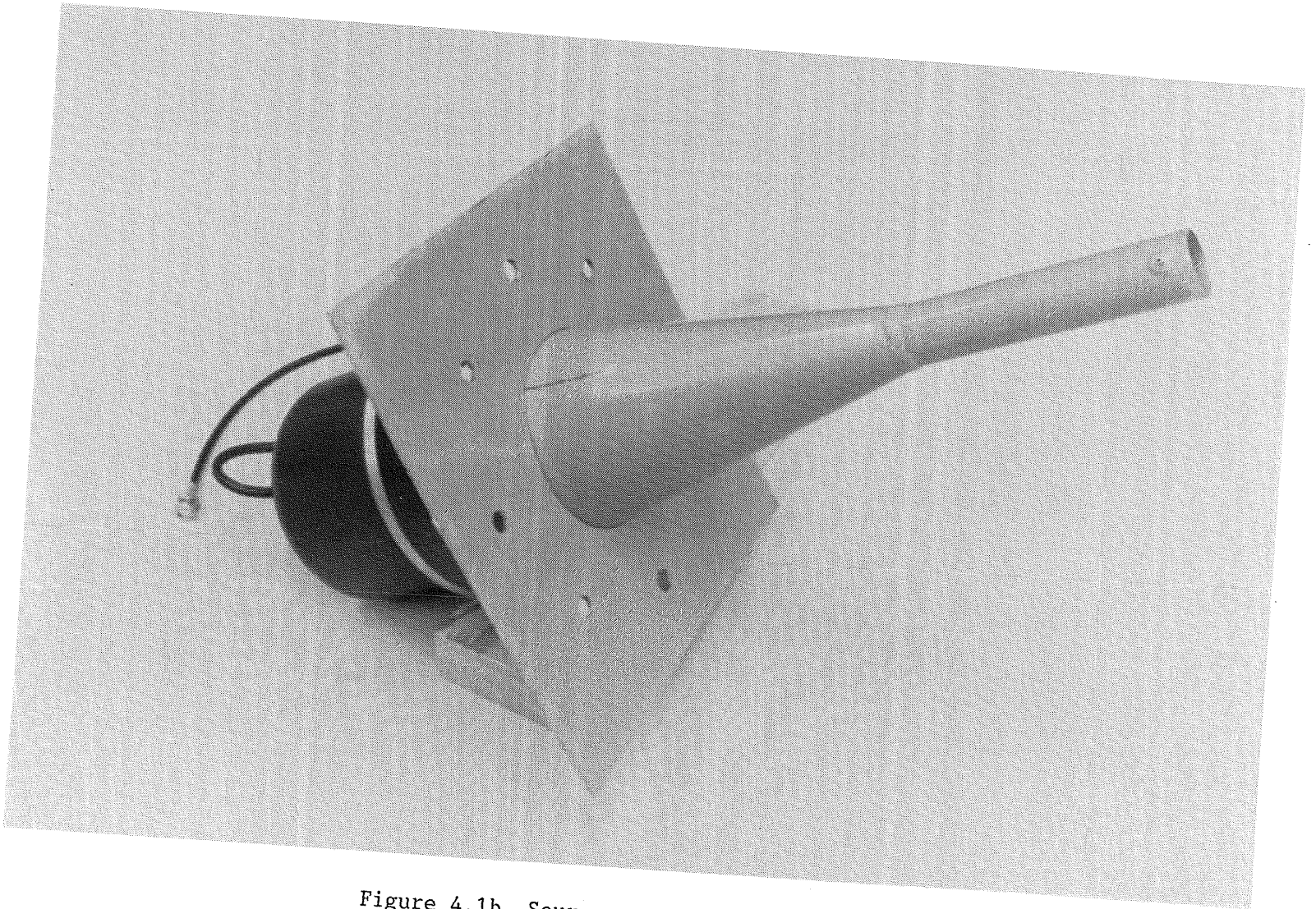

Figure 4.1b Source configuration #2

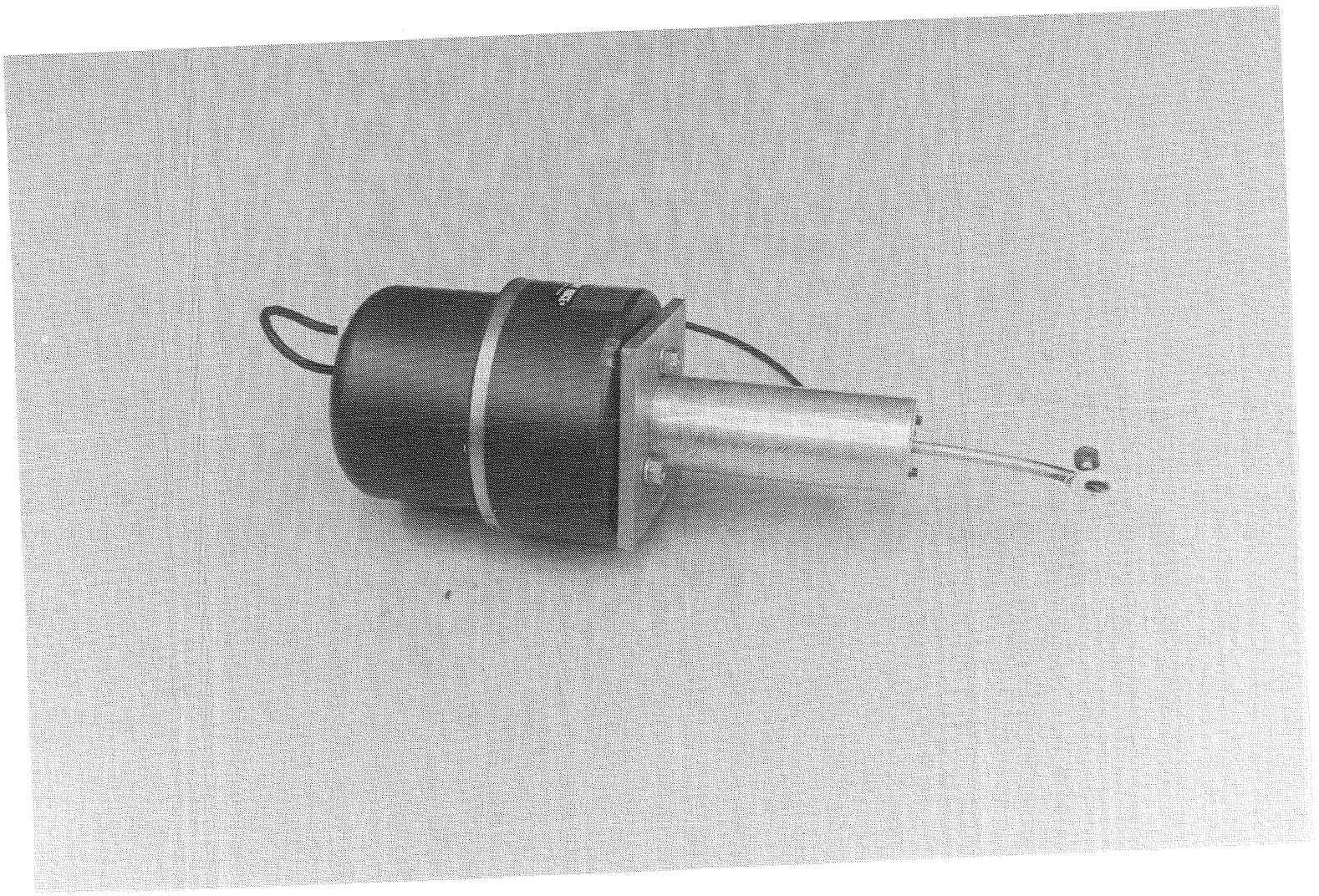

Figure 4.1c Source configuration #3

carrying the sound decreased in size from 3.5 cm to approximately 0.64cm. As shown in Figure 4.2, the performance of configuration #3 was comparable to that of configuration #2, but configuration #1 was far superior. (These measurements were made at about 1.2 cm from the exit along its centerline.) It was decided therefore to use configuration #1 for the designed external excitation source section.

A sketch of the new external excitation source section for Jet Flow Facility is shown in Figure 4.3. It consists of a steel sleeve clamp 1 which slips over the 10 cm air supply duct just upstream of the nozzle. Two sets of 8 tubes, 2 and 4, are welded on this tube in the fashion of the spokes of a wheel at 45^{o} intervals. These form the supports and guides for the driver assemblies 3, 5, and 6 which are connected by lugs, 9 and 10, to the fork end of rods 8 and 11, which can move in the tubes 2 and 11 and be secured with set screws. In this way the source tubes which are fitted inside the source tube sleeves 3 and secured with set screws, may be moved relative to the jet. In the sketch, the driver assembly is shown at an angle of 30^{o} to the jet axis with the 1.38 diameter source tube at its closest proximity to the jet shear layer (it could be placed closer if the exit of the source tube were smaller or made elliptical). The driver assemblies may be moved vertically to change the distance of the source tube exit from the jet and, in addition, may be pivoted about the bolt in the left hand lug 8 to change the angle. The slots in the lug 10 allow this rotation. Finally, the driver tube 5 may be moved in the sleeve 3 to allow tuning of resonant frequencies of the driver tube. Photographs of partially assembled source section are shown in Figure 4.4.

The assembled external excitation source section, mounted on the supply duct of the jet facility, is shown in photographs in Figure 4.5.

4.3 PROCEDURE TO MEASURE EXCITATION LEVELS

A constant, sufficiently high level of excitation was desired throughout the required Strouhal number range. Driver limitations however, forced the compromise on a nominal level of 147 dB, measured at the center of the nozzle exit, which was attainable over all but the upper end of the frequency range. The natural frequencies of the system, i.e., where local peaks in level occur, were chosen for the test points. At each of these frequencies, the voltage input to the power amplifiers was adjusted to produce a jet-exit centerline excitation level of 147 dB in the absence of flow. The corresponding input level was recorded and subsequently used to reproduce that condition with flow. Table 4.1 shows the test point frequencies and levels for the heated jet runs. Some details of the adjustments made to obtain the same level and phase output from each of the

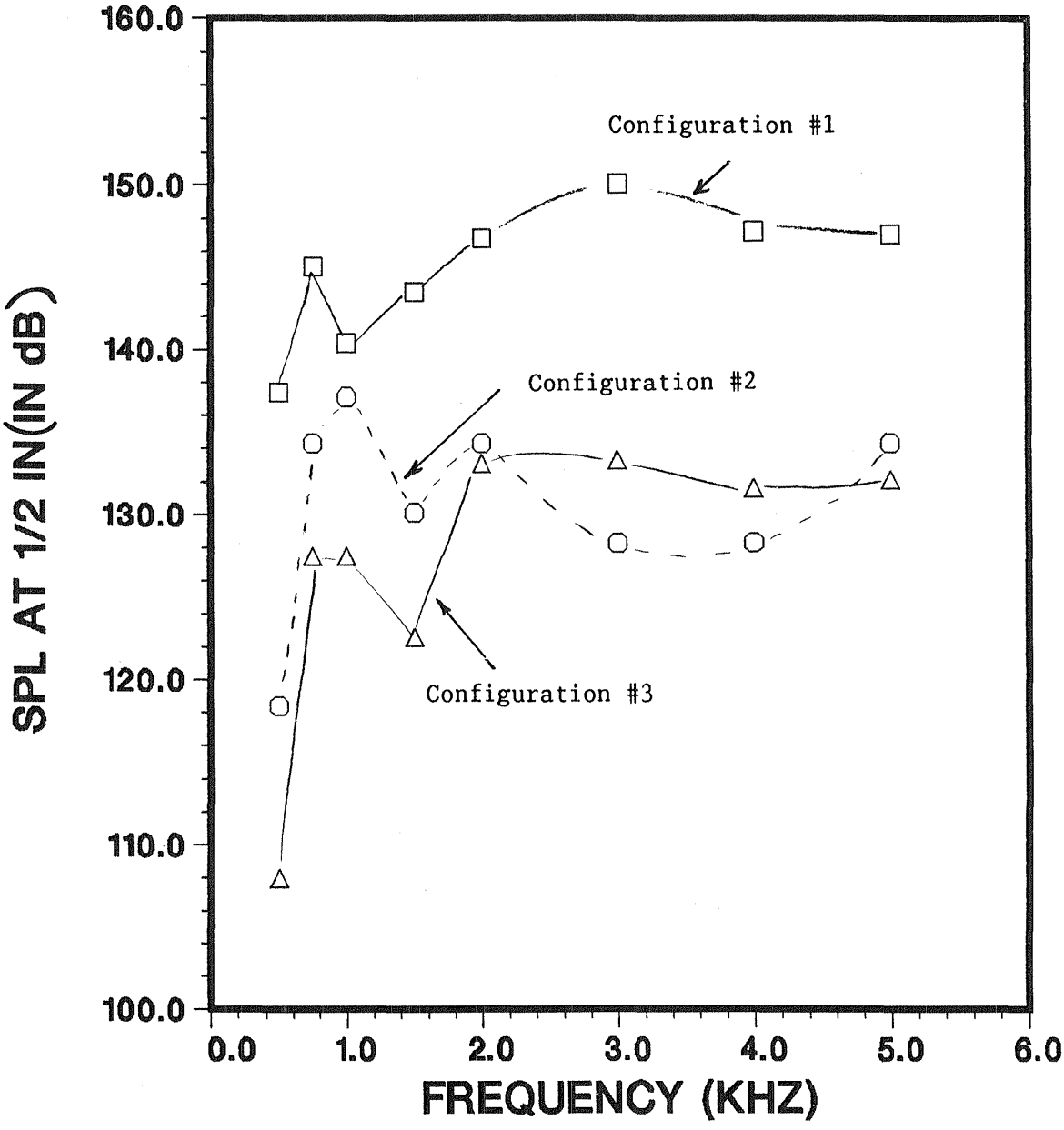

Figure 4.2 Sound pressure levels measured at 1/2 inch from the exits of the three source openings

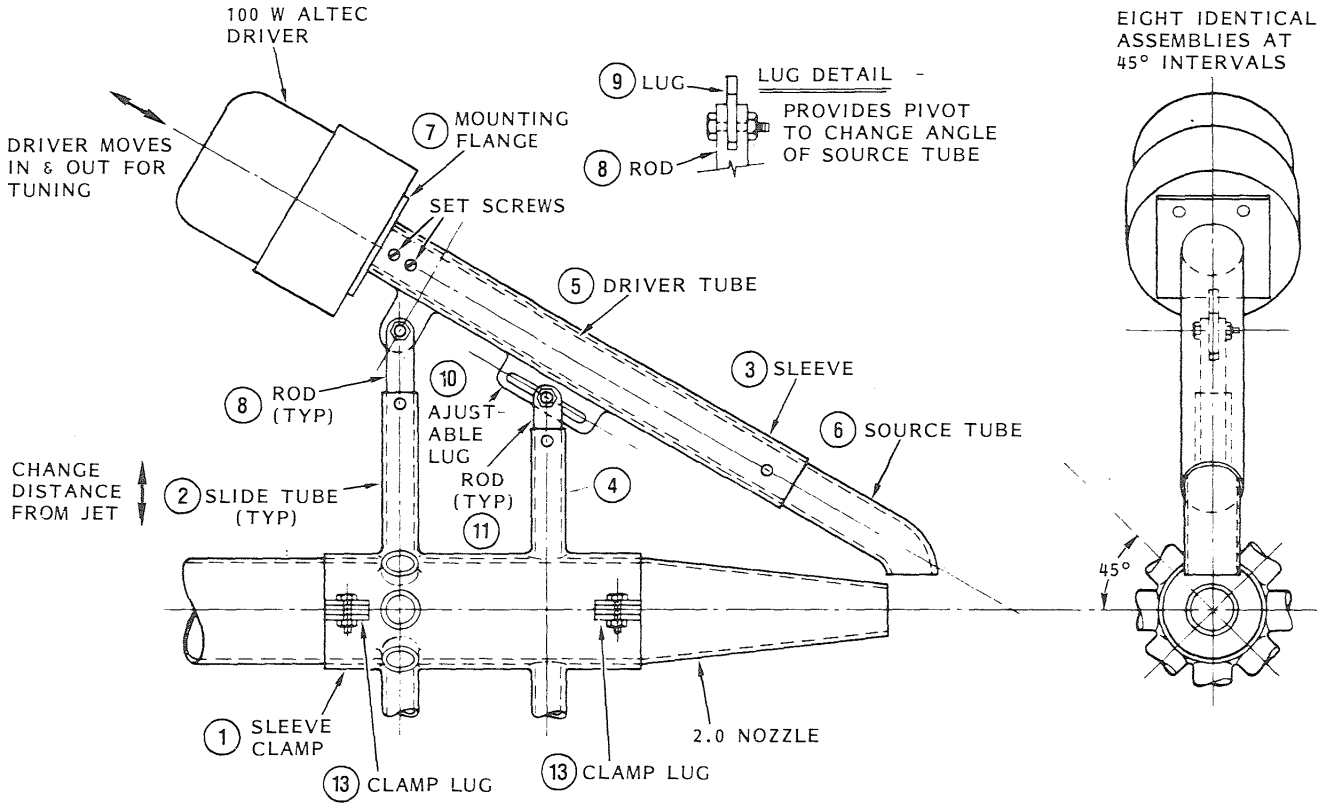

Figure 4.3 External source section

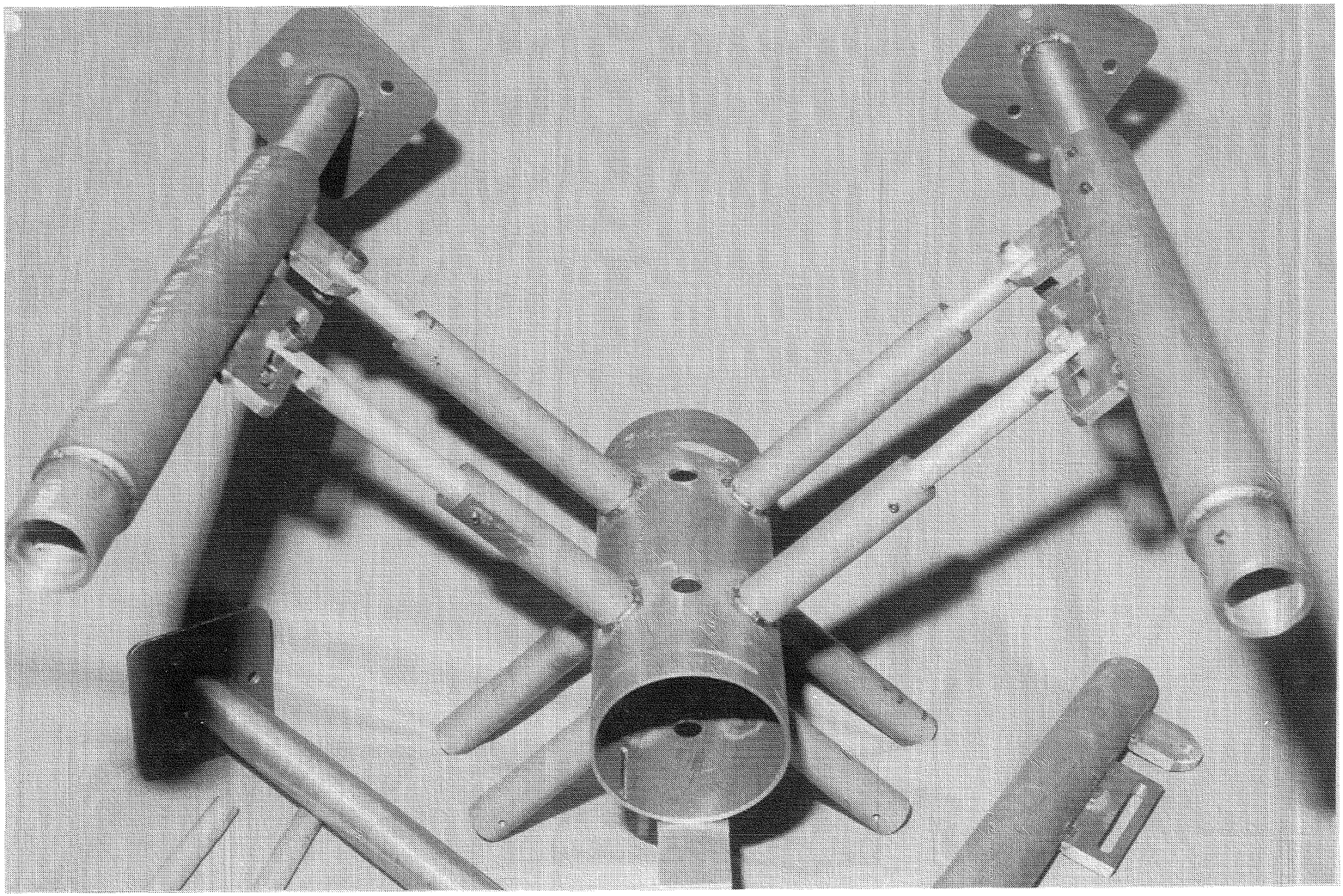

Figure 4.4a Front view of partially assembled source section

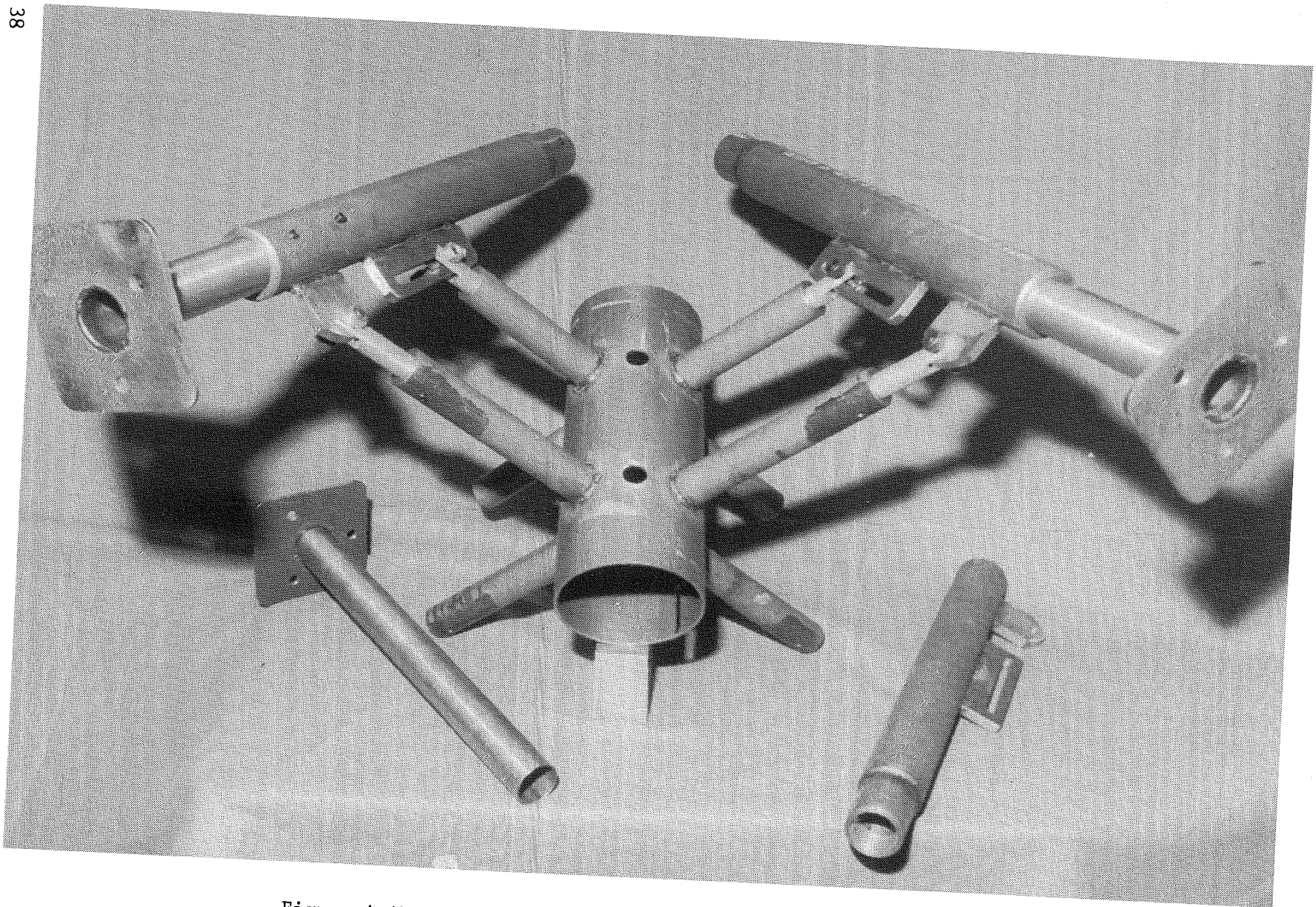

Figure 4.4b Rear view of partially assembled source section

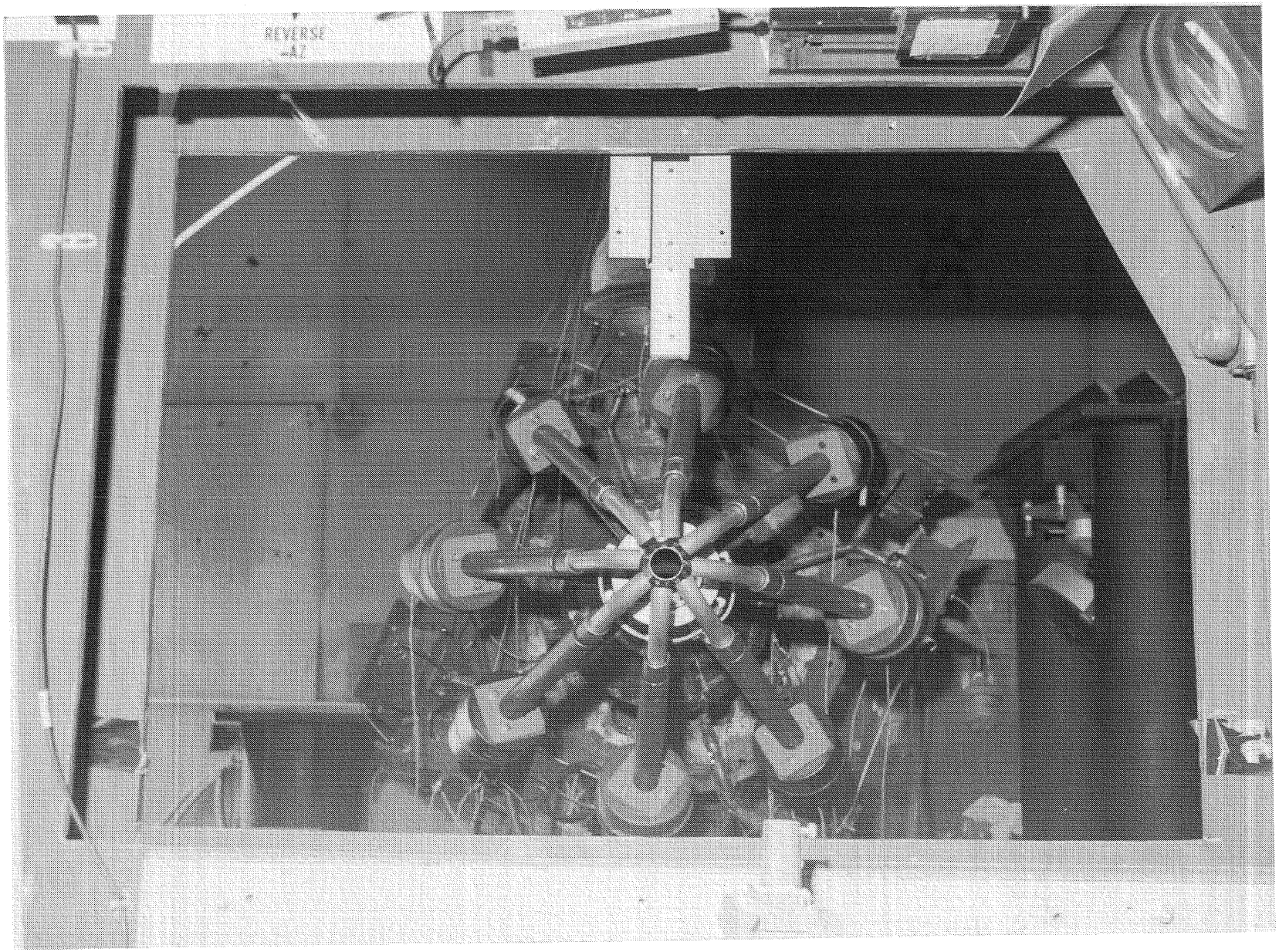

Figure 4.5a Source section - front view

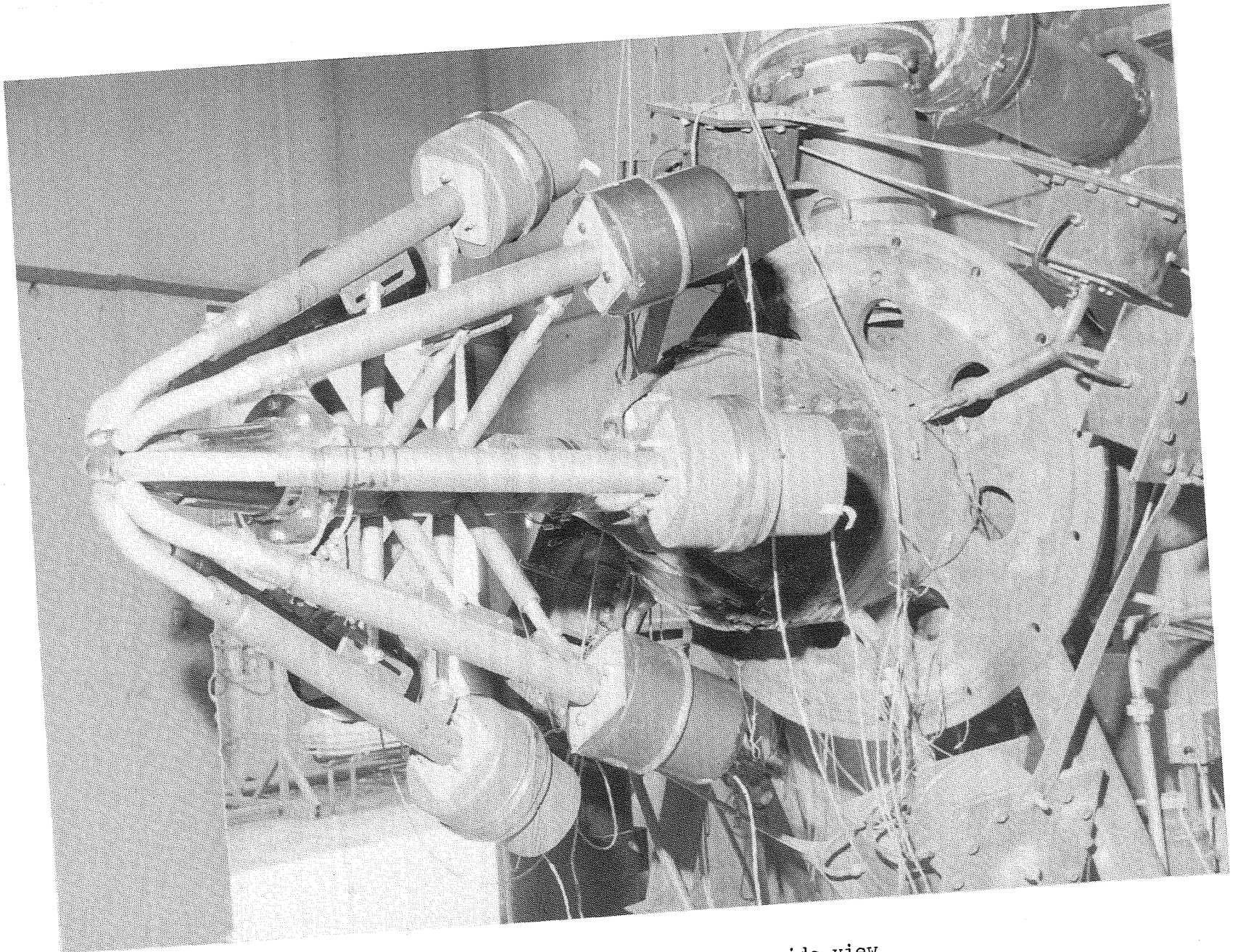

Figure 4.5b Source section - side view

PEAK FREQUENCY Hertz	EXCITATION VOLTAGE Vrms	EXCITATION LEVEL dB
1504	1.14	146.8
1894	1.065	146.8
2310	0.092	146.8
2502	1.18	146.8
2817	1.125	146.8
3009	0.94	146.8
3015	0.98	146.8
3200	1.18	146.8
3499	1.18	146.8
3702	0.99	146.8
3880	1.16	146.8
4136	1.245	143.9
4412	1.24	144.6
4700	1.29	139.6
4999	1.25	137.9
5415	1.33	141.0
5606	1.30	140.0
5994	1.33	135.1

Table 4.1 Typical excitation frequencies and levels.

acoustic drivers are discussed below.

Driver Tube Adjustment

The driver tubes shown in Figure 4.3 have a sliding section that can be used to tune the system and to compensate for differences in driver diaphragm position, cut length of the tube, or tube end position. Initial adjustment was made to peak the output of each tube, one at a time, as measured at the centerline of the jet nozzle and at a single representative frequency and driver input level. This provided the maximum output that could be achieved by length adjustment. Care was taken to assure that each path was the same in terms of effective wavelengths. That was necessary so that at other frequencies the same relative phase would exist among all the tubes.

The tubes were adjusted by watching the waveform from the jet-axis microphone as the tube lengths were varied about the minimum common length that produced a peak level. The peak was identified visually, and the tube was locked into place at that length.

Level Setting

After the initial length setting, the power amplifiers, which share a common input signal, were adjusted one at a time to obtain a common signal level at the centerline microphone. At this point, the drivers should all be producing essentially the same signal so that optimum power is delivered to the jet region.

Phase Adjustment

A final phase adjustment was made by examining the phase between the input signal to the amplifiers and the signal at the centerline microphone, again taken one driver at a time. Slight adjustments in tube length brought the phases to within a few degrees of each other at a frequency of about 4 kHz. This was considered adequate since the maximum frequency, hence the shortest wavelength and greatest phase deviation possibility, would be about 6 kHz.

Excitation Levels

The excitation levels quoted throughout this report are those measured at the nozzle axis at X/D = 0.125 at the focus of the driver tubes with no nozzle flow. The measurements were made directly in the no-flow case. The centerline level was measured using a microphone on the nozzle axis, and the amplifier setting was recorded for that level. This amplifier setting was then used to produce that same excitation level for both no-flow and flow cases.

Circumferential Measurements

After all the adjustments were made, one final check was made to verify the uniformity of the excitation level around the jet. For this check, all the drivers were operated simultaneously and at the same input level. Measurements were made along the lip line and in line with each driver tube exit. The uniformity of the excitation levels outside the nozzle lipline for the frequency that most excited the jet is shown in Figure 4.6. The measurements here correspond closely to the center of the driver tubes and to the spaces between adjacent tubes. The uniformity is seen to be quite good; the spread in level is $\pm$ 2 dB, and the maximum phase difference is 13.5 degrees. The average of the circumferential levels is 148.7 dB, while the centerline level is 149.9 $\pm$ 0.5 dB.

Measurements made outside the shear layer show higher levels with flow than without. The level with unheated flow was 2 dB $\pm$ 1 dB higher, and the level with heated flow was 1.5 dB $\pm$ 1 dB higher.

4.4 RESULTS

The major objective of this part of the study was to verify the excitability of highly heated, high speed jets using the external excitation source section. Thus, the experimental effort was focused on the following two jet operating conditions.

Test Condition	Mach Number	Total Temperature
1	0.8	290 K
2	0.8	670 K

At these jet operating conditions, experiments were carried out to determine the excitation Strouhal number that produces the strongest effects on the jet plume. As for the internal excitation, presented in Part 1, the Strouhal number optimization was based on changes of local Mach number on the jet centerline at nine nozzle exit diameters downstream of the nozzle exit plane.

Acoustic excitation conditions were restricted to a relatively narrow range because of the low response of acoustic drivers for frequencies above 6 kHz. This limits the excitation Strouhal number to the range of $St_j \leq 0.7$ at the extreme jet operating condition (Test Condition 2). The excitation level at the nozzle exit plane on the jet centerline was kept at 147 $\pm$ 2dB

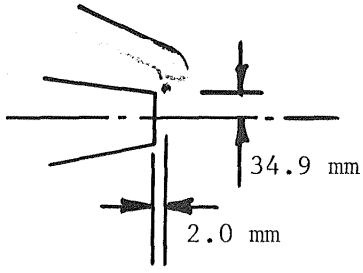

f = 1504 Hz
V_i = 1.0 Volts
G_L = 149.9 dB

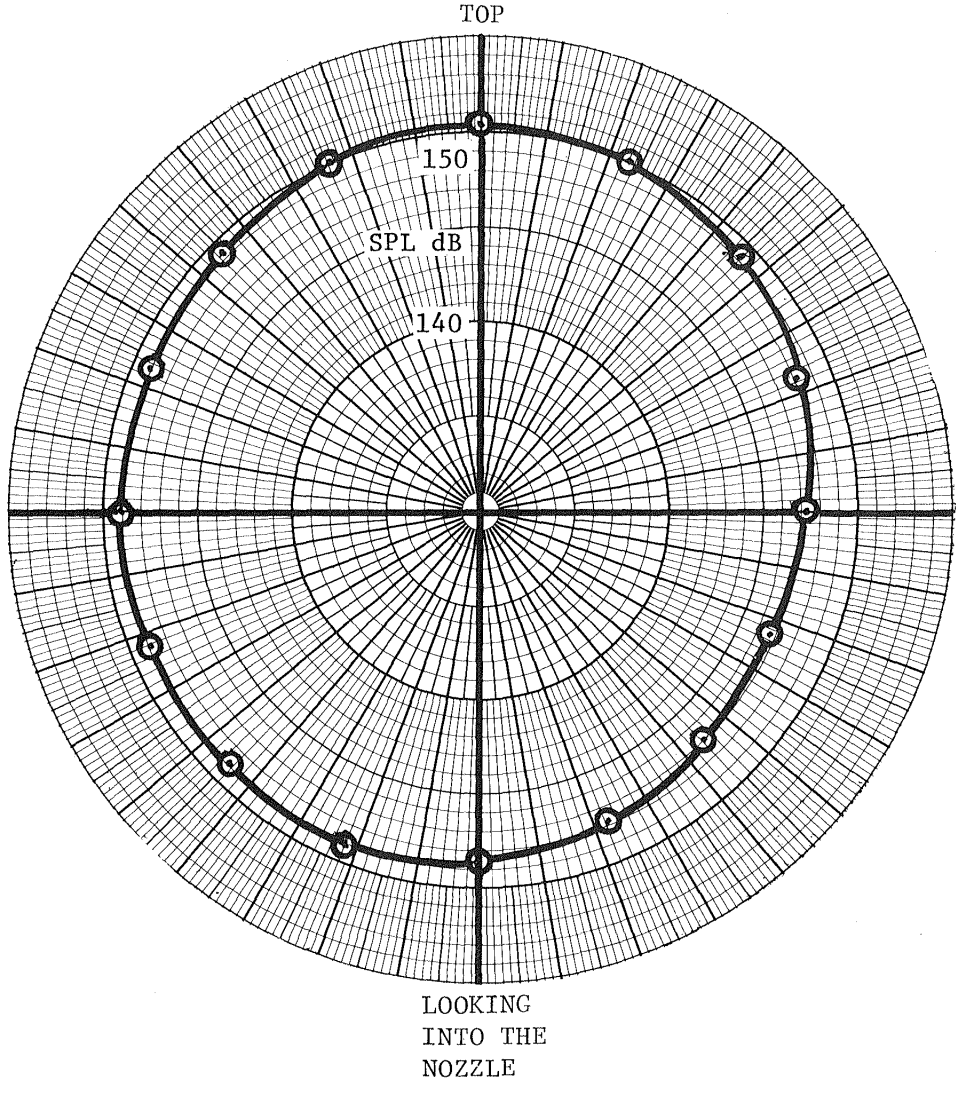

Figure 4.6 Excitation source circumferential directivity.

during the course of the experiments.

4.4.1 Unheated High Speed Jet

A distribution of relative Mach number as a function of excitation Strouhal number for the unheated jet of M_j = 0.8 is plotted in Figure 4.7. The centerline excitation level is 147 dB up to the Strouhal number 0.75. Then, the level decreases to 135 dB at the maximum plotted Strouhal number. As seen in this figure, the response of the unheated jet is very pronounced. The jet is affected at practically all examined Strouhal numbers. The most effective Strouhal number range is from 0.25 to 0.6 when the jet centerline local Mach number at X/D = 9 decreases to an average to 75% of its value for the unexcited jet. At the Strouhal number of 0.3, the jet exhibits a sharp local minimum with the relative Mach number dropping to as low as 62%. It has to be pointed out, however, that the jet shows tremendous scatter in this response in the range of Strouhal numbers from 0.23 to 0.36. Obviously, in this region, the jet is very sensitive to small changes in the excitation Strouhal number.

4.4.2 Heated High Speed Jet

The effect of excitation Strouhal number on high speed, highly heated jet (M_j = 0.8, T_t = 670 K) is shown in Figure 4.8. The centerline excitation level was kept constant at 147 dB up to the Strouhal number of 0.50. After that, the excitation level drops to 135 dB at the maximum Strouhal number. As seen in Figure 4.8, the response of this jet to the acoustic external excitation is significantly weaker than is the response of the unheated jet. Nevertheless, the relative Mach number distribution indicates that this highly heated, high speed jet is excitable at certain Strouhal numbers. Two local minima in the relative Mach number distribution can be observed. The first minimum is at the excitation Strouhal number 0.19, where the relative Mach number drops to 90% of the unexcited value. The second minimum, at the Strouhal number 0.5, is a little shallower at about 94% of the unexcited value. Thus, it appears that the heated jet of M_j = 0.8 and T_t = 670 K is excitable in two relatively narrow regions centered around Strouhal numbers 0.19 and 0.5. Outside of these two regions, no effects of excitation on heated jets were observed. The validity of this finding, of course, is restricted to the range of applied excitation levels.

In conclusion, it was a worthwhile exercise to conduct these tests with the external excitation in that they showed that if high enough excitation levels are used, the heated jet, even at high speeds can be modified by artificial excitation. The precise mode in which coupling takes place in this case can, however, be determined only by further work.

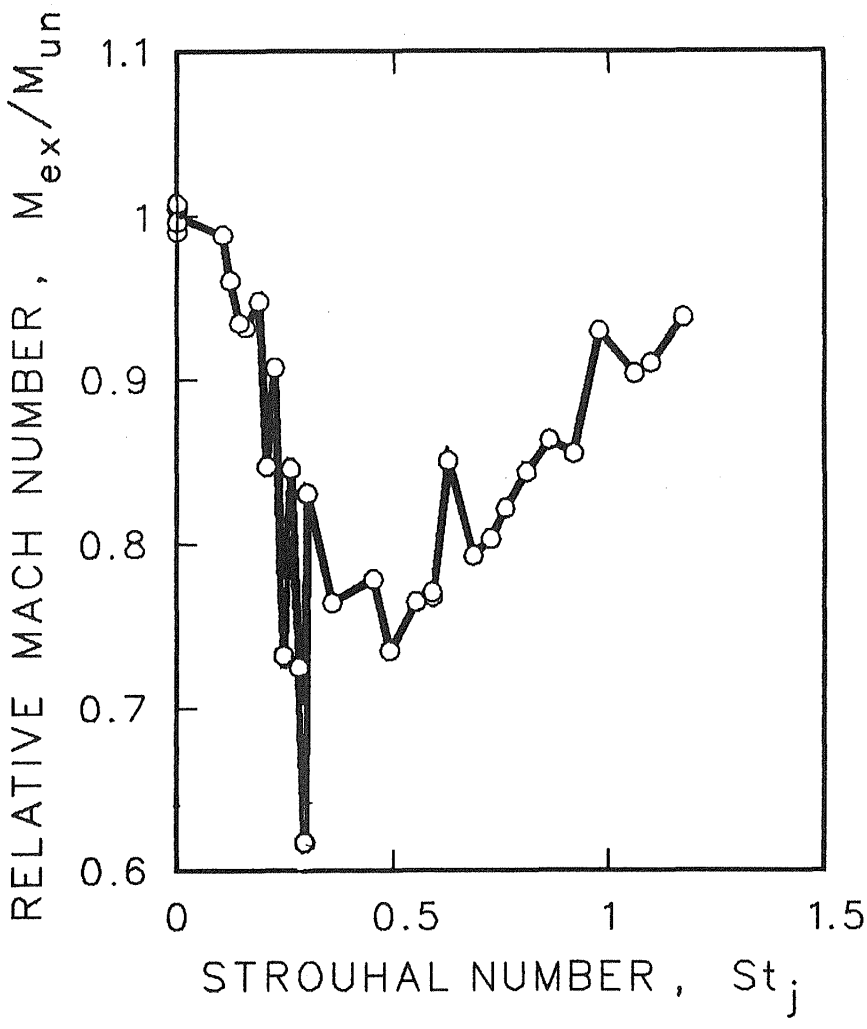

Figure 4.7 Excitation Strouhal number effects on relative Mach number on jet centerline at X/D = 9. M_j = 0.8; T_t = 290 K (unheated)

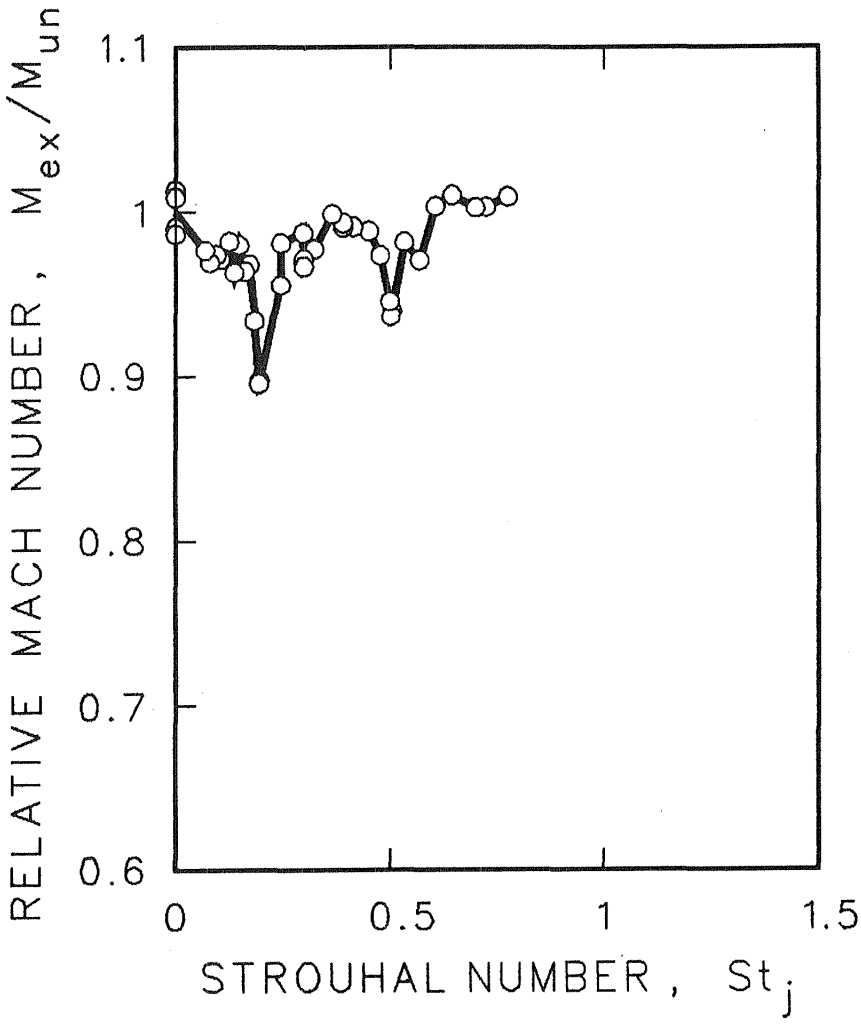

Figure 4.8 Excitation Strouhal number effects on relative Mach number on jet centerline at X/D = 9. M_j = 0.8, T_t = 670 K (heated)

5.0 EFFECTS OF NOZZLE-EXIT BOUNDARY LAYER CONDITIONS ON JET EXCITABILITY

5.1 INTRODUCTORY REMARKS

An experimental program carried out under this contract took various turns during the course of its conduct. Tasks were modified or added to the original program in accordance with the updated NASA-Lewis requirements in an effort to demonstrate that fluid mixing in high-speed highly heated jets can be enhanced by artificial excitation. This resulted in a requirement to thoroughly investigate the effects of nozzle-exit boundary layer conditions on excitability of heated free jets. Similar experiments were already initiated under the Phase I effort in 1983. However, they were not completed as intended because of funding limitations. Due to these limitations, the accomplished results of these experiments in 1983, reported in Part I, Section 5, did not satisfactorily answer the question of the role of nozzle exit boundary layer conditions on jet excitability.

The current set of experiments on the effects of nozzle-exit boundary-layer conditions on jet excitability was carried out in three stages. The first stage consisted of a thorough investigation of nozzle-exit boundary-layer behavior under various jet operating conditions. The second stage was devoted to boundary layer modification to eliminate the dependence of the exit boundary layer on jet operating conditions. Finally, in the third stage, after eliminating the nozzle exit boundary layer dependence on jet operating conditions, the external excitation experiments were carried out for selected jet operating conditions.

5.2 NOZZLE-EXIT BOUNDARY LAYER CHARACTERISTICS

5.2.1 Boundary Layer Total-Head Velocity Profiles

Boundary-layer velocity profiles were calculated from total-head velocity distributions measured across the nozzle-exit boundary layers. All the velocity profiles were calculated assuming a flow with constant static temperature equal to the core flow temperature. The reason for this simple approach was that the temperature distribution across the investigated heated-flow boundary layers was unknown.

For a given profile survey, all the calculated velocity values at discrete points across the boundary layer were fitted with an analytical curve based

on the parametric cubic spline fitting subroutine ICFSKU from the IMSL library [5.1]. As examples, four velocity profiles containing the experimental points as well as their fitted curves are shown in Figure 5.1.

Boundary-layer thicknesses $\lambda_{0.995}$ and λ were calculated from the fitted analytical curve as distances from the nozzle inner wall where the local velocity reaches 99.5% and 100% of the velocity value in the jet core. A distribution of the boundary-layer thickness $\lambda_{0.995}$ as a function of the nozzle operating conditions, expressed in terms of the jet exit Reynolds numbers, is shown in Figure 5.2. As seen in this figure, the boundary-layer thickness rapidly decreases from an initial value with an increasing jet Reynolds number and reaches its minimum for a critical Reynolds number of $Re_J = 0.3*10^6$. After that, the boundary-layer thickness rapidly increases, reaches a local maximum and then decreases again. In spite of a noticeable scatter of the boundary-layer thickness values, it is clear from Figure 5.2 that the flow temperature does not play any significant role for nozzle operating conditions below the critical Reynolds number. Above the critical Reynolds number ($Re_J = 0.3*10^6$), however, the effects of the elevated flow temperatures are clearly traceable. Three separated branches appear to emerge for the nozzle operating conditions above the critical Reynolds number, each associated with a certain jet total temperature (285 K, 500 K, and 700 K). Thus, in this region, the flow temperature must be considered as an additional parameter to the jet-exit Reynolds number, influencing the nozzle-exit boundary-layer development.

5.2.2 Integral Characteristics

Boundary-layer integral characteristics provide a basic description of the velocity distribution behavior in a particular boundary layer. The three commonly used integral characteristics are displacement, momentum, and energy thicknesses (δ, θ, ε). These characteristics are defined as follows [5.2]:

$$\delta = \int_0^{\lambda} \left(1 - \frac{\rho}{\rho_\lambda}\frac{u}{U_\lambda}\right) dy$$

$$\theta = \int_0^{\lambda} \frac{\rho}{\rho_\lambda}\frac{u}{U_\lambda}\left(1 - \frac{u}{U_\lambda}\right) dy$$

$$\varepsilon = \int_0^{\lambda} \frac{\rho}{\rho_\lambda}\frac{u}{U_\lambda}\left(1 - \frac{u^2}{U_\lambda^2}\right) dy$$

where λ is the boundary layer entire thickness (a radial distance where a local velocity reaches the core-flow velocity) and subscript λ denotes

a.

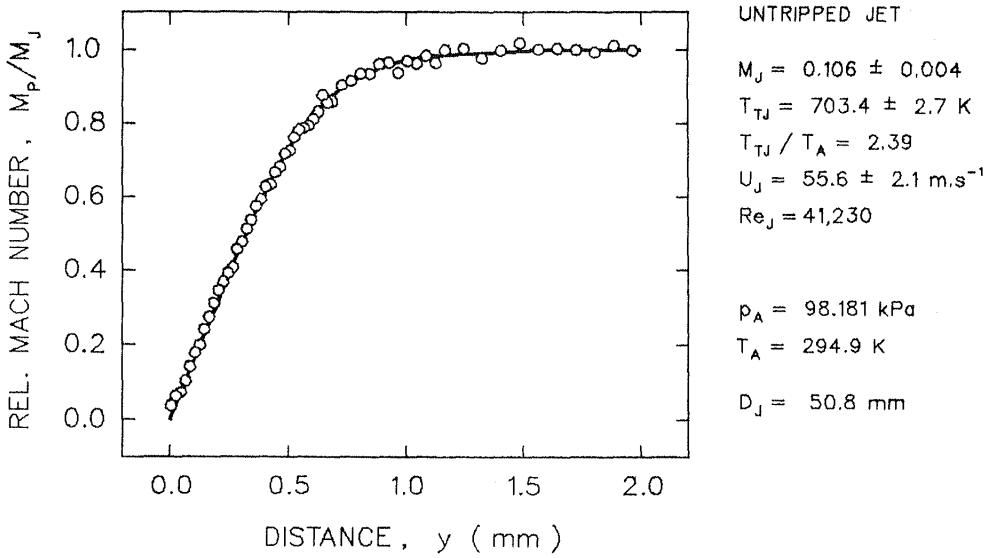

b.

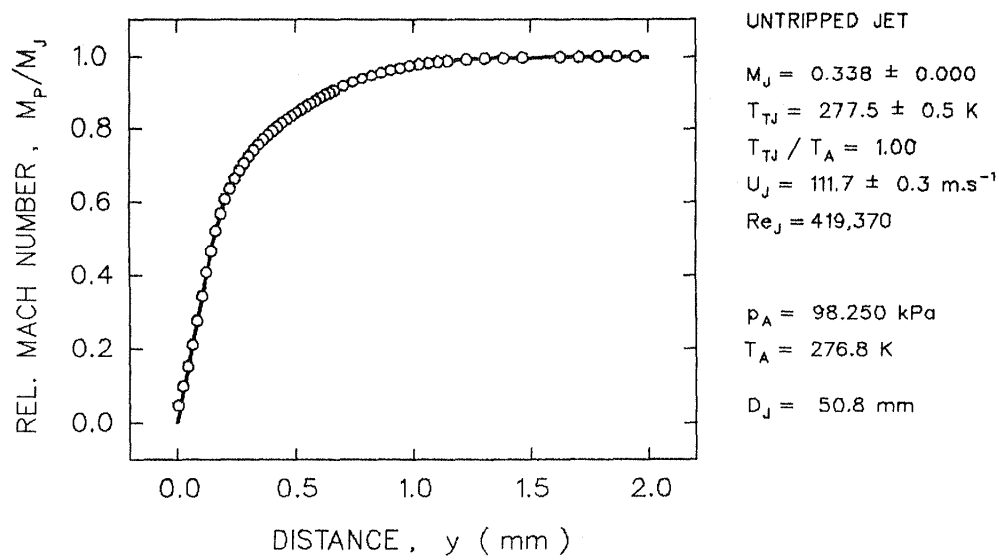

Figure 5.1a,b Nozzle exit boundary layer head-velocity profiles.

c.

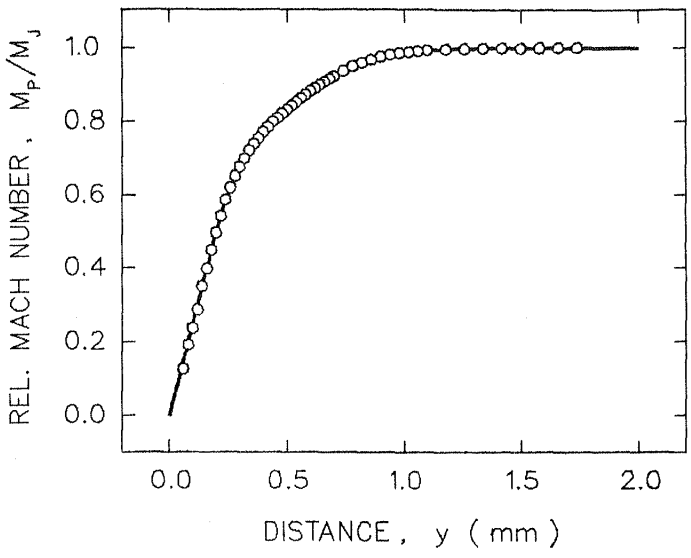

UNTRIPPED JET

M_J = 0.860 ± 0.002
T_{TJ} = 499.7 ± 1.8 K
T_{TJ} / T_A = 1.75
U_J = 359.4 ± 1.4 m.s^{-1}
Re_J = 585,560

p_A = 97.630 kPa
T_A = 284.8 K

D_J = 50.8 mm

d.

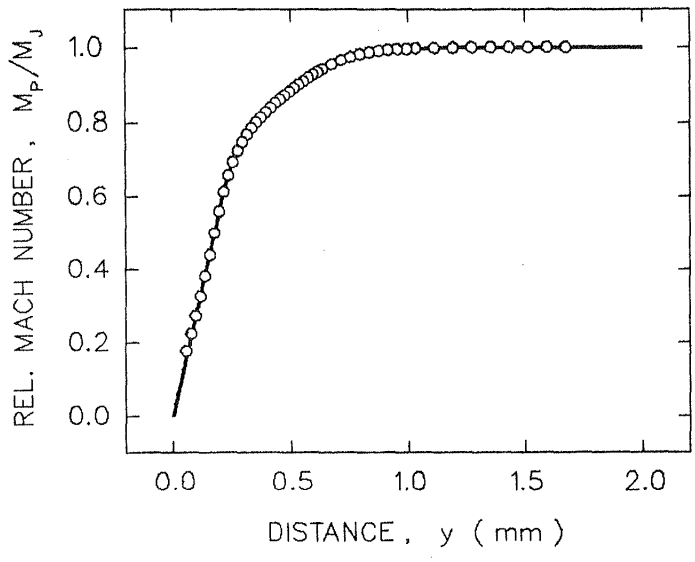

UNTRIPPED JET

M_J = 0.956 ± 0.001
T_{TJ} = 280.4 ± 0.3 K
T_{TJ} / T_A = 1.00
U_J = 295.4 ± 0.3 m.s^{-1}
Re_J = 1,412,630

p_A = 97.837 kPa
T_A = 281.1 K

D_J = 50.8 mm

Figure 5.1c,d Nozzle exit boundary layer head-velocity profiles.

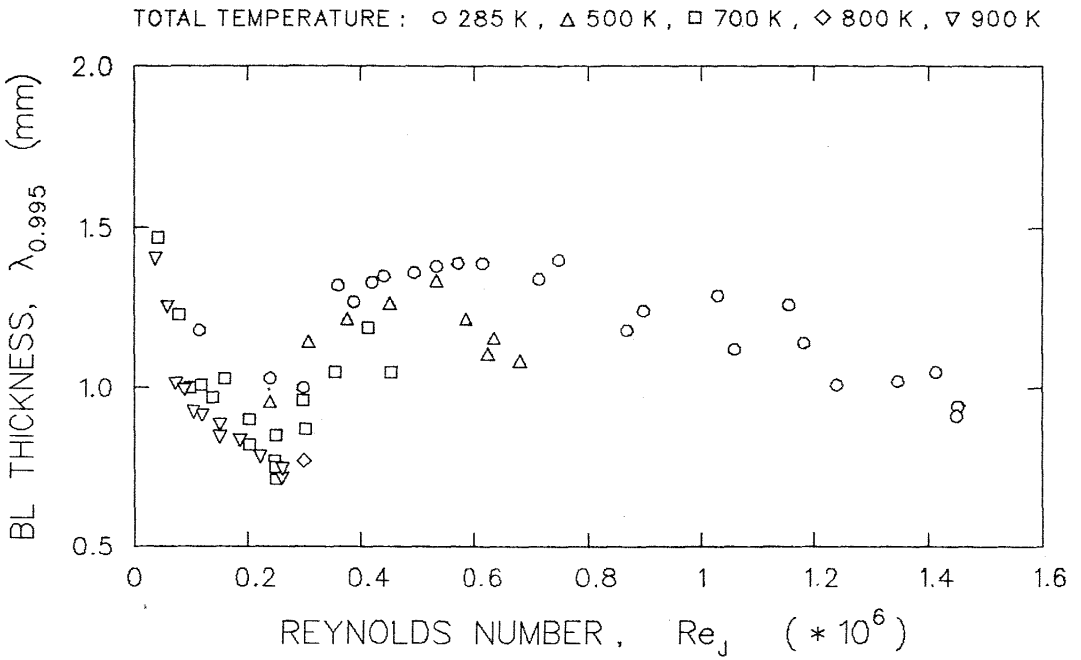

Figure 5.2 Nozzle exit boundary layer thickness distribution.

values at the outer edge of the boundary layer. As mentioned above, the velocity calculation is based on an assumption of a constant flow temperature. The calculation of the integral characteristics is based on the assumption of a constant property fluid (T_T = const, ρ = const). The integral characteristics were calculated from fitted analytical curve using numerical integration utilizing the IMSL subroutine DCADRE [5.1].

A dependance of the integral characteristics on jet operating conditions is shown in Figure 5.3. As seen in this figure, the jet exit Reynolds number has a dramatic effect on these characteristics, resembling behavior of the boundary-layer thickness distribution shown in Figure 5.2. The data scatter in these plots appears to be smaller than that for the boundary-layer thickness distribution.

Consider displacement thickness in Figure 5.3a. It decreases rapidly with an increasing jet Reynolds number and reaches its minimum for a critical Reynolds number of $Re_J = 0.3*10^6$. Beyond the critical Reynolds number, the displacement thickness suddenly increases and then remains more or less constant until the nozzle exit velocity approaches the transonic region where the displacement thickness starts slowly to drop off ($Re_J = 1.2*10^6$, T_T = 285 K). A closer inspection of this plot reveals that above the critical Reynolds number the displacement thickness always drops off when the jet exit velocity reaches the transonic region which, for the elevated jet total temperatures, occurs at lower jet-exit Reynolds numbers ($Re_J = 0.6*10^6$, T_T = 500 K and $Re_J = 0.4*10^6$, T_T = 700 K). Again, the effect of the jet temperature on the nozzle-exit boundary layer-development is independent from the effect of the jet-exit Reynolds number alone.

A similar trend exists in the remaining plots in Figure 5.3 for the momentum and energy thickness development. The three branches for the flow temperatures of 285 K, 500 K, and 700 K are even more distinguishable in the region above the critical Reynolds number. After reaching their maxima beyond the critical Reynolds number, both the momentum and energy thicknesses gradually decrease with an increasing jet-exit Reynolds number without a noticeable drop off in the vicinity of the transonic region.

5.2.3 Shape Factors

Shape factors describe the shape of the boundary-layer velocity profile. The displacement-momentum and energy-momentum shape factors are defined as [5.2]:

$$H_{\delta\theta} = \delta / \theta$$

and

$$H_{\varepsilon\theta} = \varepsilon / \theta.$$

The significance of the boundary-layer shape factors lies in detection of boundary layer transition from laminar to turbulent. For example, it is well established that for a flat-plate boundary layer, the displacement-momentum shape factor exhibits a sudden drop from a value of 2.6 for the laminar layer to a value of about 1.4 for the turbulent boundary layer [5.2].

As seen in Figure 5.4, at the jet Reynolds number of $Re_J = 0.3*10^6$, the displacement-momentum shape factor $H_{\delta\theta}$ drops from 2.5 to 1.9 for the unheated flow (T_T = 285 K), to 2.1 for the flow heated to 500 K, and only to 2.3 for the flow heated to 700 K. Thus, the jet Reynolds number $0.3*10^6$ marks the end of the laminar regime of the nozzle exit boundary layer. In the transitional and turbulent regions, the value of the displacement-momentum shape factor strongly depends on the flow total temperature, as was already noticed in the case of the integral characteristics. It is higher for higher flow temperatures. After the boundary layer transition, the value of the displacement-momentum shape factor increases with an increasing jet Reynolds number.

Analogous behavior can also be observed for the energy-momentum shape factor $H_{\varepsilon\theta}$. In this case, however, the value of the shape factor increases for the laminar/turbulent transition. The increasing flow total temperature diminishes the rise of this factor during transition in comparison with the laminar boundary-layer value.

As the nozzle exit velocity approaches the transonic region, both shape factors exhibit a reversal in their trends. This is obvious at least for the unheated flow ($Re_J = 1.2*10^6$, T_T = 285 K). For the heated flows ($Re_J = 0.6*10^6$, T_T = 500 K and $Re_J = 0.4*10^6$, T_T = 700 K), the experimental scatter prevents drawing a similar conclusion with sufficient confidence. The reason for this trend reversal is not quite apparent.

The findings from this part of the study can be summarized as follows:

- For the laminar nozzle-exit boundary layer, the boundary layer thickness and integral characteristics are functions of the jet Reynolds number only. Shape factors, for the laminar exit boundary layer, are constant. No difference between heated and unheated jets was observed.

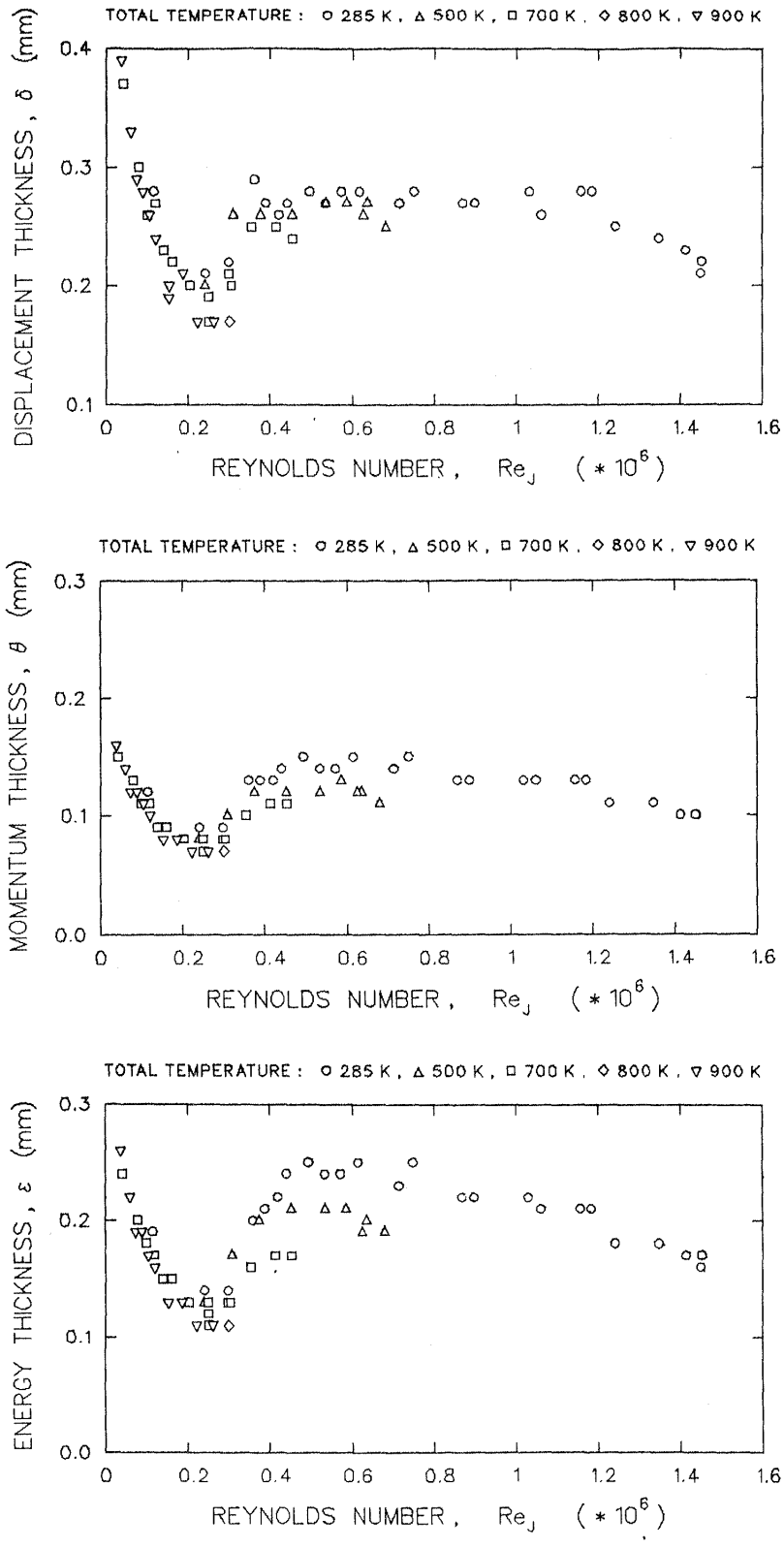

Figure 5.3 Boundary layer integral characteristics.

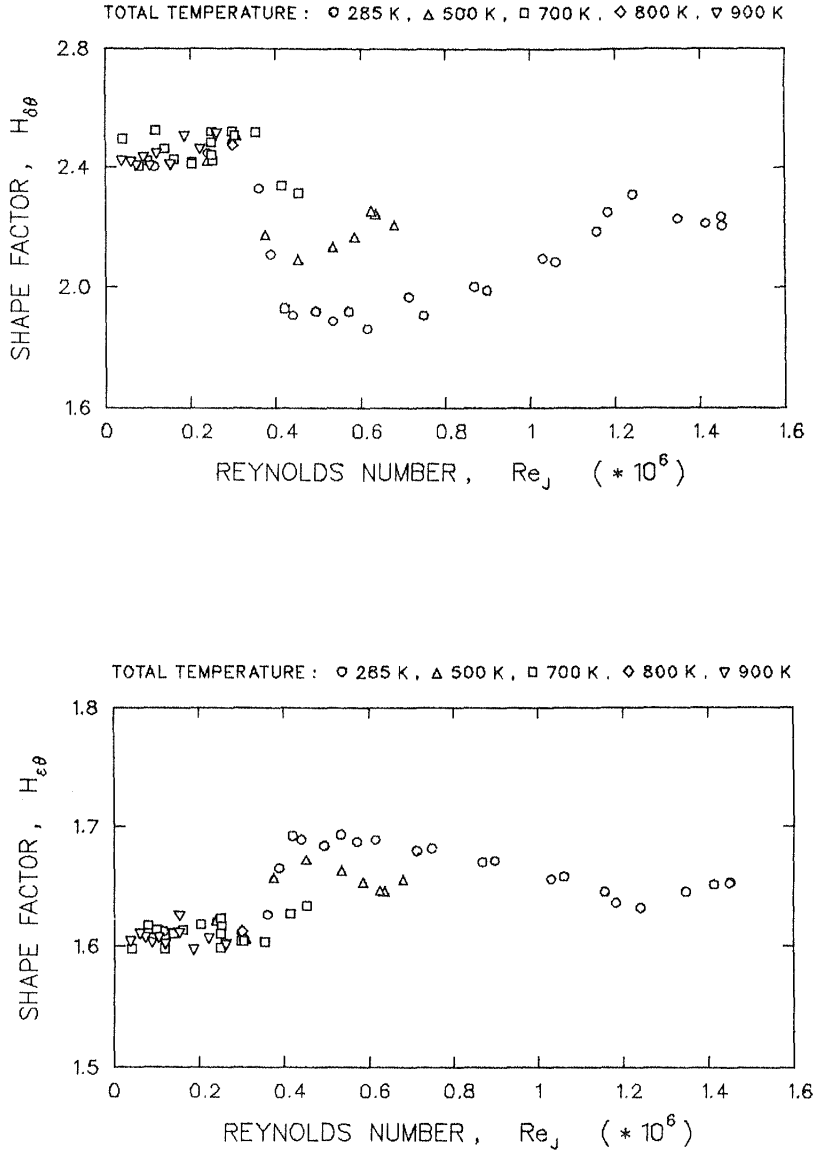

Figure 5.4 Shape factor distributions.

- For the turbulent nozzle-exit boundary layer, the boundary layer thickness, integral characteristics, and shape factors are functions of the jet exit Reynolds number and flow temperature. The results show that the flow temperature, for the turbulent exit boundary layer, must be considered as an independent parameter.

5.3 BOUNDARY LAYER MODIFICATION

Boundary layer modification was aimed at elimination of the nozzle-exit boundary layer dependence on jet operating conditions. A number of parameters may characterize the nozzle-exit boundary layer conditions. The important parameters, from our point of view, are boundary layer displacement-momentum shape factor $H_{\delta\theta}$ and boundary layer momentum thickness θ. Thus, the main objective of the boundary layer modification was to keep these two parameters constant, therefore, independent of the jet operating conditions.

To achieve the above stated goal, it was decided to trip the boundary layer inside the test nozzle, similarly as it was done under the Phase I effort. This time, however, the tripping rings were placed relatively far upstream of the test-nozzle exit plane. (The test facility has been redesigned, after the Phase I experiments, to enable an easier access inside the test nozzle.)

The main effort was devoted to nozzle-exit boundary layer modification of a high speed, highly heated jet of Mach number 0.8 and jet total temperature of 670 K. Several tripping rings of different ring and wire diameters were employed. The most satisfactory results were achieved for a ring placed 67 mm upstream of the nozzle exit plane. The ring wire diameter was 1.63 mm.

The effect of jet operating conditions on untripped nozzle exit boundary layers is shown in Figure 5.5. This figure shows nozzle-exit boundary layer profiles for unheated and heated jets at Mach number 0.8. As seen in this figure, there is a significant difference between the nozzle-exit boundary layer profiles for an unheated jet and jet heated to 700 K. The unheated jet has a displacement-momentum shape factor ($H_{\delta\theta}$) of 2.084 and momentum thickness (θ) of 0.13 mm. The shape factor value indicates that the nozzle-exit boundary layer is in the transition between laminar and turbulent states. The jet heated to 700 K (Figure 5.5b), however, has a laminar nozzle-exit boundary layer profile with the following characteristics: $H_{\delta\theta} = 2.517$, $\theta = 0.10$ mm.

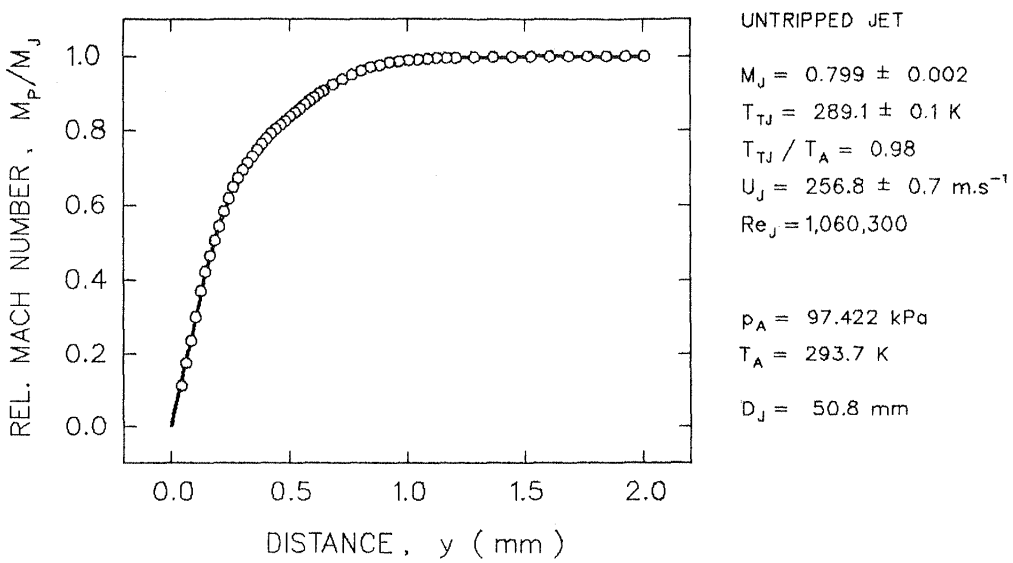

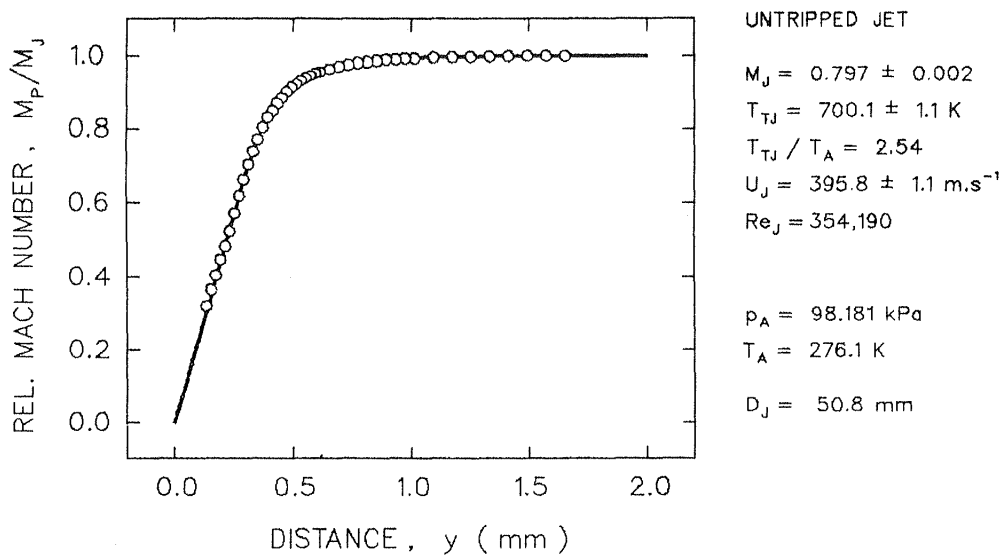

Figure 5.5 Nozzle exit boundary layer profiles of unheated and heated, untripped, Mach number 0.8 jets.

The tripped boundary layer profiles for similar jet operating conditions are shown in Figure 5.6. As seen in this figure and in the previous one, there is no significant difference between untripped and tripped nozzle exit boundary layer profiles for unheated jets. The unheated tripped jet nozzle-exit boundary layer characteristics ($H_{\delta\theta}$ = 1.901, θ = 0.13 mm) are close to those of the unheated untripped jet. However, the heated-tripped jet boundary-layer profile noticeably differs from that for the untripped jet and it is similar, as planned, to the unheated jet nozzle-exit boundary layer profile. The boundary layer profile of the heated tripped jet has the following characteristics: $H_{\delta\theta}$ = 1.911 and θ = 0.15 mm.

As seen from the above discussed results, the nozzle-exit tripped-boundary-layer characteristics at a Mach number of 0.8 are not significantly altered with a change in jet total temperature. Thus, the selected way of boundary layer modification satisfied the requirement of elimination of the nozzle-exit boundary layer dependence on jet operating conditions. A summary of all nozzle-exit boundary layer characteristics for a jet Mach number of 0.8 is given in Table 5.1.

Similar experiments were conducted also for a jet exit Mach number of 0.3. A summary of boundary layer characteristics for untripped and tripped conditions for this jet exit Mach number is given in Table 5.2. As seen in this table, the same tripping ring generated a thicker, more turbulent nozzle-exit boundary layer at the jet Mach number of 0.3 than it did for the higher jet exit Mach number of 0.8.

It should be noted here, that the tripped boundary layer momentum thicknesses of the Mach number 0.8 jet for unheated and heated conditions stay within the range of momentum thickness values generated naturally in the untripped jet (Figure 5.3). In the case of Mach number 0.3 jets, however, the tripped boundary layer momentum thicknesses are twice or three times the corresponding values for untripped jets.

None of the tripping rings used generated identical nozzle-exit boundary layers for both, low and high jet exit Mach numbers. To exchange the tripping rings during excitation experiments, however, the external excitation section must be dismounted (Figure 4.5.). Because the excitation source tuning and calibration are laborious and time consuming procedures, it was decided to conduct excitation experiments only with the tripping ring which satisfied the main condition: that the nozzle-exit boundary layers for unheated and heated high speed jets be similar.

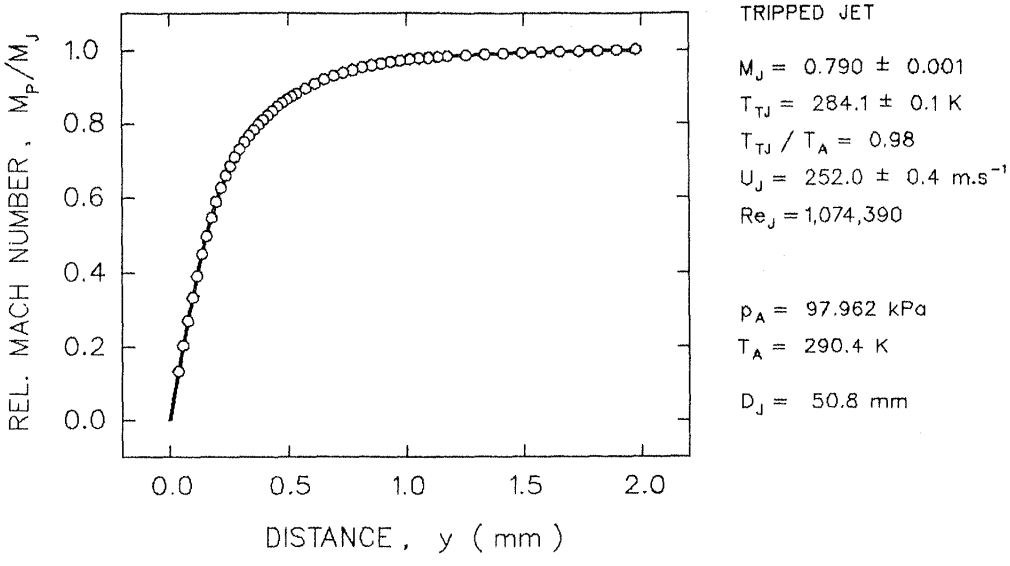

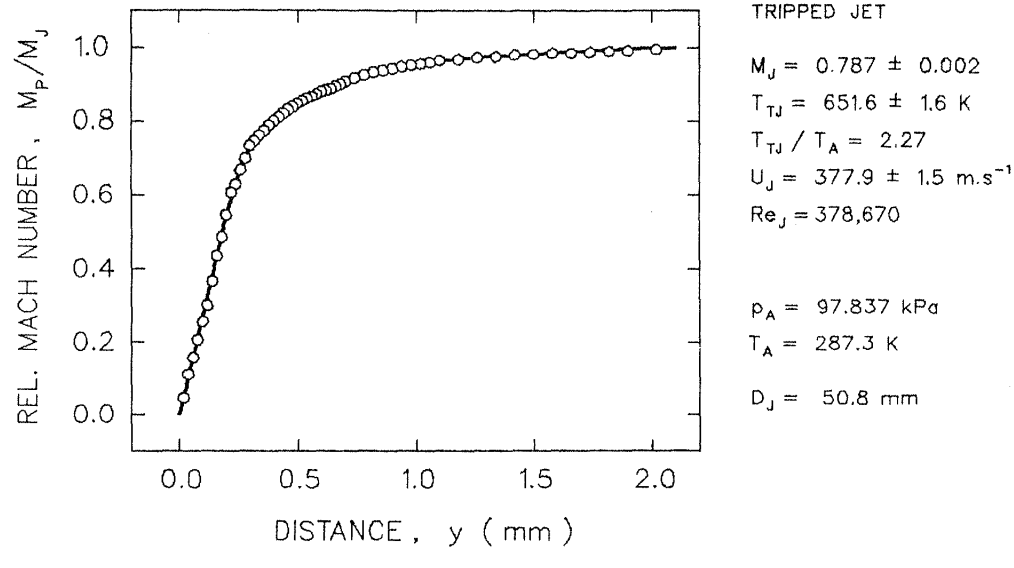

Figure 5.6 Nozzle exit boundary layer profiles of unheated and heated, tripped, Mach number 0.8 jets.

	M_J	T_T (K)	$H_{\delta\theta}$	$H_{\delta\varepsilon}$	δ (mm)	θ (mm)	ε	Re_θ	Re_J
Untripped	0.80	289	2.084	1.658	0.26	0.13	0.21	2633	1,060,300
	0.80	700	2.517	1.603	0.25	0.10	0.16	694	354,190
Tripped	0.79	284	1.901	1.700	0.25	0.13	0.22	2747	1,074,090
	0.79	652	1.911	1.717	0.29	0.15	0.26	1115	378,670

Table 5.1 Nozzle exit boundary-layer characteristics of Mach number 0.8 jet

	M_J	T_T (K)	$H_{\delta\theta}$	$H_{\delta\varepsilon}$	δ (mm)	θ (mm)	ε (mm)	Re_θ	Re_J
Untripped	0.30	284	2.328	1.626	0.29	0.13	0.20	887	359,420
	0.30	700	2.522	1.598	0.27	0.11	0.17	246	118,690
Tripped	0.30	279	1.590	1.775	0.33	0.21	0.36	1470	364,170
	0.30	653	1.516	1.790	0.43	0.29	0.51	732	129,800

Table 5.2 Nozzle exit boundary layer characteristics of Mach number 0.3 jet

5.4 EXCITATION TESTS WITH MODIFIED BOUNDARY LAYERS

After having finished the nozzle-exit boundary layer modification experiments, external excitation tests commenced. The excitation tests were conducted in the same manner as described earlier in Section 4.0. The jet response to the excitation Strouhal number was determined by measurement of flow Mach numbers at the jet centerline at nine nozzle exit diameters downstream of the nozzle exit plane. Accurate probe positioning at the jet centerline required repeated measurements of both vertical and horizontal jet-velocity profiles. This procedure was necessary because the nozzle geometric axis moved due to thermal expansions when the flow was heated.

5.4.1 Unexcited Jets

Radial profiles of unheated and heated unexcited jets of Mach number 0.8 are shown in Figure 5.7. As seen in this figure, at this jet exit Mach number the effect of heating the flow was to provide noticeable decrease of the centerline local Mach number at X/D = 9, thus indicating considerable broadening of the jet plume.

Low speed unheated and heated jets of Mach number 0.3, however, behaved differently. As seen in Figure 5.8, where radial profiles for Mach number 0.3 jets are depicted, no significant decrease of the centerline local Mach number at X/D = 9 was observed due to the flow heating. These findings are summarized in Figure 5.9. In this figure, only the peak values of jet radial profiles are shown. The figure clearly points out the differences between the effects of flow heating at low and high jet exit Mach numbers.

Radial profiles at X/D = 9 for Mach number 0.8 jets with tripped nozzle boundary layers are plotted in Figure 5.10. A comparison of Figures 5.7 and 5.10 shows that a change in nozzle-exit boundary layer conditions itself caused changes in the flowfield of a heated Mach number 0.8 jet. For the heated jets, the flow Mach number at the jet centerline at X/D = 9 increased from 75% of the jet exit Mach number for the untripped jet to 82% of the tripped jet. For the unheated jets, however, the change is hardly noticeable.

These results show the significance of the nozzle-exit boundary layer parameters on high Mach number free jet development. As described in the previous subsection, the applied boundary layer modification did not alter the nozzle-exit boundary layer parameters for the unheated jets of Mach number 0.8. In accordance with that, no significant changes in the jet flow Mach number at X/D = 9 were observed.

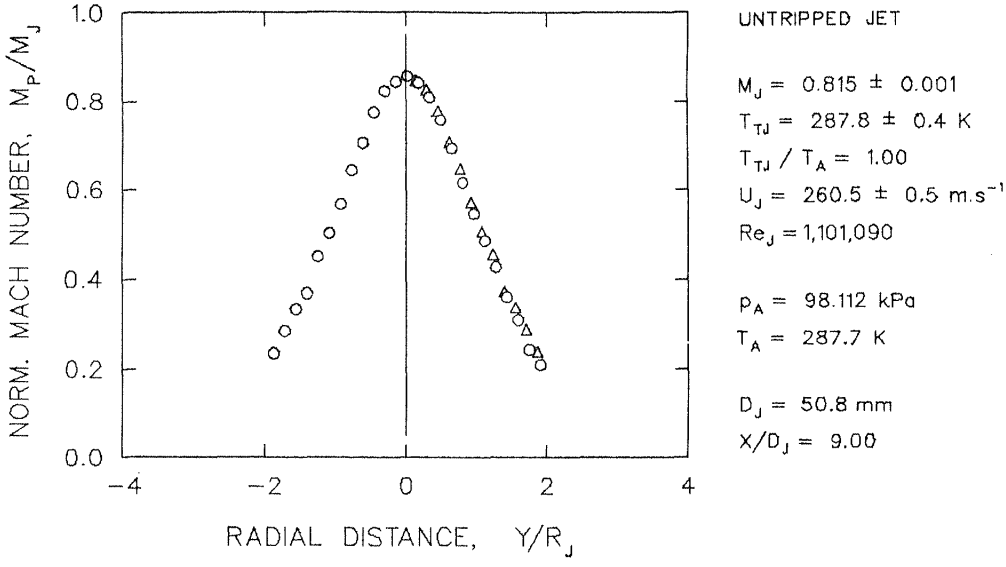

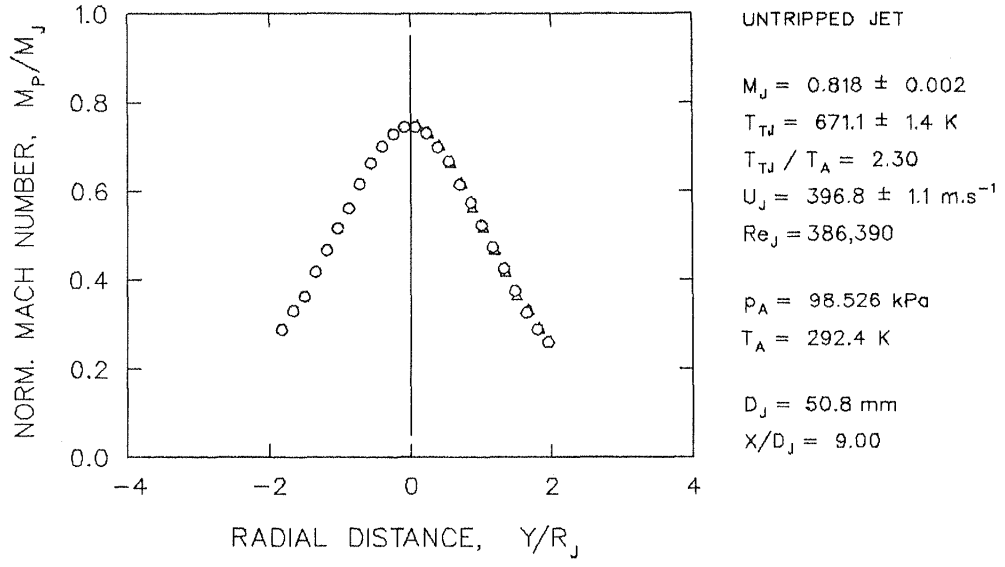

Figure 5.7 Radial profiles at X/D = 9 of unheated and heated, untripped, Mach number 0.8 jets.

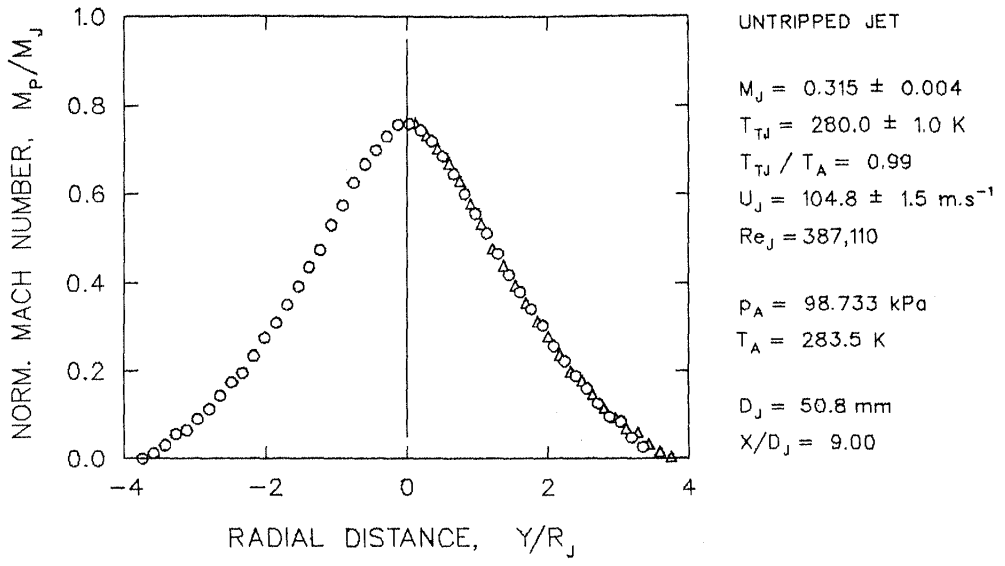

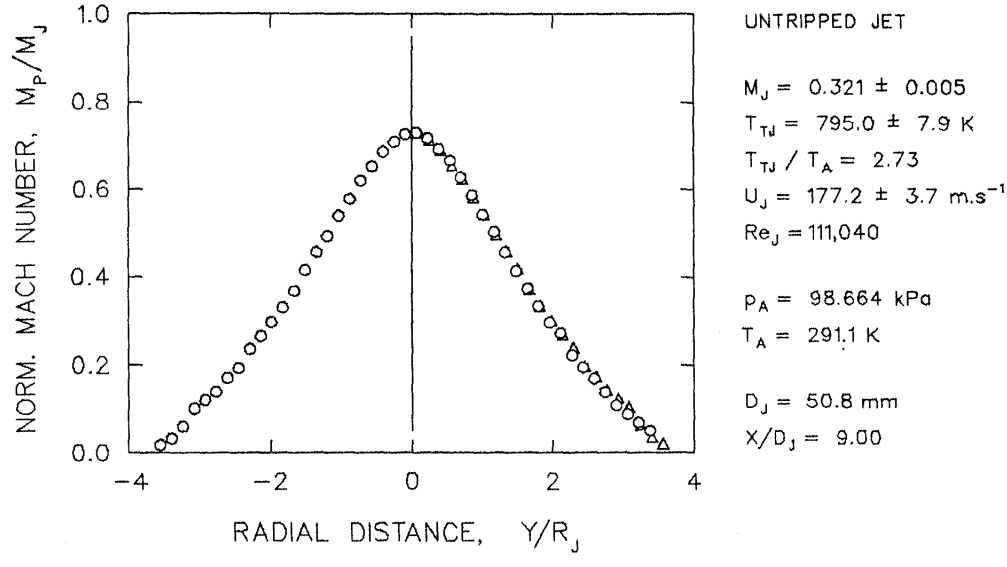

Figure 5.8 Radial profiles at X/D = 9 of unheated and heated, untripped, Mach number 0.3 jets.

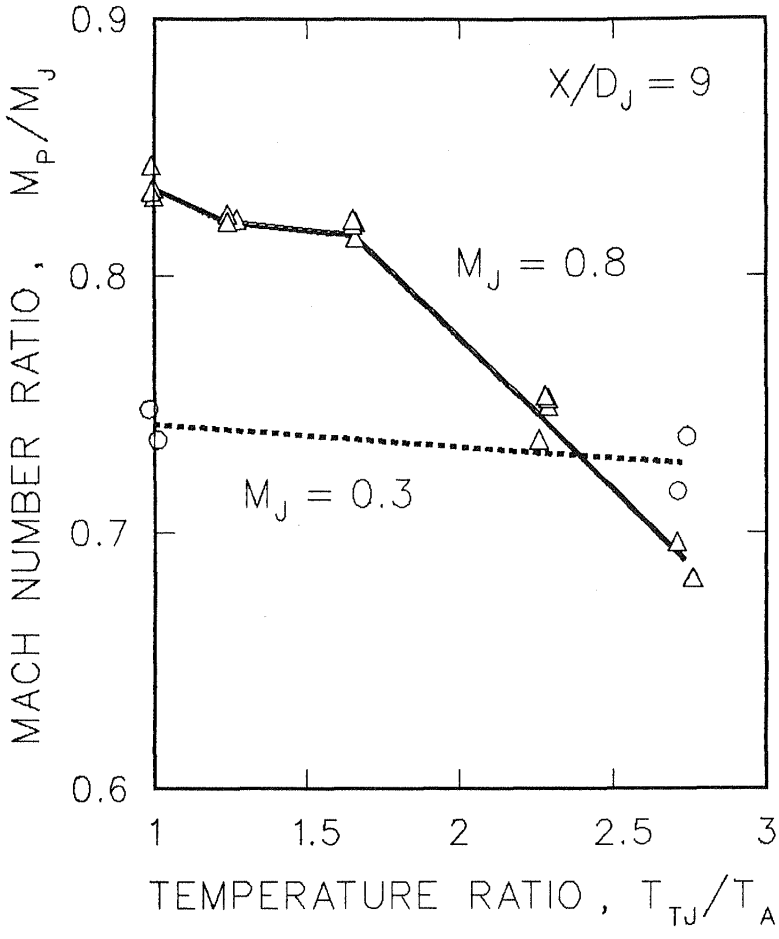

Figure 5.9 Total temperature effects on centerline local Mach number at X/D = 9 of unexcited jets.

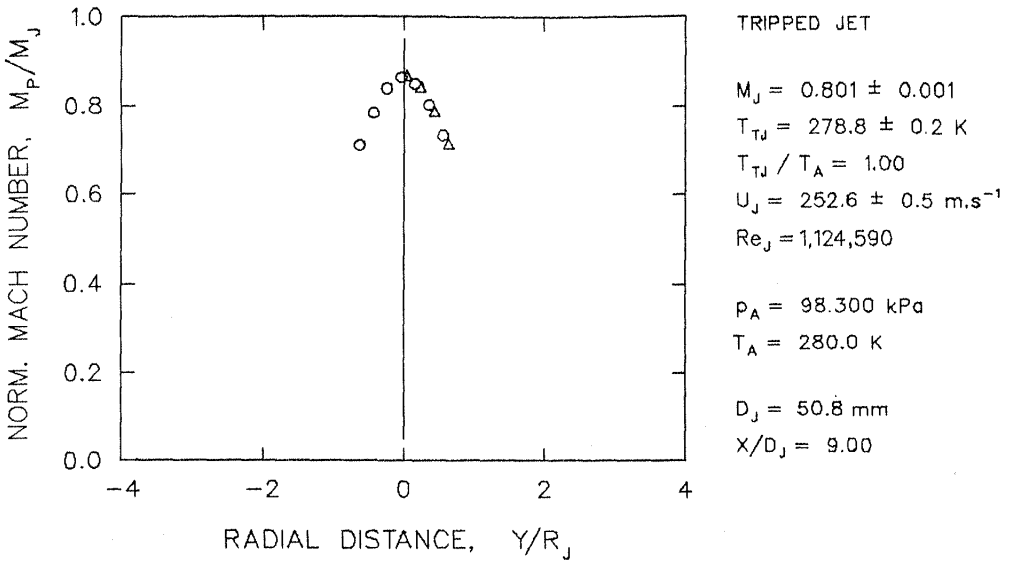

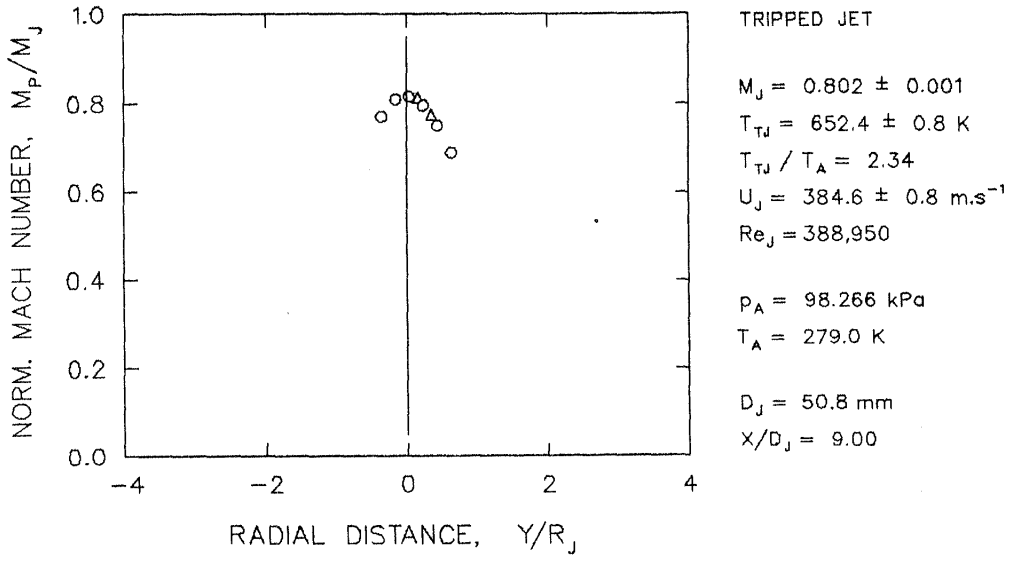

Figure 5.10 Radial profiles at X/D = 9 of unheated and heated, tripped, Mach number 0.8 jets.

For the Mach number 0.8 heated jets, however, the boundary layer tripping changed the nozzle-exit boundary layer characteristics, namely the momentum thickness and the displacement-momentum shape factor. Correspondingly, the flowfield measurements indicate closing of the jet plume and decreased mixing for the tripped, thicker, turbulent boundary layer in comparison to the untripped, thinner, laminar nozzle-exit boundary layer. This indicates that free jet mixing and development may also be controlled by nozzle exit boundary layer modification.

Radial profiles for tripped unheated and heated Mach number 0.3 jets are shown in Figure 5.11. These radial profiles do not noticeably differ from the profiles for untripped Mach number 0.3 jets (Figure 5.8). No firm conclusions are presently based on this fact because, as mentioned above, the tripped nozzle exit boundary layer thickness of Mach number 0.3 jet is far beyond the range of naturally developed boundary layer thickness for these jet operating conditions.

5.4.2 Excited Jets

As mentioned above, the jet response to the acoustic excitation was determined by measurement of flow local Mach numbers at the jet centerline at X/D = 9. The excitation Strouhal number effects for the untripped jets of Mach number 0.8 were already discussed in Section 4.4. For convenience, the relevant plots are shown here again in Figures 5.12 and 5.13 with the corresponding excitation levels added. In these figures, the flow Mach number of the excited jet is compared with the Mach number at the same point in the jet flowfield, but in the absence of acoustic excitation (peak values from Figure 5.7). As seen in Figure 5.12, the unheated jet is affected at practically all examined Strouhal numbers. The heated jet (Figure 5.13), however, shows significantly weaker response to the applied acoustic excitation. Furthermore, the jet response is limited to certain frequencies only.

The excitation Strouhal number effects on unheated and heated tripped jets are shown in Figures 5.14 and 5.15. Apart from a small shift in the optimum excitation frequency, both jets show the same response to the acoustic excitation. For the optimum excitation frequency, the centerline flow Mach number at X/D = 9 drops to 80% of the unexcited value, indicating the jet plume opening and increased mixing due to acoustic excitation. The similar response to external acoustic excitation by both, unheated and heated tripped jets is a significant result showing the nozzle-exit boundary layer conditions play key roles in jet excitability and mixing. When the nozzle-exit boundary layer conditions were identical, there was no difference between heated and unheated jets.

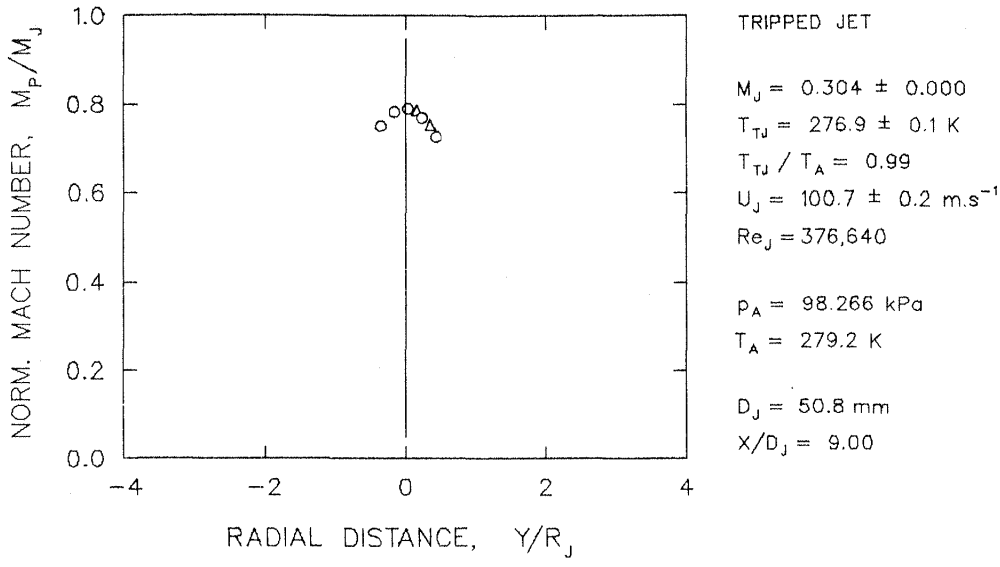

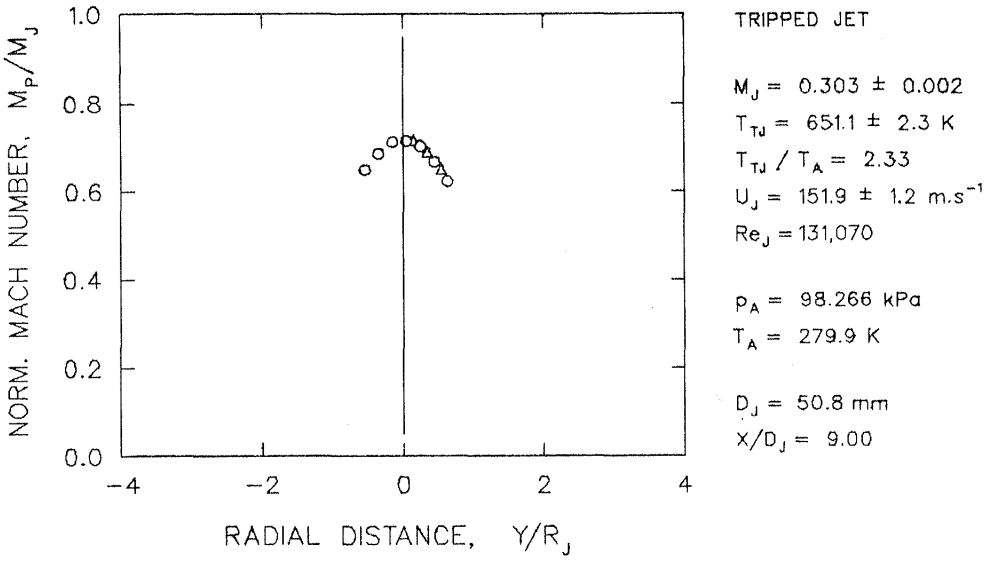

Figure 5.11 Radial profiles at X/D = 9 of unheated and heated, tripped, Mach number 0.3 jets.

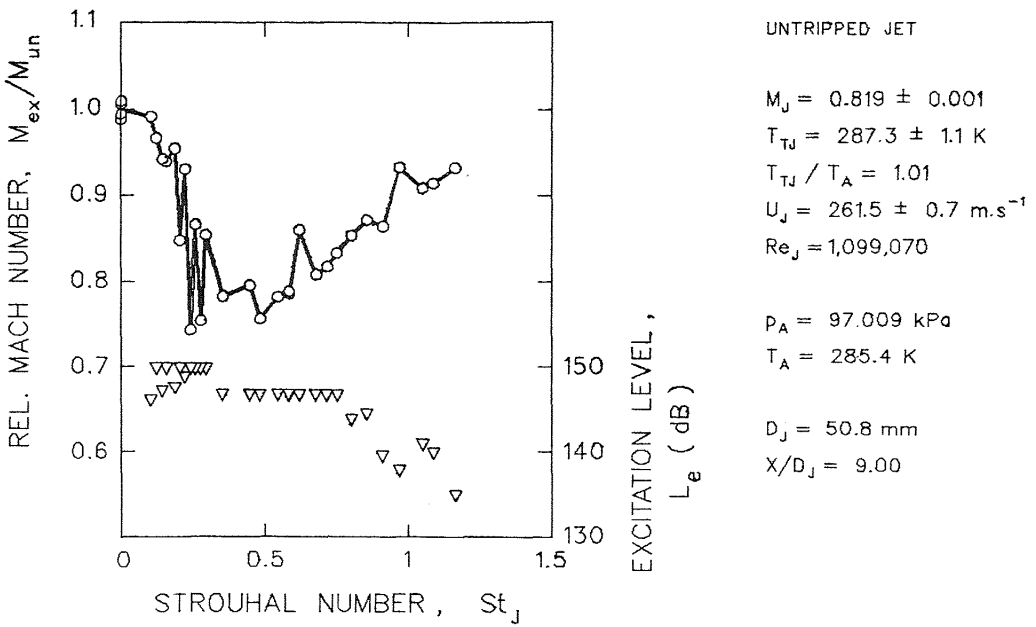

Figure 5.12 Excitation Strouhal number effects on unheated, untripped, Mach number 0.8 jet.

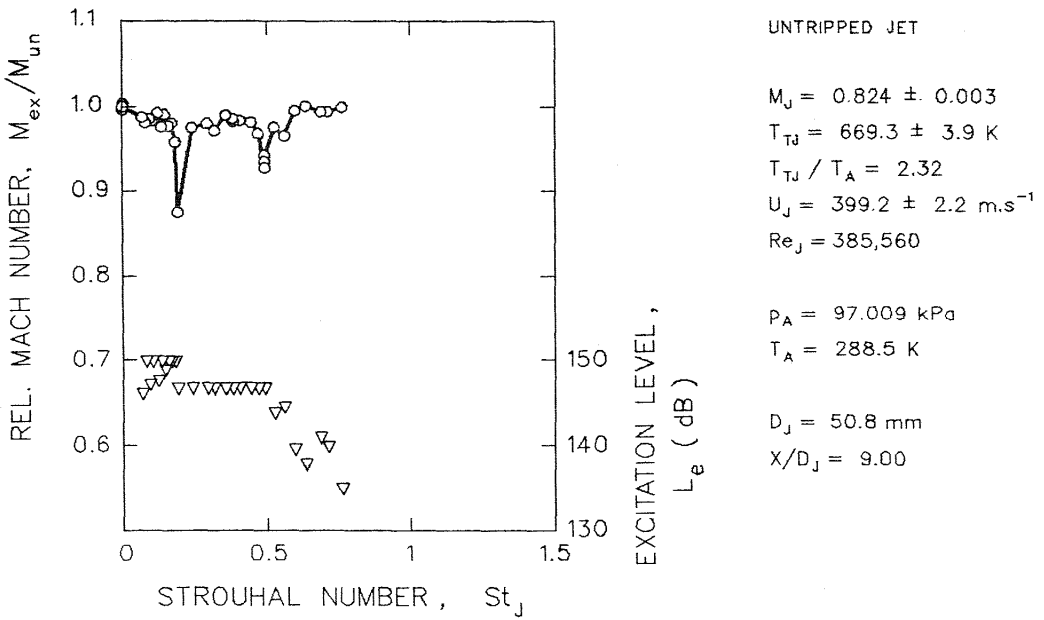

Figure 5.13 Excitation Strouhal number effects on heated, untripped, Mach number 0.8 jet.

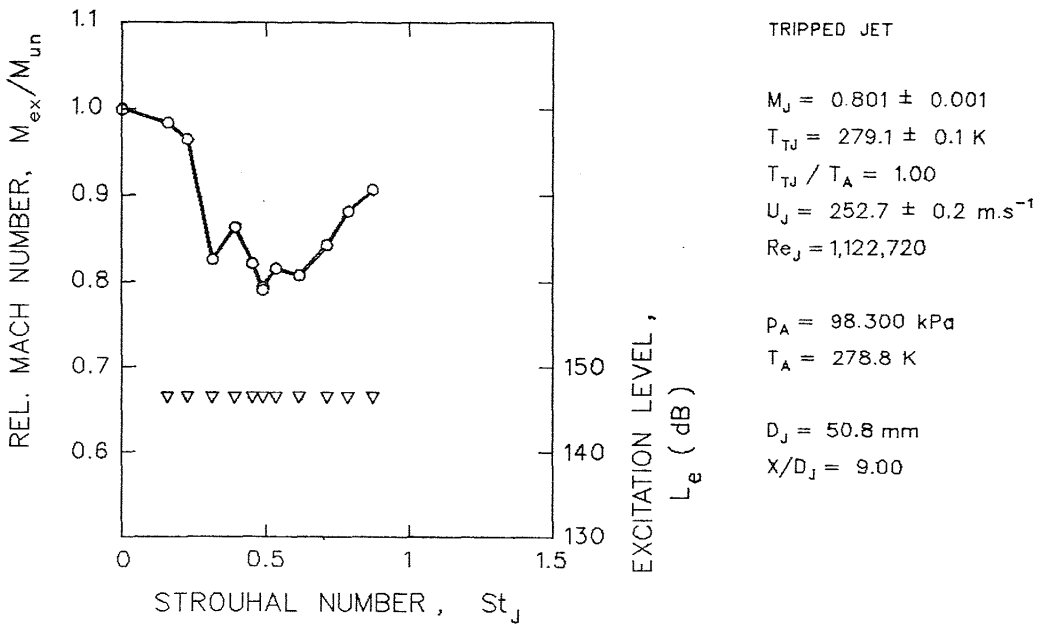

Figure 5.14 Excitation Strouhal number effects on unheated, tripped, Mach number 0.8 jet.

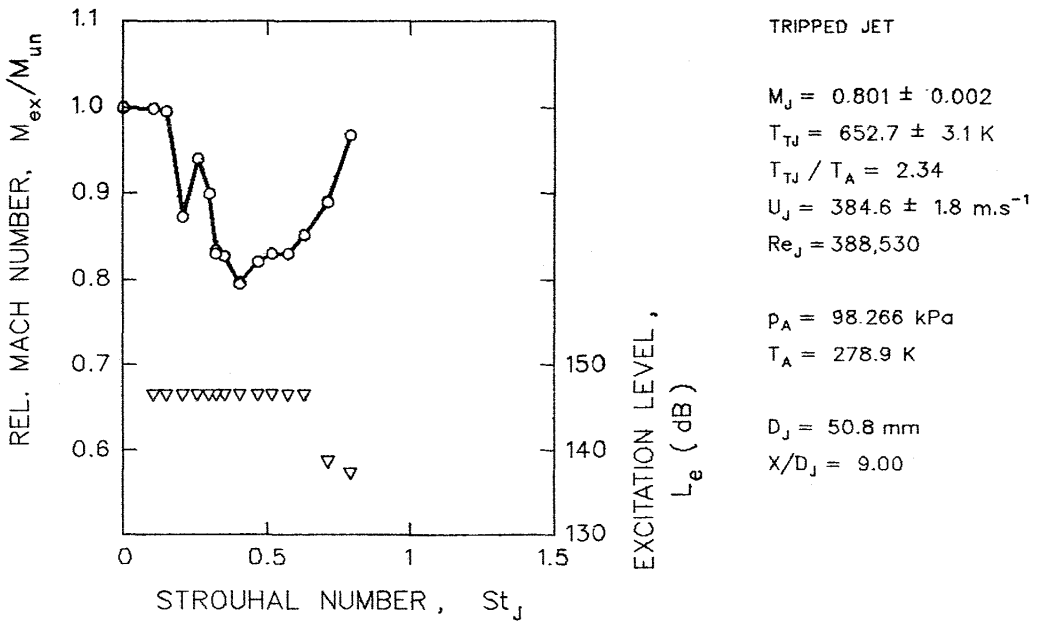

Figure 5.15 Excitation Strouhal number effects on heated, tripped, Mach number 0.8 jet.

To assess the net gain of jet mixing enhancement due to acoustic excitation, the results must be compared on a common basis. In Figures 5.12 through 5.15, the jet excitability was judged based on a relative change between excited and unexcited states. In Figures 5.16 through 5.19, however, the flow Mach number at X/D = 9 is normalized by the jet exit Mach number. There are no surprises for unheated untripped and tripped jets (Figures 5.16 and 5.18). Both jets respond similarly to the acoustic excitation. For heated jets, as shown above in Figures 5.13 and 5.15, the tripped jet seemed to be more excitable than the untripped one. However, the heated tripped jet's initial centerline Mach number at X/D = 9 was substantially higher than the one for the untripped jet. It appears that the greater excitability of the heated tripped jet results from the decreased jet mixing due to the boundary layer tripping as discussed above. A closer inspection of Figures 5.17 and 5.19 reveals that for the same excitation level of 147 dB the centerline flow Mach number at X/D = 9 drops to approximately 65% of the jet exit Mach number regardless of the flow temperature or nozzle exit boundary layer conditions. It appears free jet mixing and development may be controlled by flow excitation as well as nozzle exit boundary layer modifications.

For completeness, the results of excitation experiments for tripped, unheated and heated, Mach number 0.3 jets are shown in Figures 5.20 through 5.23. No conclusions are derived from these results because of the noncompatibility of the nozzle-exit boundary layer conditions between untripped and tripped states for this jet exit Mach number.

5.5 CONCLUSIONS

Based on the above described experiments for Mach number 0.8, unheated and heated jet, the following conclusions were derived:

1. The free jet mixing rate strongly depends on nozzle exit boundary layer conditions.

2. Relative jet excitability, in terms of a ratio of flow local Mach numbers of excited and unexcited states at the optimum excitation frequency, is a strong function of nozzle exit conditions but is independent of flow temperature.

3. Absolute jet excitability at the optimum excitation frequency, in terms of the ratio of the flow local Mach number to the jet exit Mach number for an optimum, appears to be a function of the excitation level only.

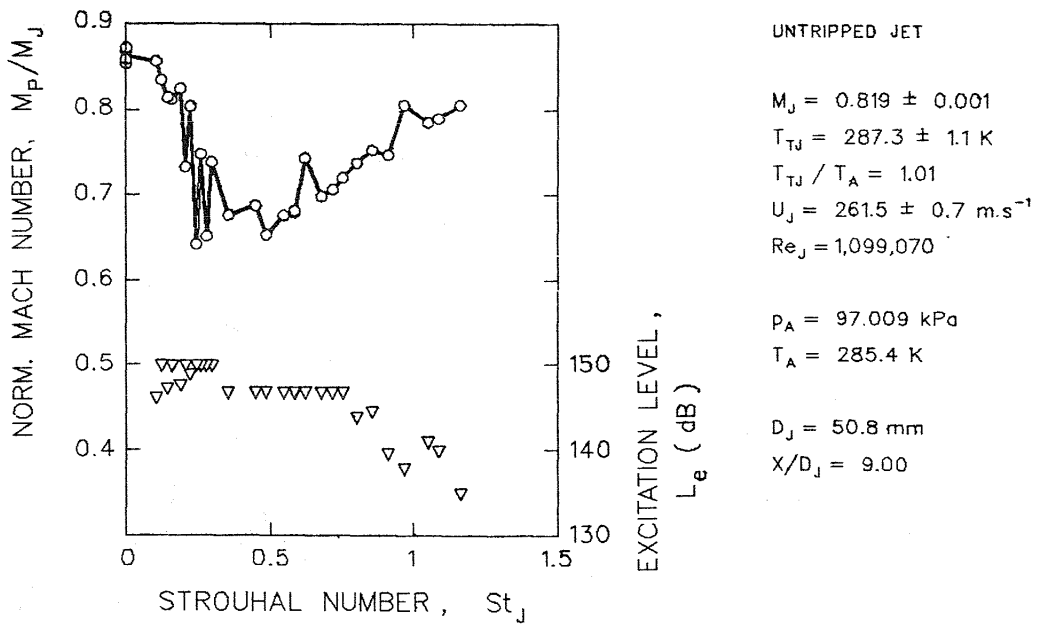

Figure 5.16 Excitation Strouhal number effects on unheated, untripped, Mach number 0.8 jet.

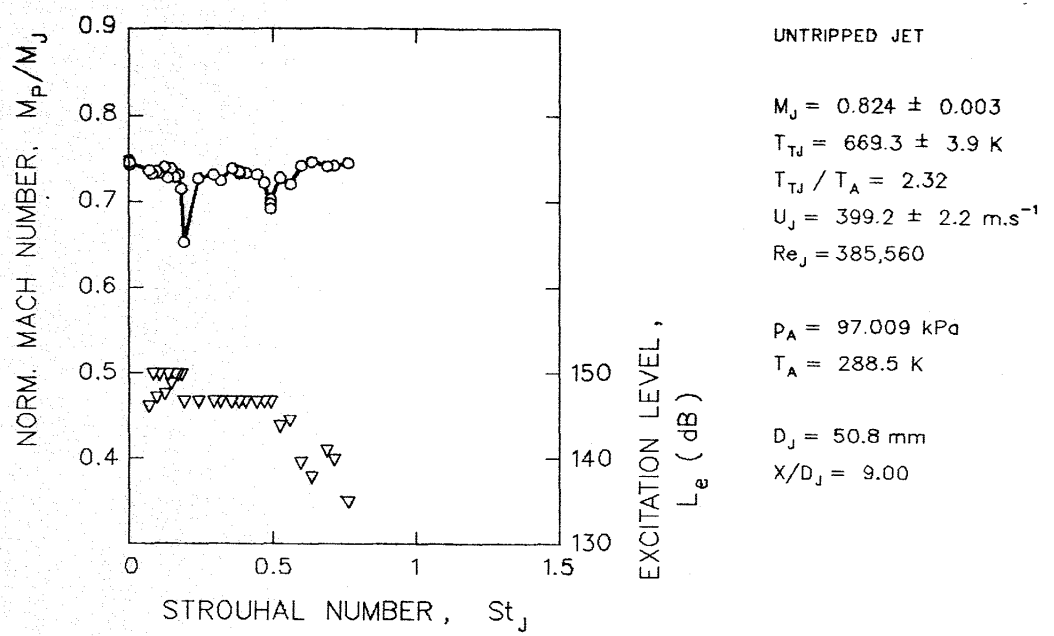

Figure 5.17 Excitation Strouhal number effects on heated, untripped, Mach number 0.8 jet.

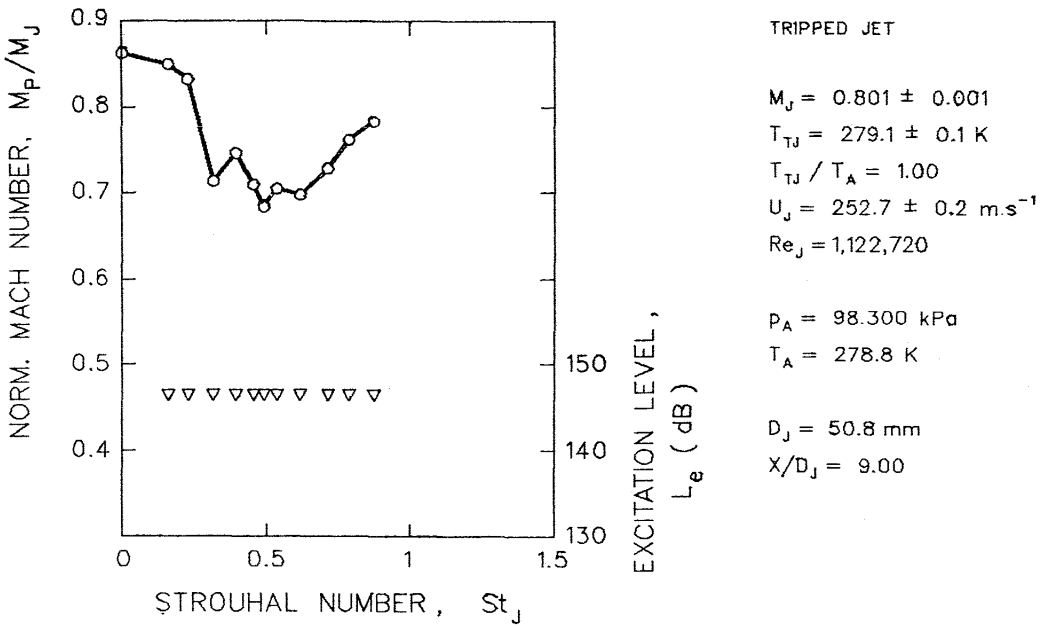

Figure 5.18 Excitation Strouhal number effects on unheated, tripped, Mach number 0.8 jet.

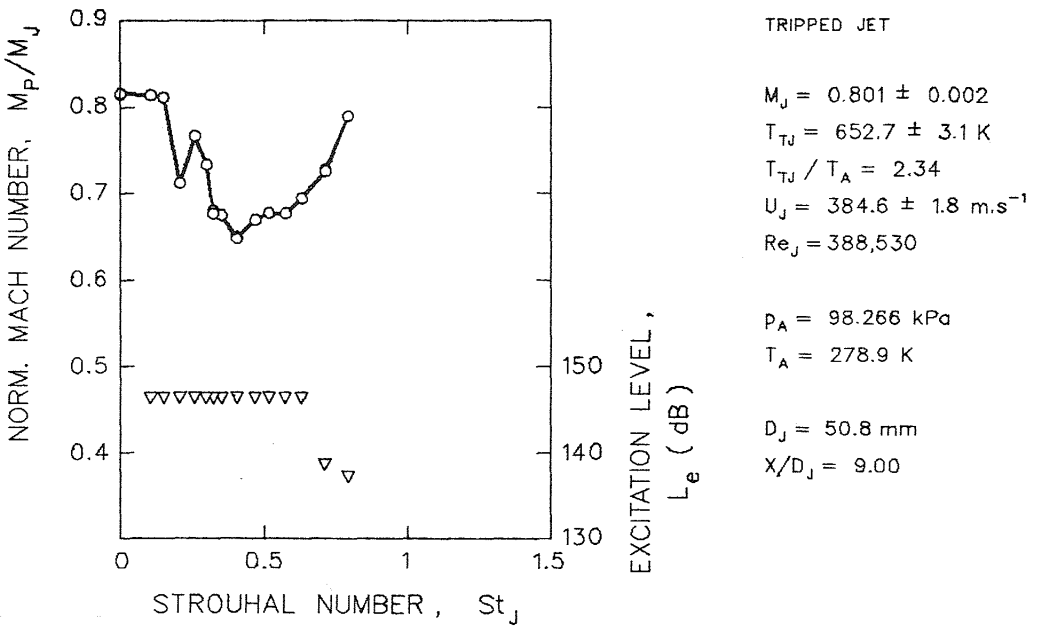

Figure 5.19 Excitation Strouhal number effects on heated, tripped, Mach number 0.8 jet.

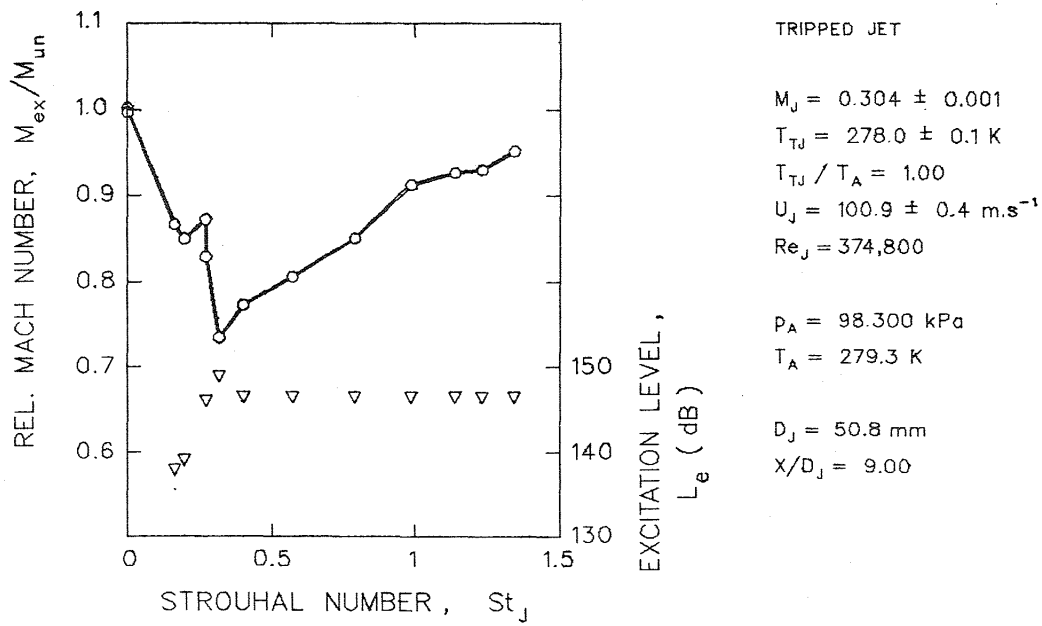

Figure 5.20 Excitation Strouhal number effects on unheated, tripped, Mach number 0.3 jet.

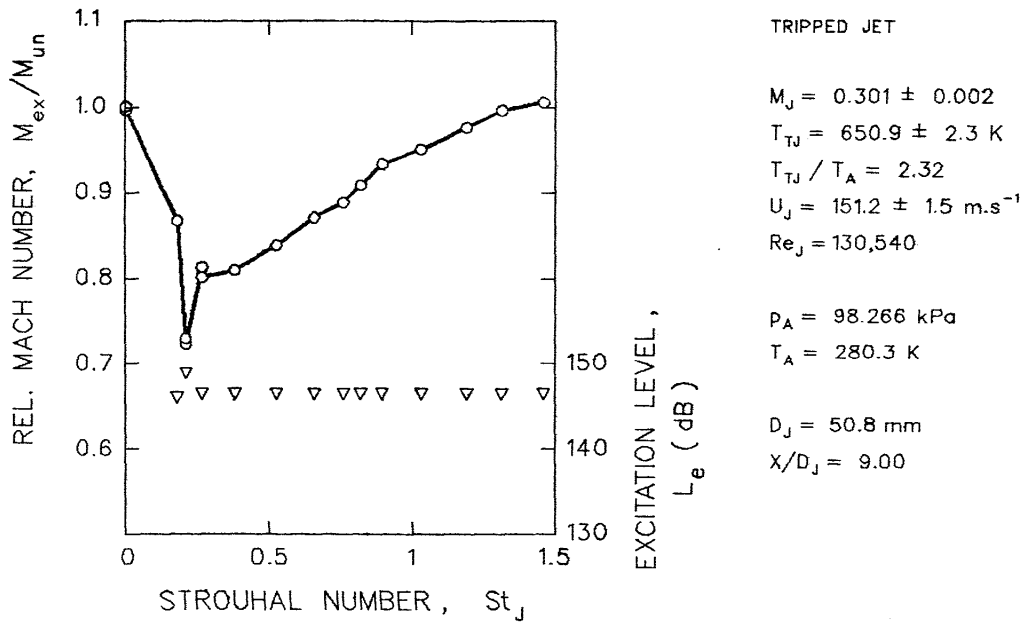

Figure 5.21 Excitation Strouhal number effects on heated, tripped, Mach number 0.3 jet.

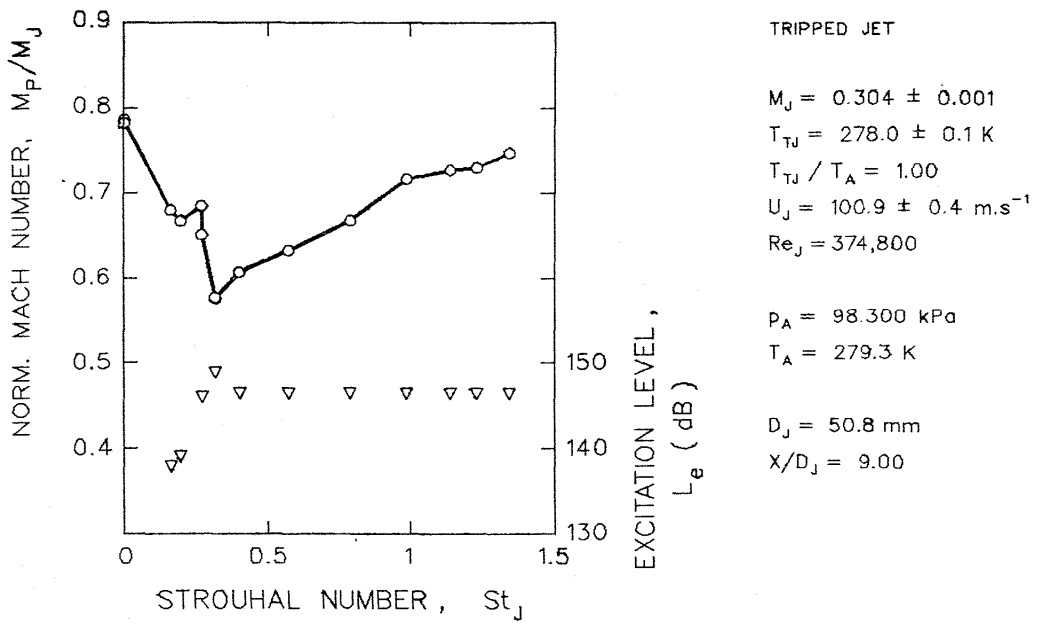

Figure 5.22 Excitation Strouhal number effects on unheated, tripped, Mach number 0.3 jet.

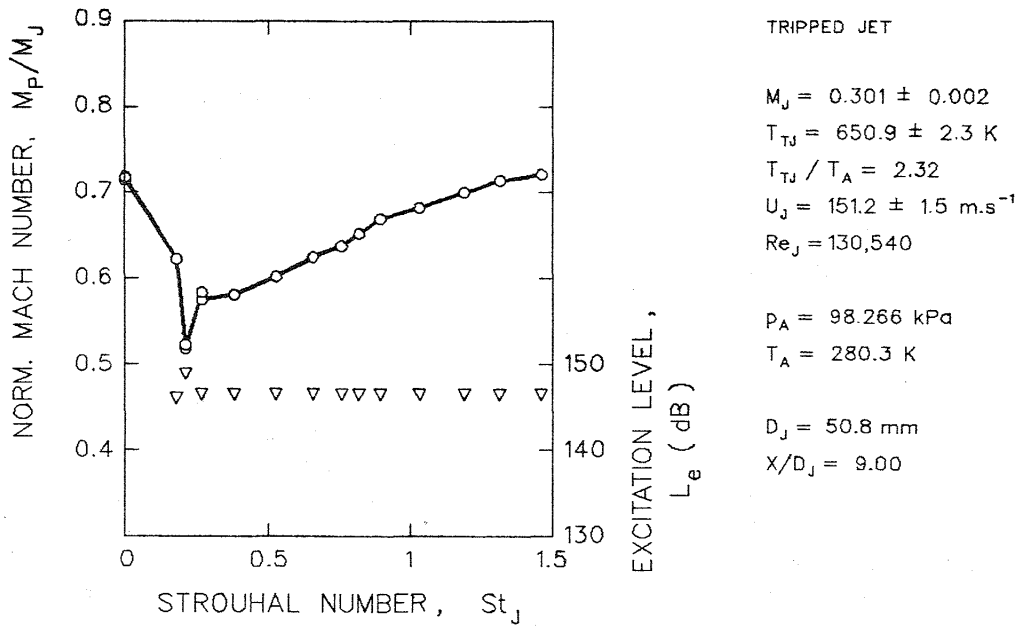

Figure 5.23 Excitation Strouhal number effects on heated, tripped, Mach number 0.3 jet.

4. Jets with a thin laminar nozzle exit boundary layer appear to be more selective as far as the optimum excitation frequency is concerned than those with a thick turbulent nozzle exit boundary layer.

5. Free jet mixing and development may be controlled by flow excitation as well as by nozzle exit boundary layer modification.

These conclusions, as mentioned above, may apply to the Mach number 0.8 jets, flow excitation conditions investigated, and the nozzle used in these tests. Further work is needed to generalize these conclusions for a broader range of jet operating conditions.

LIST OF SYMBOLS

b	half jet width
BL	boundary layer
c_{pi}	coupling coefficient (imaginary part)
c_{pr}	coupling coefficient (real part)
D	nozzle exit diameter
f	frequency
H	shape factor
k	wave number
L	level
L*	distance
M	Mach number
p	pressure
PR	pressure ratio
R	nozzle exit radius
Re	Reynolds number
St,S	Strouhal number
T	temperature
U	axial velocity
V,v	radial velocity
V_i	driver voltage
X	axial coordinate
Y,y	radial coordinate
δ	displacement thickness
ε	energy thickness
λ	boundary layer thickness
ρ	density
θ	momentum thickness
θ*	angle

Subscripts

a,A	ambient
c	centerline
e,ex	excited
j,J	jet, based on nozzle diameter
P	probe
r	reservoir
s	static
t,T	total
un	unexcited
δ	based on displacement thickness
ε	based on energy thickness
θ	based on momentum thickness

REFERENCES

[2.1] Ahuja, K. K.; Lepicovsky, J.; Tam, C. K. W.; Morris, P. J.; and Burrin, R. H.: Tone-Excited Jet -- Theory and Experiments. NASA CR-3538, 1982.

[2.2] Lepicovsky, J.; Ahuja, K. K.; Salikuddin, M.; and Morris, P. J.: Tone-Excited Heated Jets. Lockheed Report LG84ER0032, 1984.

[2.3] Tam, C. K. W.; and Morris, P. J.: Tone-Excited Jet -- Theory and Comparison with Measurements. J. Sound Vib., Vol. 102, pp. 119-151, 1985.

[2.4] Chan, Y. Y.: Spatial Waves in Turbulent Jets. Physics Fluids, Vol. 17, pp. 46-53, 1974.

[2.5] Moore, C. J.: The Role of Shear Layer Instability Waves in Jet Exhaust Noise. J. Fluid Mechanics, Vol. 80, pp. 321-367, 1977.

[3.1] Powell, A.: The Noise Emanating from a Two-Dimensional Jet Above the Critical Pressure. Aero. Quart. Vol. 4, pp 103-122, 1953.

[3.2] Powell, A.: On the Mechanism of Choked Jet Noise. Proc. Phys. Soc., Vol. 66, Pt. 12, pp. 1039-1056, 1953.

[3.3] Yu, J. C. and Seiner, J. M.: Nearfield Observations of Tones Generated from Supersonic Jet Flows. AIAA Paper 83-0706, 1983.

[3.4] Ahuja, K. K.: Basic Experimental Study of Coupling Between Flow Instabilities and Incident Sound. NASA CR-3789, 1984.

[3.5] Ahuja, K. K.: Some Unique Experiments on Receptivity. AIAA Paper No. 85-0533.

[3.6] Masters, G. F.: The Effects of Upstream Nozzle Shaping on Incompressible Turbulent Flow from Rectangular Nozzles, Transactions of the CSME, Vol. 5, pp. 197-203, 1979.

[5.1] IMSL Library, Edition 9, International Mathematical & Statistical Libraries, Inc., Houston, 1981.

[5.2] Schlichting H.: Boundary-Layer Theory, 7th edition, McGraw-Hill Book Company, New York, 1979.

NASA
National Aeronautics and Space Administration

Report Documentation Page

1. Report No.	2. Government Accession No.	3. Recipient's Catalog No.
NASA CR-4129, Part II		

4. Title and Subtitle
Acoustically Excited Heated Jets
II - In Search of a Better Understanding

5. Report Date
June 1988

6. Performing Organization Code

7. Author(s)
J. Lepicovsky, K.K. Ahuja, W.H. Brown,
M. Salikuddin, and P.J. Morris

8. Performing Organization Report No.
LG86ER0022 (E-4002)

10. Work Unit No.
505-62-91

9. Performing Organization Name and Address
Lockheed Aeronautical Systems Company - Georgia
Dept. 72-74, Zone 403
Marietta, Georgia 30063

11. Contract or Grant No.
NAS3-23708

13. Type of Report and Period Covered
Contractor Report
Final

12. Sponsoring Agency Name and Address
National Aeronautics and Space Administration
Lewis Research Center
Cleveland, OH 44135-3191

14. Sponsoring Agency Code

15. Supplementary Notes
Project Manager, Edward J. Rice, Internal Fluid Mechanics Division, NASA Lewis Research Center. J. Lepicovsky, K.K. Ahuja, W.H. Brown, and M. Salikuddin, Lockheed Aeronautical Systems Company - Georgia. P.J. Morris, Pennsylvania State University, University Park, Pennsylvania.

16. Abstract
The second part of a three-part report on the effects of acoustic excitation on jet mixing includes results of an experimental investigation directed at resolving the question of poor excitability of some of the heated jets. The theoretical predictions discussed in Part I are examined in detail to find explanations for the observed discrepancies between the measured and the predicted results. Additional testing was performed by studying the self excitation of the shock containing hot jets and also by exciting the jet by sound radiated through source tubes located externally around the periphery of the jet. The effects of nozzle-exit boundary layer conditions on jet excitability was also investigated. It is concluded that high speed, heated jet mixing rates and consequently also the jet excitability strongly depends on nozzle exit boundary layer conditions.

17. Key Words (Suggested by Author(s))	18. Distribution Statement
Sound-flow interaction; Jet mixing; Flow visualization; Velocity and temperature measurement; Large-scale structures	Unclassified - Unlimited Subject Category 02

19. Security Classif. (of this report)	20. Security Classif. (of this page)	21. No of pages	22. Price*
Unclassified	Unclassified	88	A05

*For sale by the National Technical Information Service, Springfield, Virginia 22161

End of Document